Application of FEMA P695 (ATC-63) to Analysis and Design of Light-Frame Wood Residential Buildings

Prepared by

NAHB Research Center

400 Prince Georges Boulevard

Upper Marlboro, MD 20774-8731

www.nahbrc.com

March 2011

NAHB RESEARCH CENTER SM

Acknowledgements

This research was supported in part by funds provided by the Forest Products Laboratory, Forest Service, USDA.

This research was supported in part by funds provided by the National Association of Home Builders.

Disclaimer

March 2011

List of Reviewers for 90% Draft

Ioannis Christovasilis, Ph.D., The University at Buffalo Foundation

Gary Ehrlich, P.E., National Association of Home Builders

Charles Kircher, Ph.D. P.E., Kircher & Associates, Consulting Engineers

Philip Line, P.E., URS Corporation, American Wood Council

Doug Rammer, P.E., USDA Forest Products Laboratory

Borjen ("BJ") Yeh, Ph.D., P.E., APA – The Engineered Wood Association

Contents

Table of Figures

List of Tables

(This page intentionally left blank)

Introduction

Seismic design of buildings has its basis in a combination of (1) empirical knowledge (observational and measured data) and (2) engineering analysis. The experience accumulated from seismic events and large-scale tests provides confidence in engineering models and serves to establish acceptable levels of risk for code compliance.

The design philosophy underpinning the current seismic building code requirements is focused on the objective of life safety at the Maximum Considered Earthquake (MCE) ground motion level which corresponds to a 2% probability of exceedance in 50 years. It is expected that an MCE event will cause inelastic deformations in the seismic force-resisting system, but the structure will remain stable with a low probability of collapse. The inelastic deformations cause damage to the seismic force-resisting system but also provide a mechanism for the structure to control seismic forces – an engineering strategy for economical earthquake-resistant systems.

This design philosophy is implemented in engineering standards through the use of seismic performance factors (SPFs) which modify the elastic forces and deformations determined in accordance with Newton's second law of motion. These modified forces and deformations are intended to represent the nonlinear response of a building system. The SPFs established in ASCE/SEI 7-10 (ASCE 7) *Minimum Design Loads for Buildings and Other Structures* [1] are based on performance observations and engineering knowledge and judgment. The SPFs include:

- Response Modification Factor (R)
- Overstrength Factor (Ω_0)
- Deflection Amplification Factor (C_d)

The lack of a standardized approach for the development of SPFs was one of the reasons the Federal Emergency Management Agency (FEMA) funded the Applied Technology Council's Project 63 (ATC-63) to develop a procedure for qualification of SPFs for new and existing seismic resisting systems. This new methodology is documented in FEMA P695 "*Quantification of Building Seismic Performance Factors"* [2]. In summary, the performance of a system is benchmarked based on its ability to maintain a high rate of simulated survival (i.e., non-collapse) when subjected to a suite of ground motions scaled to the MCE level.

The following statement from FEMA P695 illustrates its potential influence on seismic design and construction:

> "The methodology…provides a basis for evaluation of current code-approved systems for their ability to achieve intended seismic performance objectives. It is possible that results of future work based on this Methodology could be used to modify or eliminate those systems or requirements that cannot reliably meet these objectives."

FEMA P695 includes an example application of the methodology to the wood light-frame wood structural panel (WSP) shear wall system designed in accordance with requirements of ASCE 7-05. The results of the FEMA P695 example application of the methodology indicate that the SPFs for wood light-frame WSP systems are consistent with the values used in ASCE 7-05.

The study presented in this report was designed to:

(1) highlight implementation considerations for the FEMA P695 methodology when applied to wood light-frame WSP shear wall systems, and

(2) improve the knowledge of the seismic performance of wood light-frame WSP shear wall systems.

This report does not attempt to qualify a new seismic force resisting system or validate existing seismic force resisting systems.

The specific objectives of this study are to use the FEMA P695 methodology to:

1. Characterize the collapse performance of a wider variety of wood light-frame building configurations than addressed by the FEMA P695 example application with focus on residential applications.
2. Characterize the collapse performance of systems in lower design categories (SDC): B and C.
3. Compare the collapse performance of varying hysteretic models (such as from experimental tests of shear walls with different load protocols) on collapse performance.
4. Compare the collapse performance of phenomenological models based on wall and connection responses.
5. Characterize the influence of finishes on collapse performance.
6. Characterize the collapse performance of soft-story configurations.
7. Improve the accuracy of analysis for high-aspect ratio walls by using hysteretic models representative of the high-aspect ratio shear wall response.
8. Evaluate the influence of using different analysis software and hysteretic formulations.
9. Through sensitivity studies, understand the effect of uncertainty assumptions on collapse performance.

Implementation of FEMA P695 Methodology

Implementation of the FEMA P695 methodology requires consideration of the framework of four key elements (Figure 1):

(1) system design requirements,

(2) system performance characteristics,

(3) system analysis methods, and

(4) ground motions.

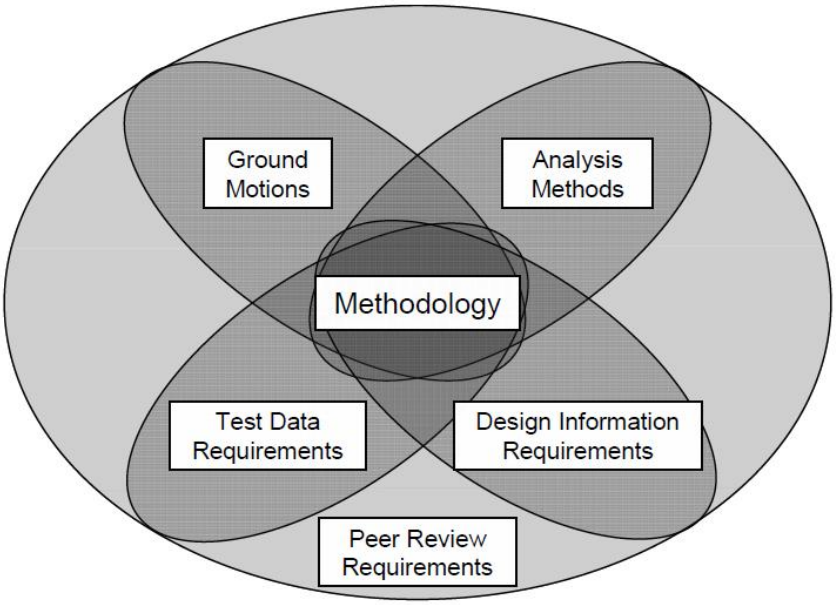

Figure 1 – FEMA P695 Methodology composition [2]

The effect of building configurations is captured though index archetypes intended to represent the possible range of configurations within design requirements. It should be noted that irregular systems and buildings in seismic design categories A and E are not considered by FEMA P695.Also, as part of the qualification of a new seismic force resisting systems, the FEMA P695 methodology requires an oversight function by a Peer Review Panel (PRP). As noted previously, qualification of a new system or existing system is not the objective of this report.

Table 1 summarizes information sources and design tools used in this study and how they relate to the four key elements of the FEMA P695 methodology. Individual sections that follow provide specific details for each of the four key elements of the FEMA P695 methodology.

Table 1 – Key elements of the analysis

FEMA P695 Key Element	Scope of This Study
System Design Requirements	IBC [3] ASCE 7-10 AF&PA SDPWS [4] AF&PA NDS [5]
System Performance Characteristics (test data)	**Sheathing Connection Behavior:** NEESWood Benchmark Test [6] **Shear Wall Behavior:** CUREE-Caltech Woodframe Project [7] APA-The Engineered Wood Association [8], [9], [10], [11] **Full-Scale Building Behavior:** CUREE-Caltech Woodframe Project [12] NEESWood Benchmark Test [6]
System Analysis Methods (nonlinear modeling)	**Shear Wall Response:** CASHEW [13] **Dynamic Nonlinear Analysis:** SAWS [14] OpenSEES [15] **Hysteretic Models:** CUREE [13] and [14] Pinching4 [15]
Ground Motions	Suite of 44 Ground Motions per FEMA P695

Appendix A provides a detailed flow-chart of procedural steps for implementing the FEMA P695 methodology used to meet objectives of this study.

System Design Requirements

System design requirements for wood light-frame shear wall buildings are in accordance with ASCE 7 with respect to determining seismic forces on the analyzed buildings including seismic design category, vertical distribution of forces, height limits, and wood frame resistance provisions. The AF&PA SDPWS provides design capacities for the wood light-frame shear walls and the applicable detailing requirements. Member and connection design is assumed to be in accordance with the AF&PA NDS.

The influence of SDPWS seismic provisions for (1) reduced design shear capacities of high aspect ratio shear walls, and (2) limitations on combining capacities of dissimilar sheathing materials, such as wood structural panel and gypsum wallboard, is investigated to evaluate their effect on collapse performance using the FEMA P695 methodology.

System Performance Characteristics

Representative shear wall response models are a key component of the building collapse simulations. The response models are typically established and validated using experimental data, from laboratory testing of the system, its components, or both, under a cyclic protocol. The test data incorporates the individual or combined behavior of materials, components, connections, assemblies, and systems. In general, the hysteretic force-displacement behavior from cyclic tests shows stiffness and strength degradation at increased displacements. The degradation mechanism is an integral part of determining the collapse behavior of the building.

As a part of this study, test programs focusing on the cyclic response of wood-frame shear walls from numerous sources have been reviewed for applicability to this study. A summary of this review is provided later in this report and includes experimental studies of (1) sheathing-to-framing connections, (2) full-scale shear walls, and (3) full-scale wood-frame structures. The sheathing-to-framing connection results are used in this study as input to CASHEW [13] for modeling of hysteretic connection response in shear walls (see description of CASHEW in the *System analysis methods* section). The full-scale shear wall data is used to fit phenomenological models (see the *System analysis methods* section for more information). Results of the full-scale house testing are used for validation of the building modeling procedure.

Sheathing Connection Response

The cyclic responses of sheathing-to-framing connections were obtained from the NEESWood Benchmark Test [6]. The primary emphasis of this NEESWood effort was to benchmark seismic performance and conduct nonlinear modeling of woodframe structures. To improve the accuracy of nonlinear shear wall modeling capabilities, the sheathing connections of 8d common nails attaching a 7/16-inch OSB panel to a framing member were tested. In this experimental series, a total of 4 configurations were tested using the CUREE cyclic displacement protocol [16]. Specifications for these test specimen configurations are provided in Table 2.

Table 2 – NEESWood Benchmark Test sheathing to framing fastener configurations [6]

Configuration	Framing Member Size	Loading Direction Relative to Framing Member Grain Direction	Number of Test Specimens
1	2x4	Parallel	13
2	2x4	Perpendicular	13
3	2x6	Parallel	13
4	2x6	Perpendicular	13

Figure 2 provides a sample of the hysteretic behavior measured in laboratory testing (Input Data) and the corresponding numerical fit (Model/Fit) for test Configurations 1 and 2 (parallel-Figure 2a, perpendicular-Figure 2b).

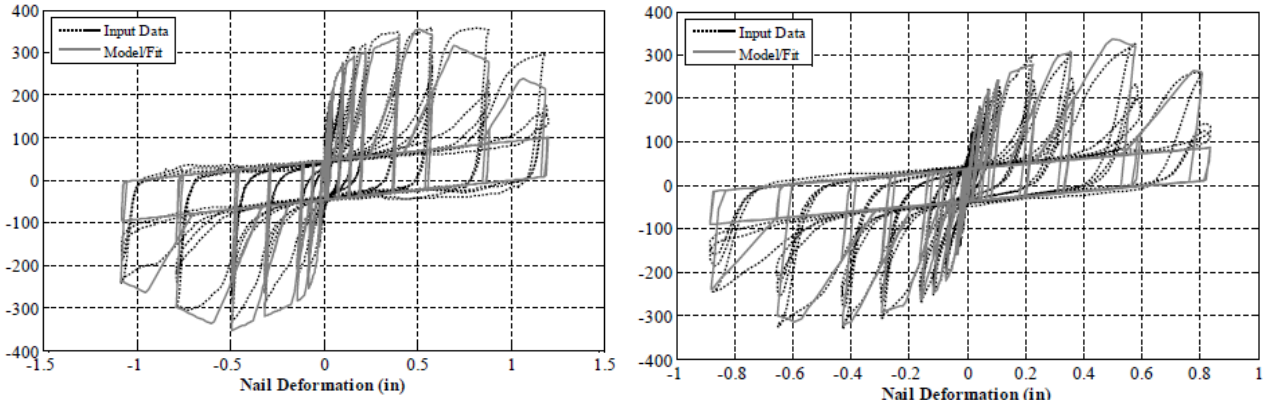

(a) Tested 2x4 connection parallel to framing grain

(b) Tested 2x4 connection perpendicular to framing grain

Figure 2 – Cyclic response comparisons for test results (Input Data) and numerical model (Model/Fit) [6]

Shear Wall Behavior

The force-displacement results for full-scale eight foot tall shear walls were obtained from laboratory tests conducted by the CUREE-Caltech Woodframe Project [7] and APA-The Engineered Wood Association [8], [9], [10], [11]. The results of these testing programs were used in this study to develop phenomenological models for input into nonlinear shear building models. Segmented shear walls (full restraint to overturning at each shear wall segment end) were investigated in this study. The shear wall aspect ratios, height/length of h/b, for segmented shear walls ranged from 0.5:1 to 4:1 (Table 3).Wood shear walls from each of these test programs demonstrate similar cyclic behavior, particularly, degradation characteristics. A summary of the primary variables considered in the shear wall tests is provided in Table 3.

Table 3 – Test data for single-sided wood sheathed shear walls[1]

Test Program	Testing Protocol	Shear Wall Type	Aspect Ratio	Sheathing-to-Framing Fasteners			Sheathing Thickness (inch)	Framing		Finishes[3,4]	Number of Specimens
				8d Nail[2]	Edge Spacing (inches)	Field Spacing (inches)		Species	Spacing (inches)		
CUREE-Caltech [7]	CUREE [16]	Segmented	0.5	Box	6[5]	12	3/8	Douglas Fir	16	None	2 (Figure 3a)
			1.23								2 (Figure 3b)
										Gypsum	2
										Stucco	2
			2.56	Common	3[5]	12				None	2 (Figure 3c)
				Box							2 (Figure 3c)
										Gypsum	2
										Stucco	2
APA [17]	SPD [16]	Segmented	1	Common	3	6	7/16		24	None	10
			2								6
			4			N/A					4
APA [9] and [10]	CUREE [16]	Segmented	1	Common	4	6	7/16				6

1. All specimen tested had a wall height of 8 feet.
2. Box nails had a shaft diameter of 0.113 inches; common nails had a shaft diameter of 0.131 inches.
3. Gypsum panels attached with #6x1-1/4 inch bugle head drywall screws at 7 inches on center.
4. Stucco finish was 3 coats and finished to a thickness of 7/8 inches, line wire and hex wire mesh was attached using 16 gauge staples with 7/8 inch legs at 7 inches on center.
5. OSB shear wall specimens were constructed using two lines of nails, staggered, along the side and top boundary of the shear wall segments.

The shear wall configurations tested for the CUREE-Caltech Woodframe Project are provided in Figure 3. Figure 3a and Figure 3b are considered low aspect ratio walls for this study because they have respective aspect ratios of 0.5 and 1.23:1, the results from the shear wall configuration Figure 3c are considered high aspect ratio walls because they have an aspect ratio of 2.56.

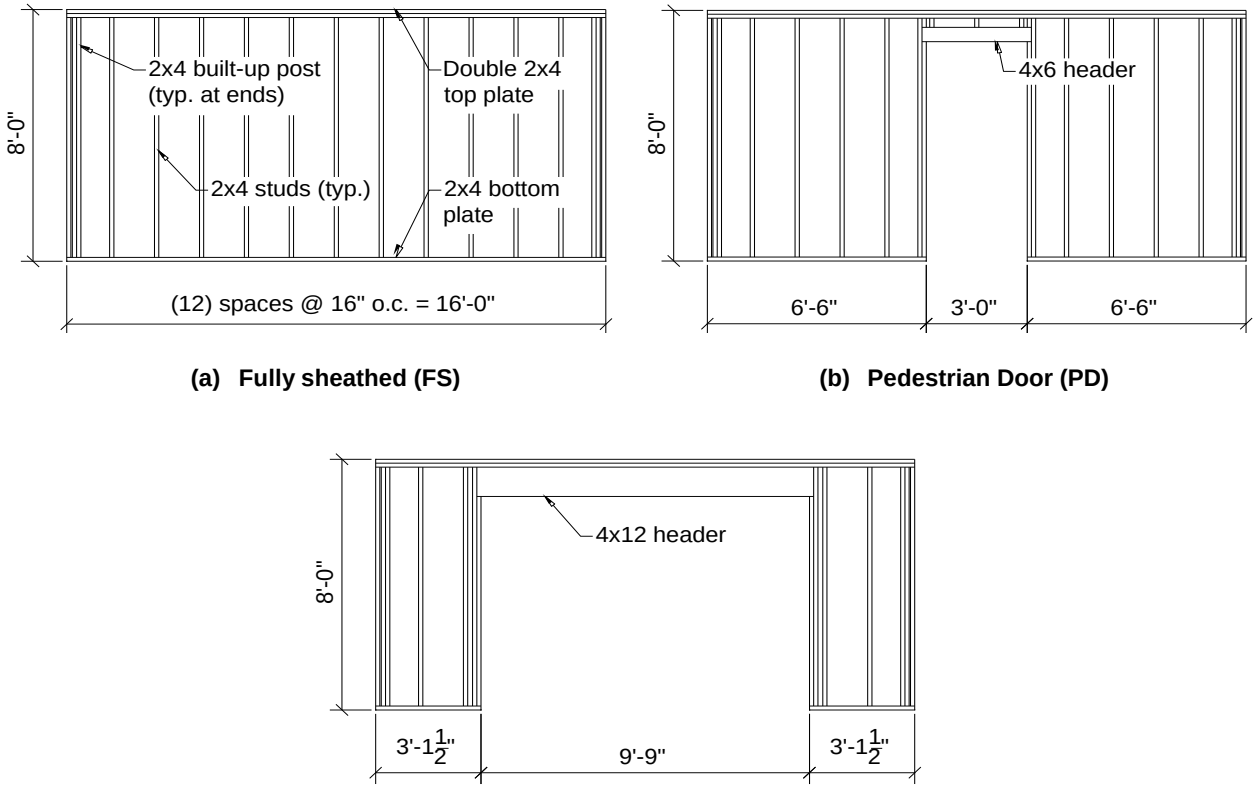

(a) Fully sheathed (FS)

(b) Pedestrian Door (PD)

(c) Garage Door (GD)

Figure 3 – CUREE-Caltech Woodframe Project wall framing configurations, after [7]

The results of shear walls tested according to two displacement protocols (Table 3, CUREE and SPD) are used in this study to develop shear wall models (SWMs) enveloping the typical behavior of WSP systems. These shear wall models are defined later in this report in the *Shear Wall Characterization* section.

Full-Scale House Testing

The lateral response of full-scale test structures from the CUREE-Caltech Woodframe Project [12] and NEESWood Benchmark Test [6] are used to determine the level of correlation between the modeling methods and system performance characteristics used in this study and results of full-scale testing (see the *Validation of Shear Wall Behavior and Modeling Methods* section for more information). Test structure details and ground motion levels used in the validation task are provided in Table 4 and building configurations are provided in Figure 4 and Figure 5.

Table 4 – Full scale residential test structures summary

Test Program (Designation)	Building Description	Floor Levels	Test Ground Motion (Scaled PGA)	Building Level	Total Weight (kips)
CUREE-Caltech Woodframe Project (9.4.F)	Single-Family	2	Canoga Park (0.5)	1	13.8
				2	10.8
NEESWood Benchmark Test (NWP1S06)	Townhome	2	Canoga Park (0.22)	1	53.12
				2	23.52

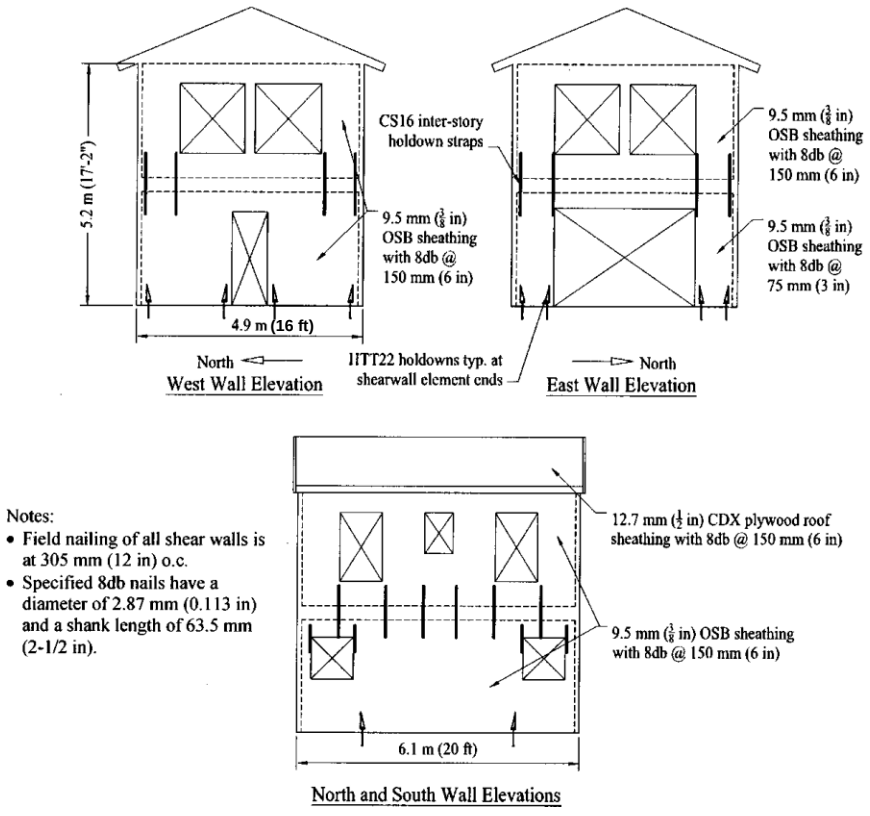

Figure 4 – CUREE-Caltech Woodframe Project two story test structure [18]

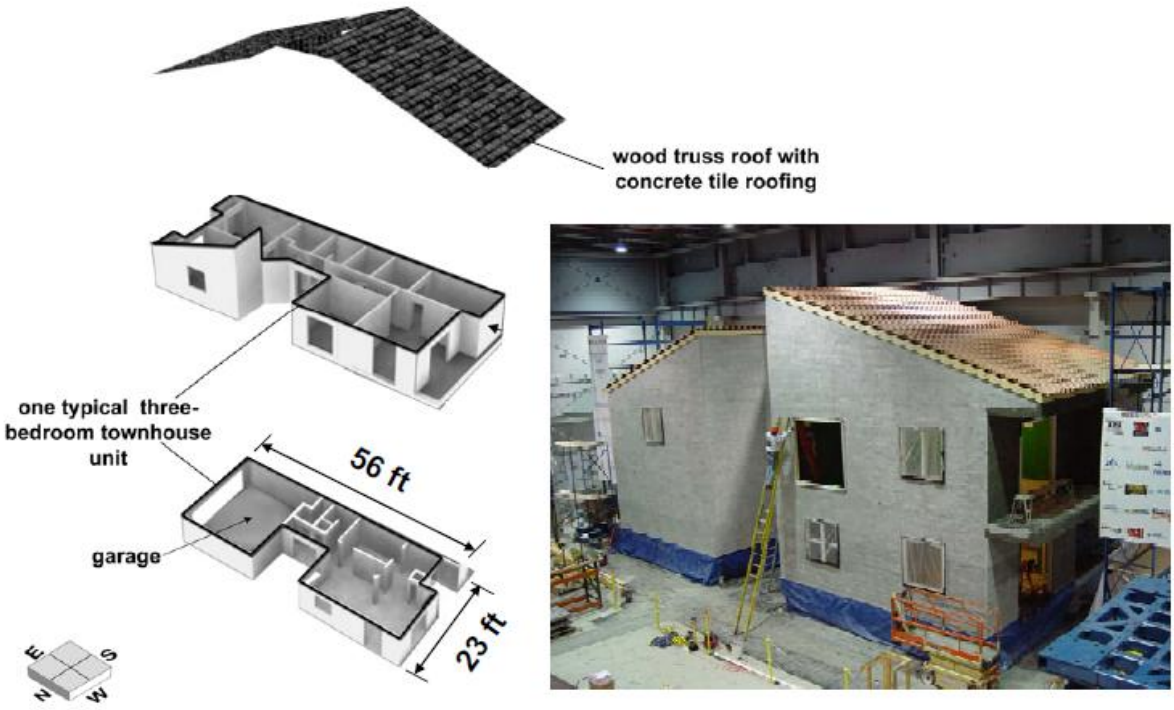

Figure 5 – NEESWood Benchmark Test two story townhouse test structure [6]

System Analysis Methods

The system design requirements and system performance characteristics are used to develop performance groups that are composed of individual building designs that can be modeled for nonlinear analysis, Individual building models, within FEMA P695, are known as index archetypes. The two nonlinear analysis procedures described in the FEMA P695 methodology include:

- Static (Pushover)
- Dynamic (Response History)

The FEMA P695 parameters of overstrength (Ω) and period-based ductility (μ_T) are obtained from the nonlinear static analysis, whereas the median collapse spectral acceleration ($\hat{S}_{CT}$) is obtained from the nonlinear dynamic analysis procedure. The static analysis of the archetype model is completed by loading the building laterally with forces distributed at each floor or roof diaphragm according to a vertical inverted triangular loading distribution. This loading differs from the fundamental mode shape vertical distribution of forces provided in FEMA P695, however the fundamental mode shape loading for WSP shear wall systems are similar to an inverted triangular loading pattern, The dynamic analysis requires the archetype model to be subjected to 44 ground motions at increasing intensities, following an incremental dynamic analysis (IDA) procedure. The ground motions are scaled to an intensity level, corresponding to $\hat{S}_{CT}$, causing simulated collapse at 22 of the 44 ground motions. Simulated collapse in this study is defined as drift in any level exceeding 7%. For further details of each of these procedures see

Sections 6.3 and 6.4, respectively, of FEMA P695 and Appendix A in this report that provides a flow chart of the FEMA P695 procedural steps as they apply to this study.

The results from the two analysis procedures are compared to limits provided in Table 7-3 of FEMA P695 for an Adjusted Collapse Margin Ratio of 20% ($ACMR_{20\%}$) and 10% ($ACMR_{10\%}$) for index archetypes and performance groups, respectively.

Three modeling programs were used in this study to evaluate wood shear wall performance (Table 5). CASHEW is used to model shear wall connection behavior, whereas SAWS and OpenSEES are used to model shear wall behavior. SAWS is the primary building analysis software used in this study. OpenSEES is used only in several analyses to enable a comparison between results obtained from different software packages and hysteretic models.

Table 5 – Nonlinear analysis modeling platforms

Nonlinear Modeling Program	Input Behavior	Output Response	Hysteretic Model
CASHEW [13]	Connection	Shear Wall	CUREE
SAWS [14]	Shear Wall	Building	CUREE
OpenSEES [15]	Shear Wall	Building	CUREE
			Pinching4

The shear wall modeling software CASHEW [13], developed as part of the CUREE-Caltech Woodframe Project, is used to determine the hysteretic response of a segmented shear wall based on the hysteretic response of individual sheathing-to-framing connections according to the CUREE hysteretic model (discussed later in this report). The shear wall model is constructed by defining sheathing size, thickness, and sheathing panel shear modulus and sheathing-to-framing fastener locations. The top plate is laterally displaced causing sheathing panel rotation. As the panel rotates, displacements occur at the sheathing-to-framing connections with forces at the connections following the CUREE hysteretic model. The sum of horizontal forces in fasteners at the bottom plate and associated lateral top plate displacement represent shear wall behavior.

The nonlinear dynamic analysis software Seismic Analysis of Woodframe Structures (SAWS) [14] uses the lateral force-displacement behavior of shear walls to predict seismic response of a building. SAWS uses the ‘pancake’ method with vertically-stacked floor masses connected by zero-length spring elements. The spring elements represent the shear wall behavior characterized by the CUREE hysteretic model.

OpenSEES [15] is a multi-dimensional nonlinear analysis software. The ‘pancake’ modeling method used in the SAWS analysis is utilized in OpenSEES to allow direct comparison with SAWS results. The shear characteristic of the beam-column element in OpenSEES is used to represent the wood shear wall response. The element is considered axially rigid and has zero moment capacity. CUREE and Pinching4 hysteretic models are available in OpenSEES and are used in comparative analyses in this study.

Hysteretic Models

Two hysteretic models are used in this study to characterize the behavior of wood light-frame WSP shear walls:

- CUREE - Figure 6a
- Pinching4 - Figure 6b

Both models are formulated to simulate the pinching response typical for wood systems that develop slack in the reloading portion of the hysteretic cycle. Both models include factors to simulate the stiffness and strength degradation also typical for light-frame shear walls subjected to cyclic displacements. One purpose for including two different hysteretic models in the scope of this study is to determine the sensitivity of collapse performance to the model used for characterization of the shear wall behavior.

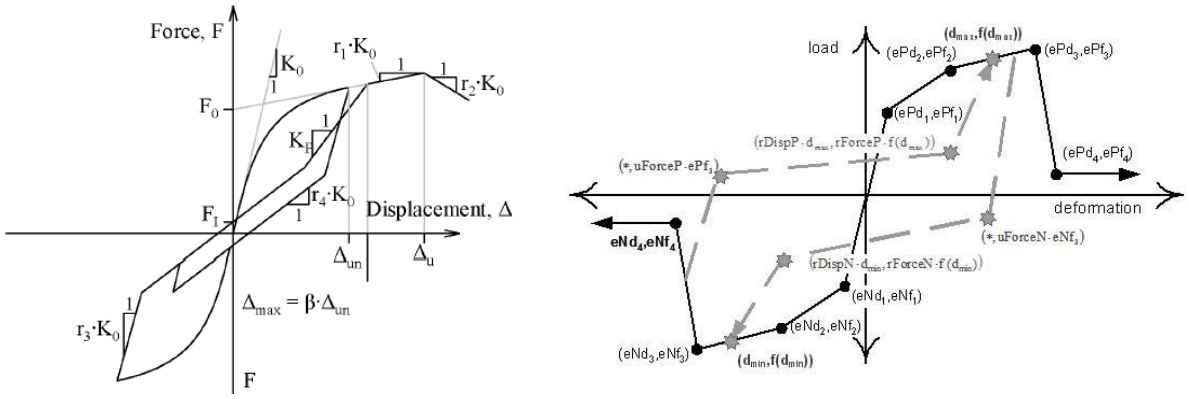

(a) 10 parameter CUREE [13] **(b) 28 parameter Pinching4 hysteretic model [15]**

Figure 6 – Hysteretic models used to characterize wood light-frame WSP shear wall cyclic behavior

The CUREE hysteretic model requires ten input parameters (Table 6): five are related to stiffness, two to force, one to displacement, and two to cyclic degradations. The CUREE hysteretic model (Figure 6a) is the only behavior used for modeling in both the CASHEW and SAWS modeling platforms and is available as an option in OpenSEES.

Table 6 – CUREE model hysteretic parameters definitions

Notation	Definition
F_0	Asymptotic y-intercept force
F_i	Pinching y-intercept force
K_0	Initial stiffness
r_1	Asymptotic stiffness ratio (e.g. post yield force)
r_2	Strength degradation stiffness ratio (e.g. post capping force)
r_3	Unloading stiffness ratio
r_4	Pinching stiffness ratio
δ_u	Displacement at capping force
α	Cyclic stiffness degradation parameter
β	Cyclic ductility parameter

The Pinching4 hysteretic model (Figure 6b), available in the OpenSEES modeling platform, requires a minimum of 28 parameters. However, many of these parameters can be set to zero for the purpose of modeling the response of wood light-frame WSP shear walls (Table 7).

Table 7 – Pinching4 model hysteretic parameters definitions

Notation	Definition	Special Notes
ePf1, ePf2, ePf3, ePf4	Force points on the envelope curve	
ePd1, ePd2, ePd3, ePd4	Displacement points on the envelope curve	
rDispP	Reloading deformation ratio	
rForceP	Reloading force ratio	
uForceP	Ratio of unloading strength	
gK1, gK2, gK3, gK4, gKLim	Unloading stiffness degradation factors	*gK2, gK3, gK4, and gKLim* = 0
gD1, gD2, gD3, gD4, gDLim	Reloading stiffness degradation factors	*gD2, gD3, gD4, and gDLim* = 0
gF1, gF2, gF3, gF4, gFLim	Strength degradation factors	*gF2, gF3, gF4, and gFLim* = 0
gE	Maximum energy dissipation	Fixed at 0.0
dmgType	Type of damage (cycle or energy)	cycle

Ground Motions

The FEMA P695 Far-Field ground motion record set is used for dynamic analysis in the current study. The Far-Field record set combines 44 historical earthquake records, M6.5 to M7.6, from locations greater than 6.21 miles (10 km) from fault rupture. The ground motions were obtained from the PEER NGA database and scaled according to Table A-4 in FEMA P695. For further information regarding the Far-Field record set see FEMA P695 Section 6.2 and FEMA P695 Appendix A [2].

Quality Rating and Uncertainty

FEMA P695 assigns to the system design requirements, system performance characteristics, system analysis methods, and ground motions a quality rating. This rating is based on the completeness and robustness of the available information related to the system under consideration, and the level of confidence in the characterization of the system behavior and performance. The quality ratings are used to quantify the uncertainty associated with the knowledge of the system's response and the accuracy of the analytical tools. The uncertainty for each FEMA P695 component is integrated with the results of the nonlinear static and dynamic analyses to characterize collapse performance on a probabilistic basis. Because the quality rating or uncertainty is a subjective measure, the current study primarily uses a total uncertainty (β_{TOT}) of 0.525 associated with a 'Good' quality rating for the design requirements, performance characteristics, and analysis methods for systems with a period based ductility greater than 3. To understand the effect of uncertainty on collapse performance, a sensitivity study is conducted to compare results using β_{TOT} = 0.525 to β_{TOT} = 0.425 and 0.725 for 'Superior' and 'Fair' quality ratings, respectively.

An example application included in FEMA P695 on light-frame wood structures used β_{TOT} = 0.500 and 0.675 for buildings incorporating low and high aspect ratio wall systems, respectively. The difference in β_{TOT} between low and high aspect ratio walls was due to the respective model quality ratings of 'Good' and 'Poor.' The high aspect ratio wall model was assigned a 'Poor' rating in FEMA P695 because SAWS did not consider uplift at wall ends as part of the system's response.

The current study evaluates the influence of the aspect ratios on the collapse performance by using phenomenological models fit into test results for walls with high and low aspect ratios. In this approach, the uplift deformation component is built into the global measured response of the tested shear walls. Therefore, a total system uncertainty of 0.525 was used in the analysis of low and high aspect ratio walls.

Nonlinear Building Model Development

In this section, the index archetype models for nonlinear static and dynamic analysis are developed based on the system design requirements and system performance characteristics of wood light-frame lateral force resisting systems. This study uses SAWS as the primary modeling software for the FEMA P695 analysis procedure. OpenSEES is used for several archetypes to evaluate the difference in the results obtained using two different analytical software platforms (SAWS vs. OpenSEES) and two unique hysteretic models (CUREE vs. Pinching4).

Identification of Index Archetype Configurations

This study considers building configuration designs that include variations within each of the FEMA P695 key elements. Table 8 provides the range for each of the considered variables for both the current study and the FEMA P695 example application. A total of thirty performance groups with eight foot tall shear walls are used in this study (Table 9). Note that this is in

comparison to the three residential performance groups with ten foot tall shear walls used in the FEMA P695 example application.

Table 8 – Archetype variables for wood light-frame systems

FEMA P695 Key Element	Variable	This Study	FEMA P695 Example Application
System Performance Characteristics	Shear Wall Type	Segmented	Segmented
	Test Protocol	CUREE and SPD	CUREE
	Aspect Ratio	Low and High	Low[1]
	Finishes	Gypsum or Stucco	None
System design requirements	Number of Stories	1, 2, 3, 4, 5	1, 2, 3, 4, 5
	Occupancies	Residential	Commercial and Residential
	Max Number of - Archetypes	8	5
	Performance Groups	30	3
	Seismic Design Categories (SDC)	B_{min}, B_{max}/C_{min}, C_{max}/D_{min}, D_{max}	C_{max}/D_{min} and D_{max}
	Aspect Ratio	Low (0.5:1, 1:1, 1.23:1, and 2:1) High (2.56:1 and 4:1)	Low (1:1 to 1.43:1) High (2.70:1 to 3.33:1)
	Wall Height	8 feet	10 feet
	Finishes	Gypsum or Stucco	None
	Soft-Story	1st Floor	None
	Edge Fastener Spacing	3”, 4”, and 6”	2”, 3”, 4”, and 6”
Nonlinear Modeling	Dynamic Nonlinear Analysis Software	SAWS and OpenSEES	SAWS
	Hysteretic Model	CUREE and Pinching4	CUREE
	Basis for Hysteretic Shear Wall Models	CASHEW Shear Wall Test Results	CASHEW
	Rayleigh Damping	1%, 3%, and 5%	1%

1. Capping displacement and post-capping behavior based on additional cyclic test data not provided in FEMA P695 [2].

Table 9 – Wood light-frame performance group matrix

Performance Group	System Performance Characteristics				System Design Requirements		System Analysis Methods			# of Archetypes
	Test Protocol	Test Program	Aspect Ratio (Edge Nail Spacing (inches))	Finishes	SDC	Soft-Story	Analysis Software	Hysteretic Model	Rayleigh Damping	
1	CUREE	CUREE-Caltech Woodframe Project	0.5 and 1.23:1 (6)	None	B_{min}	None	SAWS	CUREE	1%	7
2					B_{max}/C_{min}	None				7
3					C_{max}/D_{min}	None				7
4[1]					***D_{max}***	**None**				**7**
5					D_{max}	None	OpenSEES	CUREE		7
6					D_{max}	None		Pinching4		7
7				Gypsum	D_{max}	None	SAWS	CUREE		7
8				Stucco	D_{max}	None				7
9				None	D_{max}	None			3%	7
10					D_{max}	None			5%	7
11			2.56:1 (3)		B_{min}	None			1%	8
12					B_{max}/C_{min}	None				8
13					C_{max}/D_{min}	None				8
14[1]					***D_{max}***	**None**				**8**
15					D_{max}	None	OpenSEES	CUREE		8
16					D_{max}	None		Pinching4		8
17				Gypsum	Dmax	None	SAWS	CUREE		8
18				Stucco	Dmax	None				8
19				None	D_{max}	None			3%	8
20					D_{max}	None			5%	8

1. Baseline Performance Groups for shear walls with low (4) and high (14) aspect ratios for this study.

Table 9 (cont.) – Wood light-frame performance group matrix

Performance Group	System Performance Characteristics				System Design Requirements		System Analysis Methods			# of Archetypes
	Test Protocol	Test Program	Aspect Ratio (Edge Nail Spacing (inches))	Finishes	SDC	Soft-Story	Analysis Software	Hysteretic Model	Rayleigh Damping	
21	CUREE	CUREE-Caltech Woodframe Project	0.5 and 1.23:1 (6)	None	D_{max}	1st Floor (70%)	SAWS	CUREE	1%	4
22			2.56:1 (3)		D_{max}	1st Floor (70%				4
23		CASHEW	1.23:1 (6)		D_{max}	None				7
24			2.56:1 (3)		D_{max}	None				8
25		APA-The Engineered Wood Association	1:1 (4)		D_{max}	None				8
26	SPD		1:1 (4)		D_{max}	None				8
27			2:1 (4)		D_{max}	None				8
28			4:1 (4)		D_{max}	None				8
29	CUREE	CUREE-Caltech Woodframe Project	0.5 and 1.23:1 (6)		D_{max}	1st Floor (60%)				4
30			2.56:1 (3)		D_{max}	1st Floor (60%				4

1. Baseline Performance Groups for shear walls with low (4) and high (14) aspect ratios for this study.

The aspect ratio is a component of two FEMA P695 key components because the aspect ratio has an effect on the system response (generally higher aspect ratio walls have an increased displacement capacity) and system design requirements (high aspect ratio walls require a reduction in shear capacity).

The shear walls noted as having a high aspect ratio in Table 9 are walls that have an aspect ratio greater than 2:1. The 2:1 aspect ratio walls (Performance Group 27) are considered low aspect ratio walls because they do not require a reduction in shear capacity. Because of observations on the cyclic envelope behavior (see *Shear Wall Characterization* section) 2:1 aspect ratio walls from the same test program form one performance group.

Expanding upon the five residential building configurations considered in the FEMA P695 example application, eight common residential building configurations were developed for this test program (Table 10). General floor plans for each of the building configurations of this study are provided in Appendix B. The tributary weights provided in Table 10 are from dead loads (Appendix C) for typical residential construction materials (ASCE 7 Table C3-1) and are used in the seismic loading calculations provided in Appendix C. Index archetypes where the design required shear wall lengths were greater than the building dimensions were not considered in the analysis.

Table 10 – Archetype configurations for wood light-frame systems

Archetype Configuration	Floors	Description	Floor Level	Tributary Floor Weight used for Shear Wall Design (kips)
1	1	Single-family	1	13.72
2	1	Single-family	1	23.52
3	2	Single-family	1	21.32
			2	18.08
4	2	Townhouse	1	7.80
			2	6.18
5	3	Townhouse	1	11.45
			2	11.06
			3	10.15
6	3	Multi-family (Apartment)	1	23.61
			2	23.61
			3	12.33
7	4	Multi-family (Apartment)	1	24.16
			2	24.16
			3	24.16
			4	12.60
8	5	Multi-family (Apartment)	1	24.16
			2	24.16
			3	24.16
			4	24.16
			5	12.60

Shear Wall Characterization

This section discusses the curve fitting procedures developed by the NAHB Research Center and Forest Products Laboratory (FPL) to characterize shear wall responses for the CUREE hysteretic model. Shear wall test results and numerical fit comparisons (hysteresis and dissipated energy) are provided in Appendix D. Appendices E and F provide CUREE parameters for shear wall test results as determined by the NAHB Research Center and FPL, respectively.

NAHB Research Center Curve Fitting Procedure

The CUREE parameters were determined through regression analysis and data filtering performed on the force-displacement results for both positive and negative drift excursions. Therefore two sets of parameters were determined from each cyclic shear wall test.

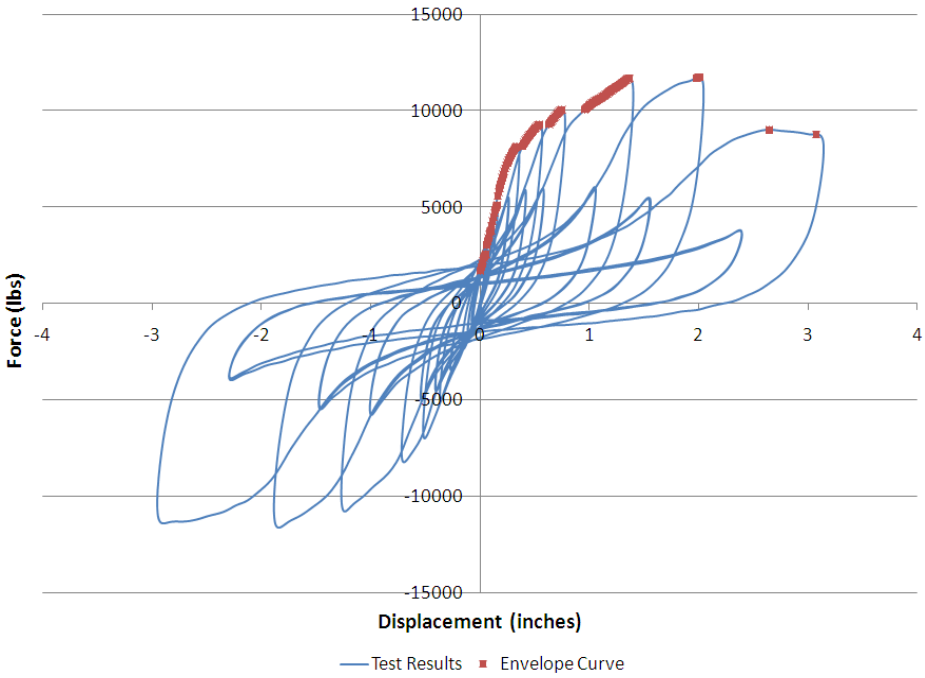

Figure 7 – Cyclic force-displacement response and backbone curve, CUREE-Caltech Specimen 4a-n

Parameters for modeling the backbone response of the shear wall up to δ_u (taken directly from measured shear wall response) were derived through a least square regression on the positive or negative drift envelope curve using the following equation:

$$S = \sum_{i=1}^{n} \left(F_i - F_{test,i}\right)^2 \qquad \textbf{Equation (1)}$$

where $F_{test,i}$ is the test force at δ_i, n is the number of experimental data points forming the backbone curve up to δ_u and F_i is the force at test displacement (δ_i) determined following procedures of the Foschi curve (after [13]):

$$F_i = sgn(\delta_i) * (F_0 + r_1 K_0 |\delta_i|) * \left[1 - e^{-\left(\frac{K_0|\delta_i|}{F_0}\right)}\right] \qquad \textbf{Equation (2)}$$

where the parameters K_0, F_0, and r_1 are defined in Table 6. The backbone curve parameters are determined when S in Equation (1) is minimized through a parametric analysis on experimental backbone curve data points. Figure 8 provides an example comparison plot of the test results envelope curve and the CUREE backbone curve. The remaining backbone curve parameter (r_2) is determined based on displacements and strengths beyond δ_u using Microsoft Excel's (2007) slope function.

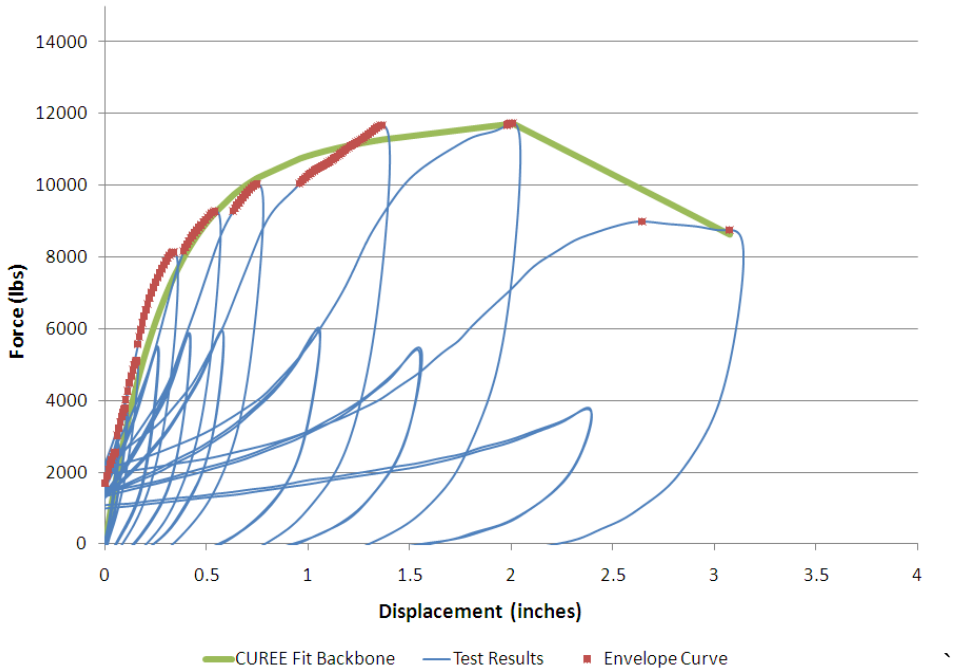

Figure 8 – Comparison of test data and numerical backbone curves, CUREE-Caltech Specimen 4a-n

The unloading stiffness ratio is limited to a minimum of 1.0 in the SAWS nonlinear software. It was observed that this parameter can often be less than 1.0, but because of the limit set by the software a consistent factor of 1.0 was used for r_3.

The remaining parameters of the CUREE model define the cyclic behavior of the model. The first of these, r_4, is a factor of K_0 and is the general slope of the force-displacement response at the y-intercept (pinching stiffness). To determine this parameter, the slope between continuous displacements and forces were calculated for displacements within the range of ±0.25 inches. This slope initially is equal to K_0, but reduces to a stabilized slope at high displacements. This stiffness is recorded and the factor, r_4, is the ratio of the determined slope to the initial stiffness. The y-intercept force was determined by recording the forces in the displacement range of ±0.25 inches, calculating the mean, and assigning this force to F_i.

The remaining CUREE parameters (α and β) were obtained from modeling by Isoda *et al.* [19] of wood shear wall systems. Isoda used α and β values of 0.76 and 1.09 respectively for wood shear walls with single-sided vertical OSB sheathing.

Figure 9 and Figure 10 provide a CUREE fit model versus test results for the same test data presented in Figure 7. Close resemblance of the CUREE model to the experimental hysteretic test results is shown in Figure 9. For this shear wall the dissipated energy for both models, up to the excursion associated with maximum displacement, remains within a 15% error. At the excursion associated with the capping force in the positive drift an error of approximately 7.3% exists. As mentioned previously, because test data is cyclic, the two sets of parameters were determined for both positive (-p) and negative (-n) drifts and forces.

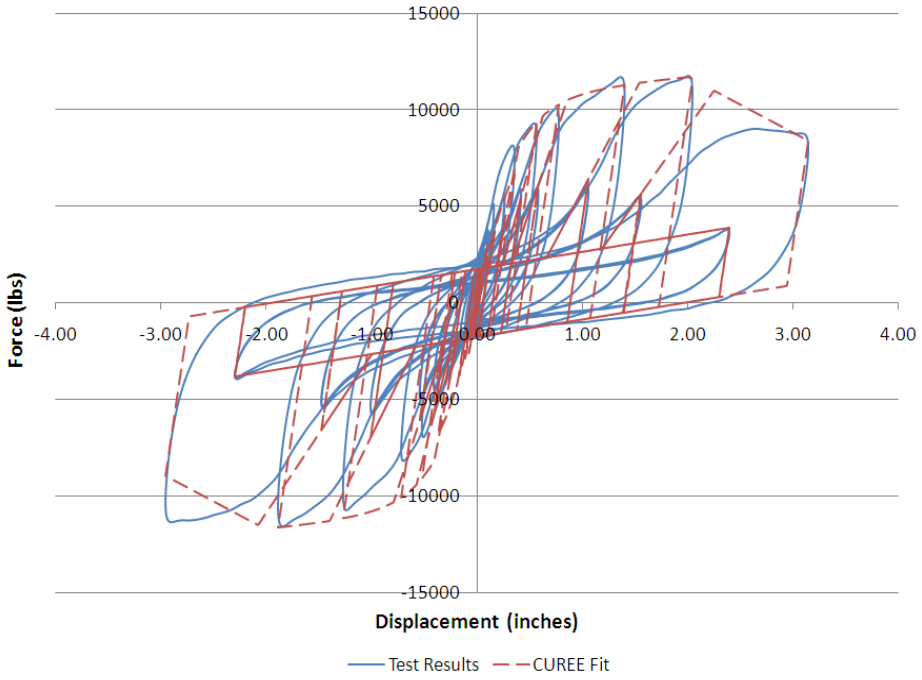

Figure 9 – Hysteretic response for test results and CUREE Fit, , CUREE-Caltech Specimen 4a-n

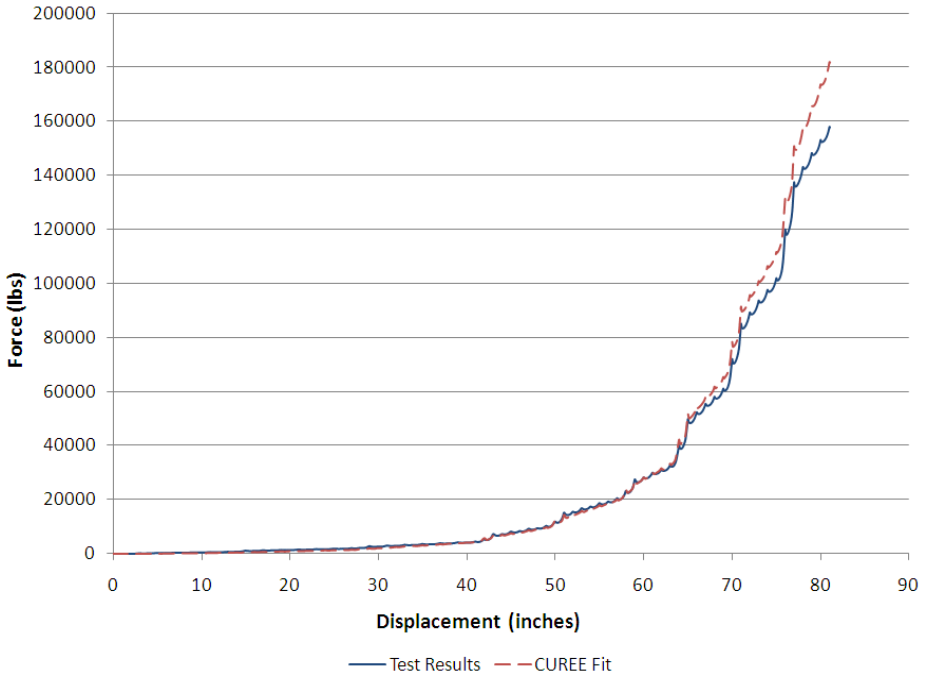

Figure 10 – Dissipated energy for test results and CUREE Fit, , CUREE-Caltech Specimen 4a-n

The fitting of the CUREE hysteretic model to the experimental test results was simplified through programming methods. A Microsoft Excel (2007) VBA application was developed for data analysis and the nonlinear dynamic analysis software SAPWood [20] was utilized for determining the CUREE model response under the test displacements. Parameters for the test

results from the CUREE-Caltech Project were determined using the NAHB Research Center curve fitting technique. The parameters for each wall specimen are provided in Appendix E.

FPL Curve Fitting

The CUREE parameters from the APA tests were provided by Doug Rammer [21] of FPL. Figure 11 provides a demonstration of the curve fitting strategy used by FPL to obtain the backbone, pinching, and unloading CUREE parameters; this method is similar to the NAHB Research Center curve fitting procedure described in the previous section, although the measured response in both the positive and negative drifts is used concurrently to calculate the average CUREE parameters. Figure 12 and Figure 13 provide a comparison of the hysteretic and dissipated energy for the fit model to test data, Appendix D provides comparison plots and Appendix F provides CUREE parameters for the shear wall test data from APA testing for this study.

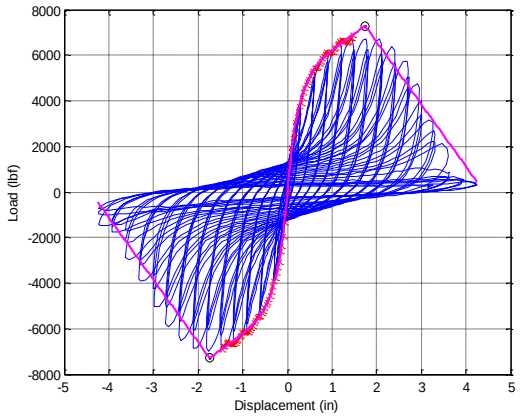

(a) – Data used for determining CUREE backbone (highlighted)

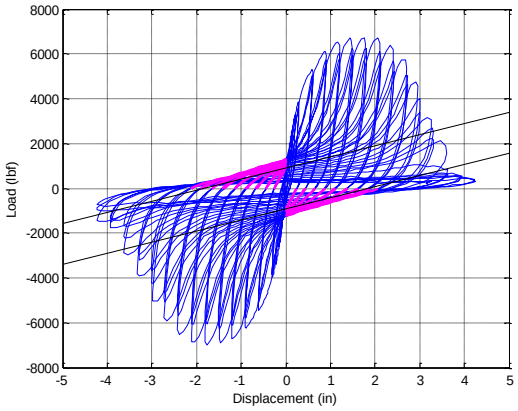

(b) – Data (highlighted) used for determining pinching parameters

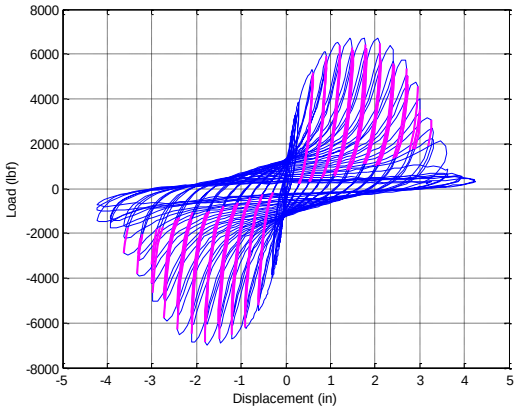

(c) - Data (highlighted) used for determining unloading parameter

Figure 11 – Demonstration of FPL's curve fitting procedure [21]

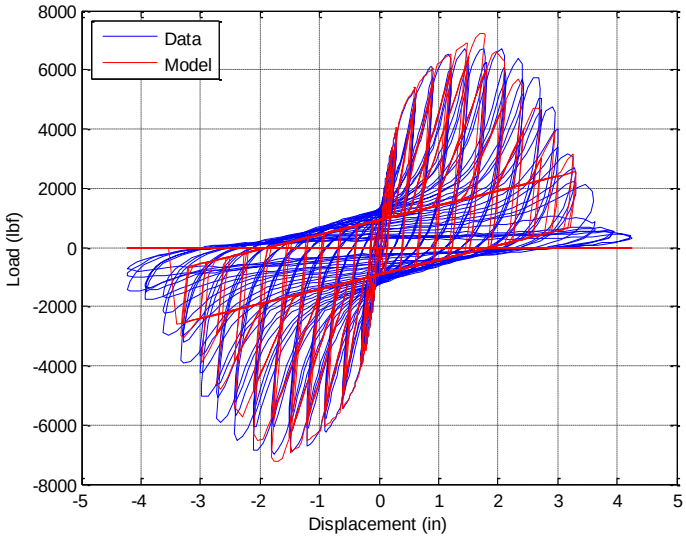

Figure 12 – Hysteretic response for test results (Data) and CUREE Fit (Model), APA T2003-22 Specimen 1 [21]

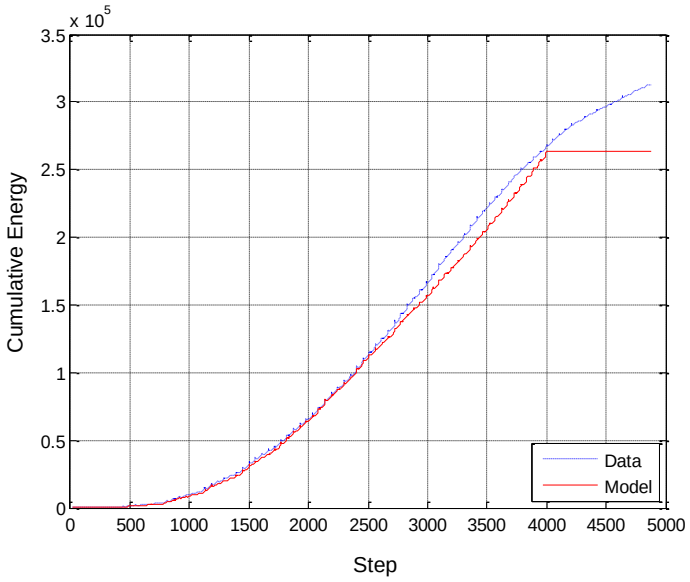

Figure 13 – Dissipated energy for test results (Data) and CUREE Fit (Model), APA T2003-22 Specimen 1 [21]

Curve Fitting Results Summary

A total of twelve eight foot tall wood OSB shear wall models were developed based on wall detailing and testing procedures (Table 11 and Figure 14). CUREE parameters provided in Table 11 are the median values for each shear wall configuration. Strength and stiffness values are per linear foot of shear wall. Figure 14 plots the shear wall envelope curves for OSB sheathed shear walls normalized to the nominal (un-factored) SDPWS wall capacities. Figure

15 plots the shear wall envelope curves for OSB sheathed shear walls with gypsum or stucco finishes normalized to the nominal (un-factored) SDPWS wall capacities.

The CASHEW models were constructed according to the details of the walls tested for the CUREE-Caltech test program. The force-displacement responses for the individual connections were characterized by the CUREE hysteretic model. As part of the NEESWood Benchmark Test, the mean parameters for each connection configuration (Table 2) were determined through regression (Table 11). The highlighted parameters (All Tests in Table 11) are used in this study with CASHEW nonlinear modeling software to characterize the shear wall hysteretic response (SWM-7 and SWM-8 in Table 12 and Figure 14.

Table 11 – Mean fastener parameters for 7/16-inch OSB, 8d common nails, CUREE hysteretic model, after [6]

Configuration	K_0 (lbs/in)	r_1	r_2	r_3	r_4	F_0 (lbs)	F_1 (lbs)	Δ_u (in)	α	β
1	8,144.3	0.025	-0.027	1.028	0.005	242.4	35.0	0.470	0.77	1.24
2	6,063.8	0.026	-0.047	1.021	0.010	238.1	34.2	0.559	0.67	1.31
3	6,659.5	0.026	-0.026	1.021	0.004	203.2	25.7	0.448	0.75	1.30
4	6,039.9	0.026	-0.053	1.010	0.013	228.9	32.8	0.540	0.70	1.29
All Tests	6,643.8	0.026	-0.039	1.020	0.008	228.3	32.0	0.508	0.72	1.29

Table 12 – CUREE model parameters from test data for single-sided shear walls

Performance Group (see Table 9)	Shear Wall Model (SWM)	Test Protocol, Aspect Ratio, Data Source or Finish	Number of Wall Results used for Analysis	Nominal SDPWS Strength Capacity (lbs/ft)	CUREE Parameters							
					F_0 (kips/ft)	F_i (kips/ft)	K_0 (kips/in/ft)	r_1	r_2	r_3	r_4	δ_u (inch)
1-5, 7, 9-10, 21, and 29	1	CUREE, Low, CUREE-Caltech	4	730	0.62	0.10	2.44	0.03	-0.05	1.00	0.02	1.96
11-15, 17, 19-20, 22, and 30	2	CUREE, High, CUREE-Caltech	4	1370	1.16	0.21	3.47	0.04	-0.04	1.00	0.03	3.52
26	3	SPD, Low, APA	10	1260	0.88	0.15	4.44	0.03	-0.11	1.01	0.04	1.18
27	4	SPD, Mid, APA	6	1260	0.77	0.14	3.23	0.05	-0.14	1.01	0.04	1.84
28	5	SPD, High, APA	4	1260	0.65	0.13	1.90	0.04	-0.15	1.01	0.03	3.48
25	6	CUREE, Low, APA	6	980	0.65	0.10	3.17	0.04	-0.07	1.01	0.01	2.25
23	7	CUREE, Low, CASHEW	1	730	0.53	0.08	2.10	0.04	-0.03	1.00	0.01	2.26
24	8	CUREE, High, CASHEW	1	1307	1.10	0.15	3.32	0.03	-0.07	1.00	0.01	3.12
7	9	CUREE, Low, OSB and Gypsum	2	250	0.18	0.02	2.07	0.06	-0.02	1.00	0.02	0.57
8	10	CUREE, Low, OSB and Stucco	2	360	0.38	0.04	2.56	0.04	-0.36	1.00	0.02	1.70
18	11	CUREE, High, OSB and Gypsum	2	250	0.17	0.03	1.17	0.03	-0.02	1.00	0.03	2.51
19	12	CUREE, High, OSB and Stucco	2	360	1.14	0.19	3.74	0.05	-0.02	1.00	0.02	3.13

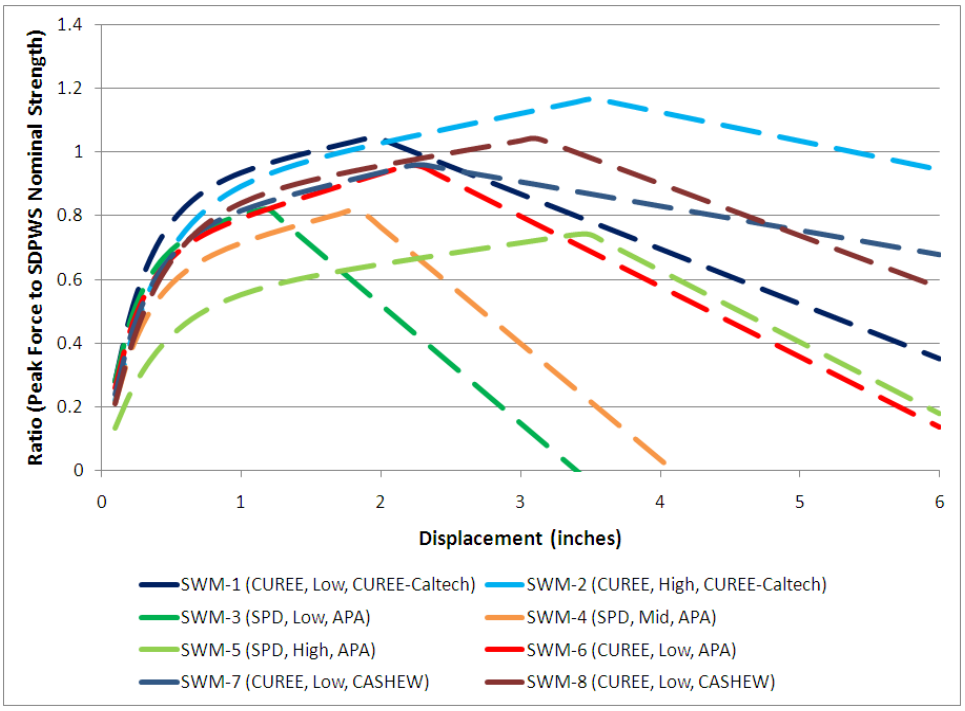

Figure 14 – Normalized numerical backbone curves for OSB sheathed shear walls in parenthesis (test protocol, aspect ratio, data source)

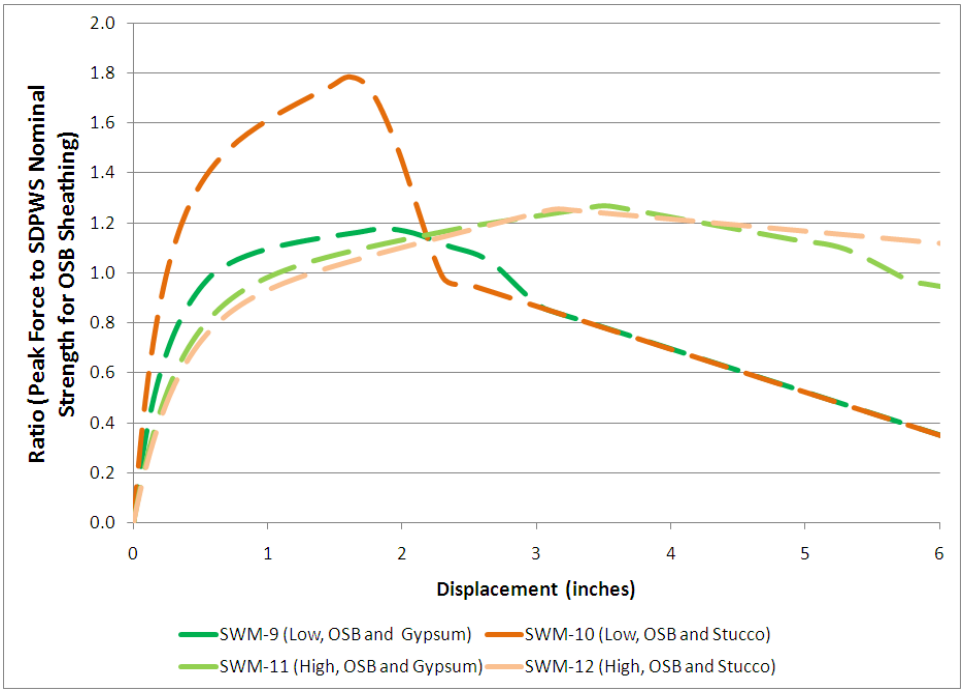

Figure 15 – Normalized numerical backbone curves for OSB sheathed shear walls with finishes in parenthesis (aspect ratio, finish)

Observations on shear wall configurations from Figure 14 demonstrate the effect of aspect ratio, and displacement protocol. Walls with high aspect ratios have the highest displacement capacities (greater than three inches). Walls subjected to the SPD displacement protocol show a reduction in strength relative to walls tested under the CUREE protocol and relative to the SDPWS nominal values.

Validation of Shear Wall Behavior and Modeling Methods

In this section, the results from the CUREE-Caltech Woodframe Project and NEESWood Benchmark Test full-scale house testing are compared to the results from building models constructed in the SAWS software platform (Table 13). Test results for houses without finishes were used in this comparison for both testing programs. The numerical models use the measured experimental floor weights and shear wall behavior as provided in the *Shear Wall Characterization* section of this report. Because the test buildings were subjected to incremental ground motions and only limited repairs were performed after each seismic event, the input ground motion for the SAWS building models considered each of the previous time histories with five seconds between ground motions to allow for free vibration (e.g., Figure 16). This method is consistent with the approach used in validation studies in both testing programs.

Table 13 – Validation of SAWS with results of full-scale building tests

Full Scale Model	Canoga Park Scaled Peak Ground Accel.	Floor Level	Test Results			SAWS Nonlinear Model Results		
			Fundamental Frequency	Peak Displacement (inches)		Fundamental Frequency	Peak Displacement (inches)	
				West Wall	East Wall		West Wall	East Wall
CUREE-Caltech Woodframe Project [12]	0.50g	1	3.96	1.23	1.48	3.72	1.07	0.94
		2		2.27	2.55		3.28	3.16
NEESWood Benchmark Test [6]	0.22g	1	3.06	1.62	0.92	2.74	1.87	1.55
		2		0.79	0.79		0.13	0.28

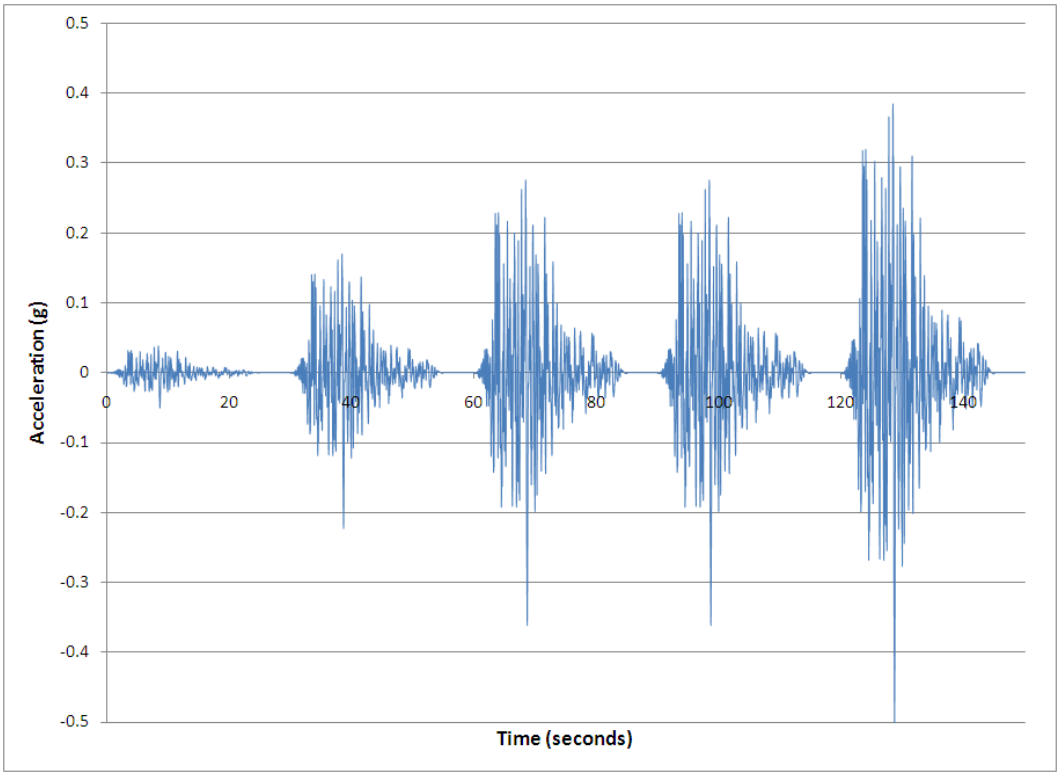

Figure 16 – Repeated Canoga Park ground motion (north-south component) for the CUREE-Caltech Woodframe Project SAWS model

In the elastic range of the structure's response, the SAWS building model demonstrates a good correlation with the results of the CUREE-Caltech Woodframe Project – fundamental frequencies of 3.72 and 3.96, respectively. However when the shear wall response enters the nonlinear range differences in peak displacement are observed between experimental and modeling results. In general, for the CUREE-Caltech SAWS model, displacements in the first floor are less than the measured results whereas displacements in the second floor exceed measured results from the full scale experiment.

Results from the NEESWood Benchmark project SAWS model differ significantly from the test structure results. The fundamental frequency demonstrates that the SAWS model has a slightly longer period (T=1/f) of 0.04 seconds demonstrating that the model is less stiff than the experimental test structure. Displacements in the first floor are greater than the measured results, whereas the displacements in the second floor are much less than the measured results.

Observations on the numerical models versus full scale experiments demonstrate the following trends:

- SAWS numerical models using experimental weights and characterized shear wall responses are less stiff than the test structure. One possible explanation for this result is

that shear wall testing does not consider gravity loads in the lateral shear wall response and these loads can increase the lateral stiffness of the shear wall.

- Maximum measured displacements in the numerical models occur in the same shear wall lines and floor level as the test structure and on average are 40% greater than measured test results.

Archetype Shear Wall Designs

Shear wall design lengths for index archetypes in each performance group were obtained using the story shear forces (V_x) provided in Appendix C and SDPWS nominal unit shear capacities (Table 14, also see Table 3 for shear wall configurations). Shear wall design lengths for each shear wall configuration at SDC D_{max} is provided in Table 15. Appendix G provides shear wall design lengths for lower SDCs.

Table 14 – LRFD factored design unit shear capacities for WSP shear wall systems

LRFD Design Seismic Unit Shear Capacity by Shear Wall Model (lb/ft)					
SWM-1	**SWM-2**	**SWM-3**	**SWM-4**	**SWM-5**	**SWM-6**
417	783	720	720	720	560

Table 15 – Shear wall design lengths for index archetypes with provided shear wall models at SDC D_{max}

Archetype Configuration	Floor	Shear Wall Design Length (feet)					
		Shear Wall Model					
		SWM-1	SWM-2	SWM-3	SWM-4	SWM-5	SWM-6
1	1	6.50	3.13	8.00	4.00	4.00	8.00
2	1	9.33	6.25	8.00	8.00	6.00	8.00
3	1	14.66	9.38	9.33	12.00	10.00	12.00
	2	9.33	6.25	8.00	8.00	6.00	8.00
4	1	6.50	3.13	8.00	4.00	4.00	8.00
	2	6.50	3.13	8.00	4.00	2.00	8.00
5	1	13.33	9.38	8.00	8.00	8.00	9.33
	2	10.66	6.25	8.00	8.00	6.00	8.00
	3	6.50	3.13	8.00	4.00	4.00	8.00
6	1	22.66	12.50	13.33	16.00	14.00	17.33
	2	17.33	9.38	10.66	12.00	10.00	13.33
	3	8.00	6.25	8.00	8.00	6.00	8.00
7	1	31.99	18.75	18.66	20.00	20.00	23.99
	2	27.99	15.63	17.33	16.00	16.00	21.33
	3	20.00	12.50	12.00	12.00	12.00	16.00
	4	9.33	6.25	8.00	8.00	6.00	8.00
8	1	41.32	21.88	23.99	24.00	24.00	30.66
	2	37.32	21.88	22.66	24.00	22.00	27.99
	3	31.99	18.75	18.66	20.00	18.00	23.99
	4	21.33	12.50	13.33	16.00	14.00	16.00
	5	9.33	6.25	8.00	8.00	6.00	8.00

Collapse Performance Evaluation

This section provides collapse performance evaluation results for the thirty performance groups considered in this study. First, the analytical tools used in this study are validated by comparing simulation results with the FEMA P695 example application. Second, an evaluation of collapse performance for systems with differences in system design requirements, system performance characteristics, and system analysis methods is completed.

Visual Basic Application Procedure Qualification

A Microsoft Excel (2007) Visual Basic Application (VBA) program was developed to execute the computer simulations and analyze results. The program's functionality includes:

(1) specifying parameters for a nonlinear SAWS building model,
(2) subjecting the building model to 44 individual ground motions,
(3) for each ground motion, incrementally adjusting acceleration intensity,
(4) determining intensity that causes simulated collapse at 22 of the 44 ground motions,
(5) subjecting the SAWS building model to quasi-static pushover, and
(6) from dynamic and quasi-static results, determining key FEMA P695 parameters (i.e., $\hat{S}_{CT}$, Ω, and μ_T).

The program was validated using the results of the FEMA P695 example application. Twelve of the sixteen FEMA P695 wood light-frame index archetypes (commercial and residential) were selected for re-simulation as part of the validation process. Table 16 provides the list of the archetypes used for comparison and the associated design and collapse characteristics. Figure 17 provides a comparison of the results obtained using the Research Center's VBA application with the results of the FEMA P695 selected example archetypes. The fundamental period and results from the quasi-static pushover analysis are shown to be approximately equal. The nonlinear dynamic analysis results from the NAHB Research Center's VBA application demonstrate collapse at a lower median spectral acceleration, by 12% on average.

Table 16 – Summary of archetype models from FEMA P695 Wood Light-Frame Systems Example Application used for validation of the NAHB Research Center's VBA application

Archetype	Number of Stories	Building Configuration	Wall Aspect Ratio	Seismic Design Category (SDC)	FEMA P695 Period	NAHB Research Center Period	FEMA P695 Collapse Spectral Acc.	NAHB Research Collapse Spectral Acc.
1	1	Commercial	Low	D_{max}	0.40	0.41	2.01	1.95
2	1	1&2 Family	High	D_{max}	0.29	0.29	2.90	2.57
3	1	Commercial	High	D_{min}	0.50	0.50	1.71	1.44
4	1	1&2 Family	High	D_{min}	0.41	0.41	2.09	1.95
5	2	Commercial	Low	D_{max}	0.46	0.48	2.23	2.22
6	2	1&2 Family	High	D_{max}	0.37	0.37	3.20	2.84
7	2	Commercial	High	D_{min}	0.61	0.61	1.95	1.71
8	2	1&2 Family	High	D_{min}	0.62	0.62	1.95	1.67
11	3	Commercial	Low	D_{min}	0.93	0.96	1.98	1.61
12	3	Multi-Family	High	D_{min}	0.69	0.69	2.34	2.10
14	4	Multi-Family	High	D_{min}	0.81	0.81	2.09	1.95
16	5	Multi-Family	High	D_{min}	0.91	0.93	1.92	1.75

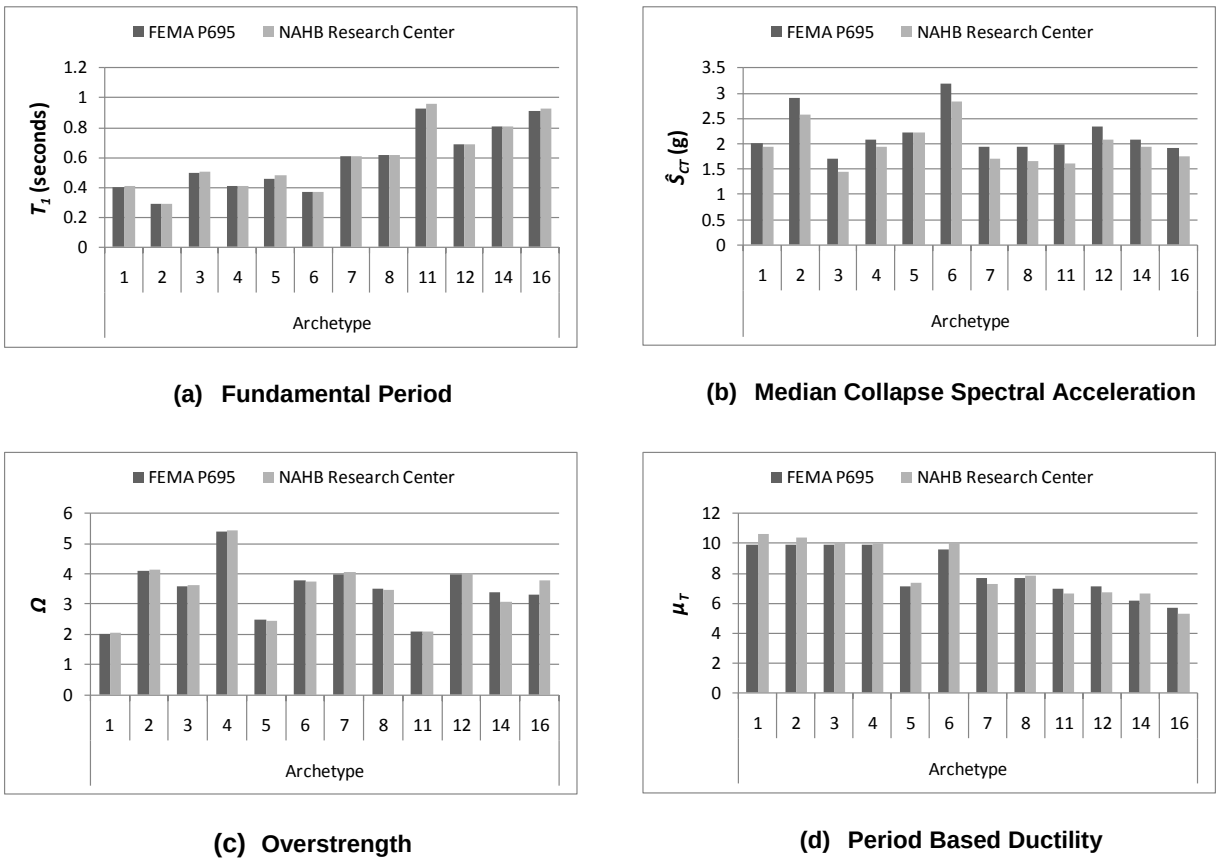

(a) Fundamental Period

(b) Median Collapse Spectral Acceleration

(c) Overstrength

(d) Period Based Ductility

Figure 17 – Comparison of wood light-frame example analysis applications

Because similar shear wall parameters, seismic weights, and modeling software are used in the analysis, variations in collapse performance between the light-frame wood example application of FEMA P695 and results from the NAHB Research Center VBA application are likely due to factoring of dynamic and quasi-static results. Discussing the example applications FEMA P695 states:

> "These examples were completed in parallel with the development of the Methodology. As such, they are consistent with the procedures contained herein, but are not necessarily in complete compliance with every requirement."

Also important to note is that the calculated $ACMR$ values from the VBA application collapse spectral accelerations do not change the Pass/Fail results of the wood light-frame example application of FEMA P695. Therefore, the VBA application module developed by the NAHB Research Center is considered validated.

Archetype Performance Group FEMA P695 Analysis

Table 17 provides the collapse performance results for the thirty performance groups (see Table 9). The groups are categorized in the study based on one or more of the FEMA P695 key

elements. A 7% drift ratio in any floor of the structure is set as the collapse drift ratio. Results for individual archetypes within the performance group are provided in Appendix H.

Because the goal of this study is to understand the influence of system design, performance, and analysis characteristics, results were compared to two 'baseline' performance groups (performance groups 4 and 14) designed for SDC D_{max} and with shear wall behavior most representative of WSP shear wall system response. Therefore, the performance evaluations conducted in this study are relative to the performance of the two 'baseline' performance groups. Because WSP shear wall systems have a history of maintaining collapse prevention under MCE ground motions, this report is not intended to draw conclusions with regard to the absolute magnitude of the individual SPFs.

The FEMA P695 collapse performance parameters listed in Table 17 are the average values for each performance group. The parameters, Ω, $\hat{S}_{CT}$, and μ_T are determined from the nonlinear static and dynamic analysis. The spectral shape factor (SSF) for index archetypes is dependent upon the SDC, fundamental period, and μ_T, FEMA P695 Table 7 provides the values of the spectral shape factors which can be interpolated. The adjusted collapse margin ratio ($ACMR$) for index archetypes is calculated by:

$$ACMR = \frac{\hat{S}_{CT}}{S_{MT}} SSF \qquad \textbf{Equation (3)}$$

where S_{MT} is the spectral acceleration at the MCE provided in FEMA P695. In the following sections, performance group average $ACMR$ is used as the primary parameter for making relative comparisons. Discussion of the results follows in several sections organized by a specific evaluation objective.

Application of the FEMA P695 methodology in this study intentionally varied inputs from those inputs used in the FEMA P695 application of the wood light-frame example. This approach was used to meet project objectives that included documenting the sensitivity of the FEMA P695 methodology on predicted collapse performance of WSP systems to various modeling, design, performance, and quality inputs. The results of this study are not intended to quantify SPFs for wood-light frame WSP shear wall systems or make recommendations thereto, but rather to further understanding of the various outcomes of application of the FEMA P695 methodology and provide discussions that highlight the relative changes in average $ACMR$ that can result from application of the methodology.

Table 17 – Collapse performance results by performance group

Performance Group	Shear Wall Model	Evaluation Variable	Evaluation Variable of FEMA P695 Key Element			Average FEMA P695 Analysis Parameters				
			System Design Requirements	System Performance Characteristics	System Analysis Methods	Ω	μ_T	$\hat{S}_{CT}$	SSF	$ACMR$
1	SWM-1	SDC B_{min}	x			1.86	9.36	0.82	1.15	3.84
2		SDC B_{max} /C_{min}	x			1.47	10.90	0.98	1.16	2.32
3		SDC C_{max} /D_{min}	x			1.84	10.35	1.13	1.15	1.74
4 (baseline)		**SDC D_{max}**	**x**			2.03	10.16	1.56	1.33	1.39
5		Nonlinear Analysis Software			x	2.02	8.66	1.74	1.33	1.54
6		Hysteretic model			x	2.01	8.58	1.51	1.33	1.33
7	SWM-9	Finish (Gypsum)	x	x		2.56	12.07	1.66	1.33	1.47
8	SWM-10	Finish (Stucco)	x	x		3.50	7.00	1.73	1.31	1.51
9	SWM-1	Rayleigh Damping (3%)			x	2.03	10.19	1.75	1.33	1.55
10		Rayleigh Damping (5%)			x	2.03	10.18	1.92	1.33	1.70
11	SWM-2	SDC B_{min}	x			2.06	11.91	1.09	1.14	5.30
12		SDC B_{max} /C_{min}	x			1.87	12.19	1.32	1.15	3.20
13		SDC C_{max} /D_{min}	x			2.02	12.14	1.52	1.14	2.38
14 (baseline)		**SDC D_{max}**	**x**			2.35	11.23	2.05	1.33	1.87
15		Nonlinear Analysis software			x	2.37	9.18	2.10	1.32	1.86
16		Hysteretic model			x	2.29	9.28	2.05	1.32	1.80

Table 17 (cont.) – Collapse performance results by performance group

Performance Group	Shear Wall Model	Evaluation Variable	Evaluation Variable of FEMA P695 Key Element			Average FEMA P695 Analysis Parameters				
			System Design Requirements	System Performance Characteristics	System Analysis Methods	Ω	μ_T	$\hat{S}_{CT}$	SSF	$ACMR$
17	SWM-11	Finish (Gypsum)	X	x		2.68	12.11	2.18	1.33	1.93
18	SWM-12	Finish (Stucco)	x	x		2.53	14.88	2.09	1.33	1.86
19	SWM-2	Rayleigh Damping (3%)			x	2.35	11.31	2.36	1.33	2.09
20		Rayleigh Damping (5%)			x	2.35	11.52	2.59	1.33	2.29
21	SWM-1	1st Floor Soft-Story (70%)	x			2.01	8.01	1.43	1.32	1.26
22	SWM-2	1st Floor Soft-Story (70%)	x			2.49	10.03	1.96	1.33	1.74
23	SWM-7	Wall modeling		x	x	2.35	7.76	1.53	1.32	1.35
24	SWM-8	Wall modeling		x	x	3.47	8.47	2.22	1.32	1.95
25	SWM-6	Edge nailing	x	x		1.84	9.23	1.62	1.33	1.44
26	SWM-4	Testing Protocol		x		2.24	5.54	1.01	1.27	0.86
27	SWM-5	Testing Protocol		x		1.90	6.39	1.01	1.29	0.87
28	SWM-6	Testing Protocol		x		1.48	7.67	1.41	1.32	1.24
29	SWM-1	1st Floor Soft-Story (60%)	x			2.01	8.03	1.42	1.32	1.25
30	SWM-2	1st Floor Soft-Story (60%)	x			2.49	10.37	1.92	1.33	1.71

System Design Requirements – Seismic Design Category

Using results of performance groups 1-4 and 11-14, the effects of seismic design categories on collapse performance are discussed. Performance groups 1-4 and 11-14 consider low aspect and high aspect ratio walls, respectively, for the range of seismic design categories: B_{min}, B_{max}/C_{min}, C_{max}/D_{min}, and D_{max}. Figure 18 provides a graphical representation of the average collapse performance results for the eight performance groups. FEMA P695 acceptable $ACMR_{10\%}$ levels for superior, good, and fair quality ratings are provided for reference.

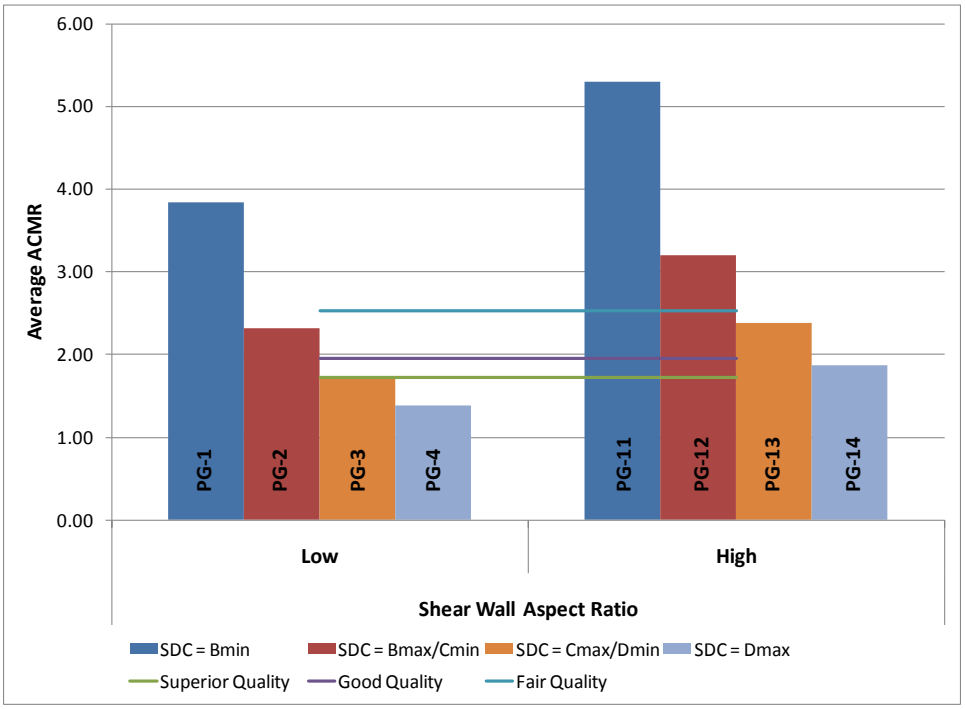

Figure 18 – Comparison plot of average *ACMR* for performance groups with different SDC's

The average ACMRs provided in Figure 18 for performance groups at SDCs C_{max}/D_{min}, and D_{max} are approximately 20% less than similar performance groups in the FEMA P695 example application. Primary differences includes ten foot tall walls and shear wall hysteretic responses developed from connection test data using CASHEW, whereas the performance groups in this analysis had 8 foot tall walls and shear wall hysteretic responses were obtained directly from shear wall test data.

Figure 18 demonstrates that design collapse performance improves in lower SDCs. These results are not necessarily intuitive because the ASCE-7 design procedures are intended to result in comparable performance across different seismic design categories by proportioning the amount of bracing based on the magnitude of spectral accelerations (S_{DS}). Although some of the difference in performance can be attributed to the nonlinear system response, the improved collapse performance in lower SDCs is primarily due to the longer building period for structures in lower SDCs as well as the associated influence of the ground scaling procedures used in FEMA P695. It should be noted that for this comparison, the shear wall amounts were optimized

for all seismic design categories such that the exact shear wall length required by design was used. This optimization was performed to remove any bias associated with "overbuilding" the walls in lower SDCs where the required wall amounts are often less than the amounts specified by the archetype wall configurations. (Note: this optimization was performed only for the SDC influence evaluation and the comparison of archetype configurations study; the specified design wall lengths were used in all other studies discussed for SDC D_{max} below. A sensitivity analysis showed that "overbuilding" is not a significant factor for index archetypes at SDC D_{max} where the required braced wall amounts are close to the amounts that are specified by the archetype wall configurations.)

The influence of the building period on collapse performance between SDCs is demonstrated through an analysis of a single degree of freedom (SDOF) system. This system, represented in Figure 19, idealizes a one-story SAWS shear model used by the VBA application. The system is subjected to input ground motions, causing inertial forces at the mass, which responds according to the spring and damper properties. A series of SAWS models were constructed to develop a collapse response spectrum in accordance with FEMA P695 (red line in Figure 20) for systems with a natural period between 0.1 and 1.0 seconds.

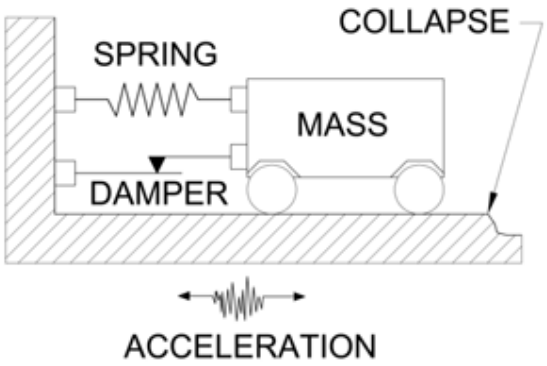

Figure 19 – Single degree of freedom system

The natural period range in Figure 20 envelopes the periods of common light-frame wood systems in the SDCs under consideration. The collapse trend was determined as the median collapse spectral acceleration, in units of (*g*), at the fundamental period of the structural system. Systems designed for higher SDCs (e.g., D_{max}) require higher ground motion accelerations to cause collapse. Figure 20 also plots the maximum considered earthquake response spectra for direct comparison to the FEMA P695 collapse acceleration spectrum at the appropriate building period.

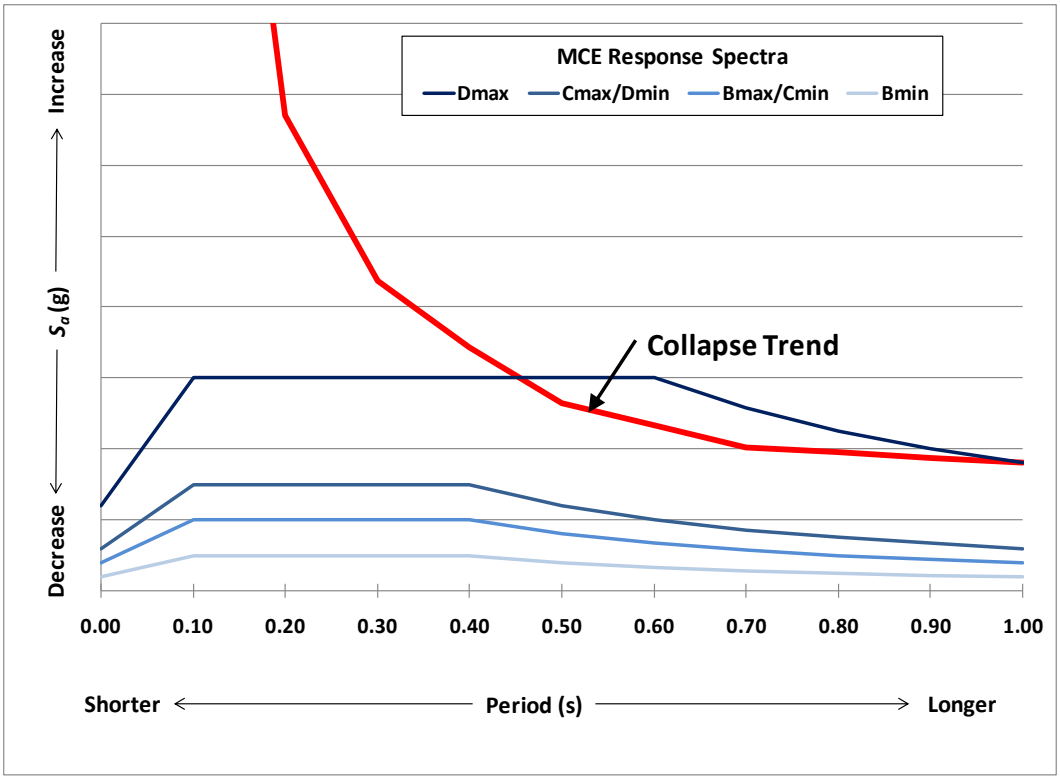

Figure 20 – Collapse response spectra for a single degree of freedom system

The factors for determining $ACMR$ in Equation (3) ($\hat{S}_{CT}$, S_{MT}, and SSF) for a structure in each of the SDCs are provided in Table 18. S_{MT} is provided for structures with a period of ≤0.25 seconds, which is the upper limit period for a one story, eight foot tall light-frame shear wall structure. Also provided is the approximate $\hat{S}_{CT}$ for structures with the approximate periods for WSP systems at the given SDCs. Lastly, the SSF for each SDC is provided – these values were obtained from FEMA P695 Table 7-1 using a period of ≤0.25 seconds and assume a period based ductility (μ_T) greater than eight. The factors were normalized to the SDC D_{max}, and through Equation (3) the expected increase of $ACMR$ was determined. The results of Table 18 show an increase ratio of $ACMR$ from D_{max} to B_{min} by a factor of 2.5.

Table 18 – Collapse analysis to determine influence of SDC for simplified period

SDC	*Approximate Fundamental Period (seconds)*	S_{MT} (T=0.25 seconds)	Ratio to D_{max} S_{MT}	$\hat{S}_{CT}$	Ratio to D_{max} $\hat{S}_{CT}$	SSF	Ratio to D_{max} SSF	*Ratio of ACMR*
D_{max}	0.35	1.50	1.00	1.95	1.00	1.33	1.00	1.00
C_{max}/D_{min}	0.47	0.75	0.50	1.44	0.74	1.14	0.86	1.27
B_{max}/C_{min}	0.58	0.50	0.33	1.20	0.62	1.14	0.86	1.62
B_{min}	0.81	0.25	0.17	0.97	0.50	1.14	0.86	2.52

Although improved collapse performance is expected in lower seismic design categories because of the longer building period, as previously demonstrated, an additional improvement in collapse performance is attributed to the use of a simplified period based on building height only without consideration for the actual building mass and stiffness, both of which vary with the SDCs. The simplified period is determined as follows:

$$T = C_u T_a \qquad \textbf{Equation (4)}$$

where C_u is an upper limit coefficient provided in ASCE 7 Table 12.8.1 and T_a is the approximate fundamental period given by:

$$T_a = C_t h_n^x \qquad \textbf{Equation (5)}$$

Where C_t and x are coefficients provided in ASCE 7 Table 12.8.2 and h_n is the building height.

Table 18 shows that the approximate fundamental period for light-frame wood buildings is longer than the simplified period determined in accordance with Equation (4). This difference increases for lower seismic design categories. Figure 21 provides results of an analysis using the FEMA P695 methodology with ground motion scaling based on the fundamental period (Trend B) as compared to the analysis based on the simplified period (Trend A).

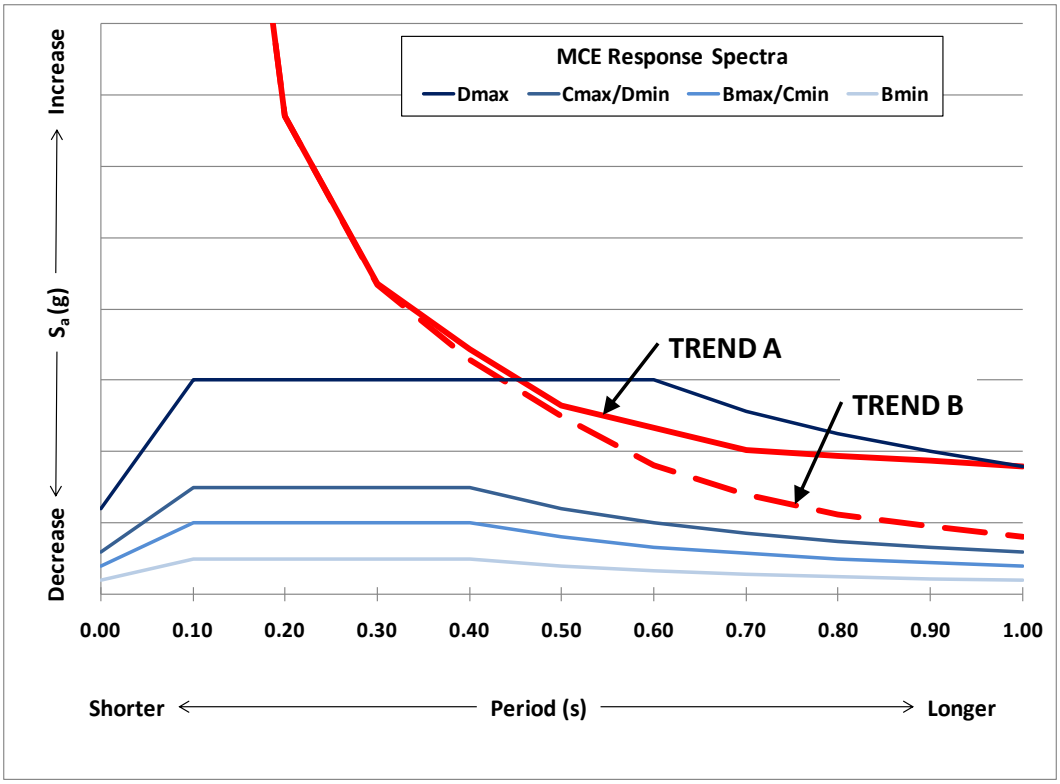

Figure 21 – Collapse response spectra analysis considering calculated period

Table 19 is similar to Table 18 except that $\hat{S}_{CT}$ was calculated using the ground motion normalization factor ($\hat{S}_{NRT}$) based on the calculated fundamental period (Trend B in Figure 43). A reduction in the ratio of $ACMR$ demonstrates that the difference in collapse performance between SDCs will reduce when the fundamental period is used for ground motion scaling in lieu of the simplified period.

Table 19 – Collapse analysis to determine influence of SDC for calculated period

SDC	Approximate Fundamental Period (seconds)	S_{MT} (T=0.25 seconds)	Ratio to D_{max} S_{MT}	$\hat{S}_{CT}$	Ratio to D_{max} $\hat{S}_{CT}$	SSF	Ratio to D_{max} SSF	Ratio of $ACMR$
D_{max}	0.35	1.50	1.00	1.91	1.00	1.33	1.00	1.00
C_{max}/D_{min}	0.47	0.75	0.50	1.37	0.72	1.14	0.86	1.24
B_{max}/C_{min}	0.58	0.50	0.33	0.97	0.51	1.14	0.86	1.33
B_{min}	0.81	0.25	0.17	0.55	0.29	1.14	0.86	1.46

The results of this analysis suggest that for short-period structures such as light-frame wood buildings, the influence of the actual building period on the results of FEMA P695 should be evaluated. The results further indicate that light-frame wood buildings may have better collapse performance characteristics in lower SDCs. It should be noted that longer period structures are

subject to higher displacement – a separate performance consideration. However, it also should be considered that the actual amount of bracing in lower SDCs will be higher than the minimum required by seismic design due to wind design requirements and practical construction and architectural considerations. A separate analysis conducted using the archetypes with specified archetype wall length that included the additional overstrength showed improved $ACMR$ indicating that the benefit gained from 'overbuilding" outweighs the potential reduction in $ACMR$ due to a shorter building period with other variables staying equal.

System Performance Characteristics – Influence of Test Protocols

This study evaluates the influence of the test protocol (CUREE vs. SPD) on the $ACMR$. The results are organized by aspect ratio such that the effect of the aspect ratio does not mask the influence of the test protocol. Figure 22 shows the cyclic backbone curves for test data from several sources. The SPD protocol results in reduction in both peak load and deformation capacity as compared to the CUREE protocol, leading to reductions in the $ACMR$ (Figure 23) of approximately 0.5 units. This demonstrates that the FEMA P695 collapse performance can reduce between 30 to 40% for systems tested under displacement protocols that significantly reduce the strength and displacement capacity of a systems. Therefore, selection of a test protocol has a significant influence on the $ACMR$ and the resulting *R*-factor for light-frame shear walls.

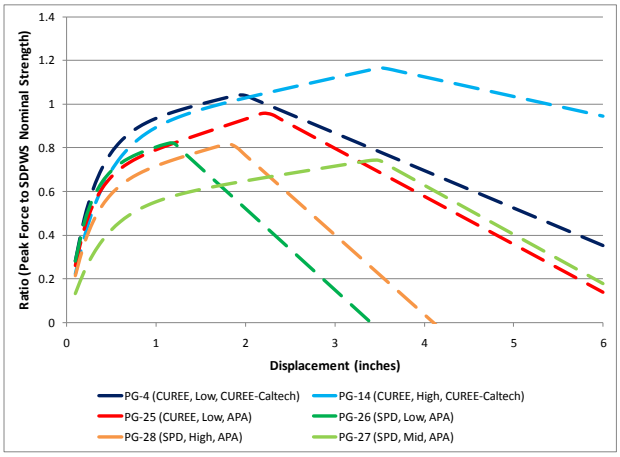

Figure 22 – Low and high aspect ratio shear wall envelope behaviors in parenthesis (test protocol, aspect ratio, data source)

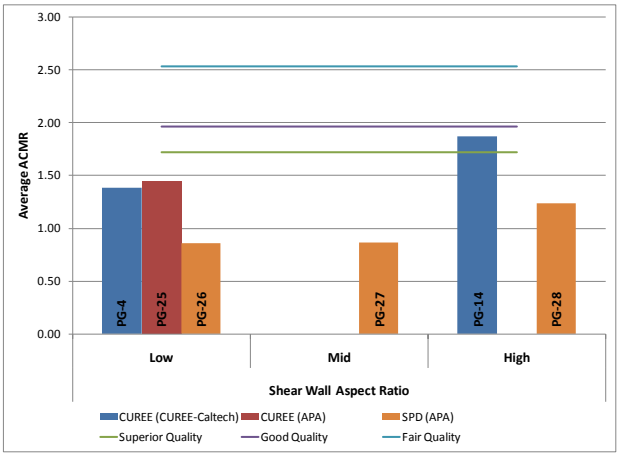

Figure 23 – Comparison plot of average $ACMR$ for performance groups with shear wall configurations tested under different protocols in parenthesis (data source)

System Performance Characteristics – Aspect Ratio

This section compares the results of performance groups that include the low and high aspect ratio shear walls (Performance Groups 4, 14, 26, and 28). Examples of these shear wall model behaviors are provided in Figure 24 and a more detailed discussion on the difference between the models can be found in *System Performance Characteristics* and in Table 3. In this analysis, the high aspect ratio adjustment factor specified in the SDPWS is not included in the calculation of the shear wall design length. Therefore, high and low aspect ratio walls are compared directly

on a performance basis. The collapse performance results for these four groups for SDC D_{max} (Figure 25) demonstrate an improved behavior for high aspect ratio walls.

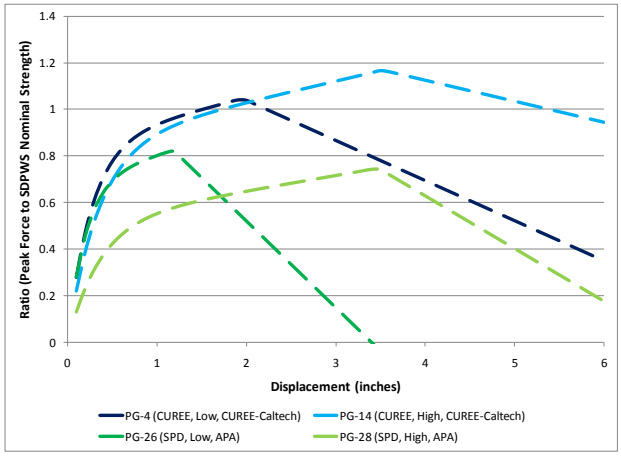

Figure 24 – Low and high aspect ratio shear wall envelope behaviors in parenthesis (test protocol, aspect ratio, data source)

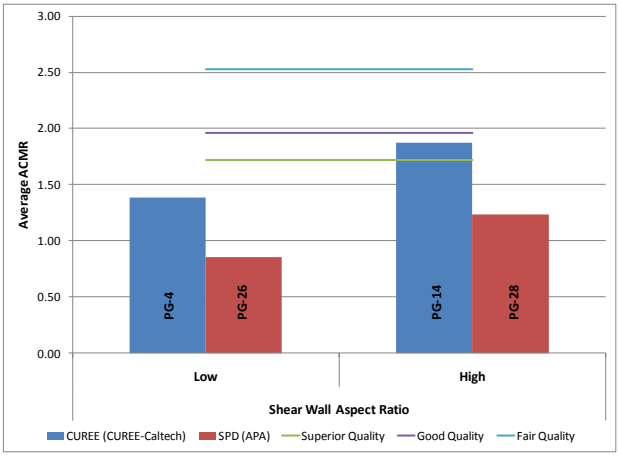

Figure 25 – Comparison plot of average $ACMR$ for performance groups with low and high aspect ratio shear wall configurations (SDC = D_{max}) in parenthesis (data source)

The improvement in the high aspect ratio wall $ACMR$ can be explained by the difference in the displacement capacity between the high aspect ratio and low aspect ratio walls (Figure 24). Independent of the test protocol the displacement at peak load almost doubles from low to high aspect ratio walls.

Figure 25 shows a consistent improvement in collapse performance for high aspect ratio walls for both testing protocols. This improvement is achieved without applying the high aspect ratio strength reductions required by the SDPWS for seismic design of shear walls. Therefore, the applicability of seismic strength reductions on the high aspect ratio segments should be re-evaluated. Considerations regarding potential for higher deformations should be addressed separately through the appropriate drift calculations and limits. The effect of gravity loads on shear wall response and modeling were not considered in this study of WSP aspect ratios.

System Performance Characteristics – Contribution of Finishes

This section evaluates the influence of finishes on the $ACMR$. Similar to the aspect ratio study, gravity loads were not considered in the analysis. Figure 26 shows envelope curves for four performance groups with finishes (PG-7, PG-8, PG-18, and PG-19) and the two baseline performance groups without finishes (PG-4 and PG-14). Only walls tested in accordance with the CUREE cyclic protocol are included in this evaluation. The performance groups evaluated here include both high and low aspect ratio walls. Discussion of the influence on collapse performance of high and low aspect ratio walls is presented separately. The contribution of finishes is not included in the seismic design of the archetypes, as consistent with the SPDWS provisions. As discussed previously, the backbone curves are showing a distinctly different deformation capacity between high and low aspect ratio walls. The finishes have relatively small

influence on the cyclically-tested backbone curve, with some increase in the initial stiffness and peak force, and only a small decrease (if any) on the deformation capacity. One exception is the backbone curve for low aspect ratio walls with stucco that shows a nearly 80 percent increase in peak force, but nearly the same magnitude decrease in deformation capacity. Figure 27 provides $ACMR$ values for all six performance groups.

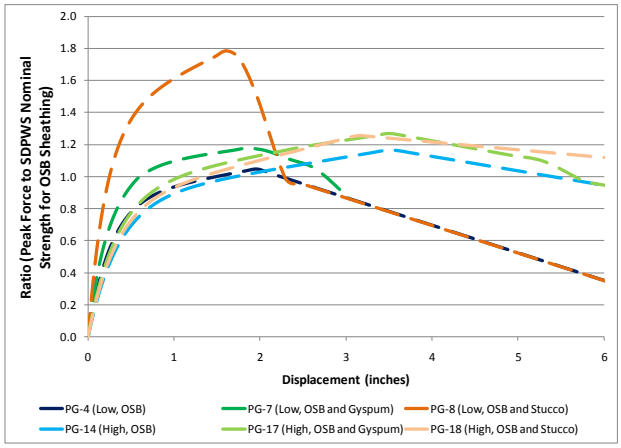

Figure 26 – Low and high aspect ratio shear wall envelope behaviors in parenthesis (aspect ratio, data source)

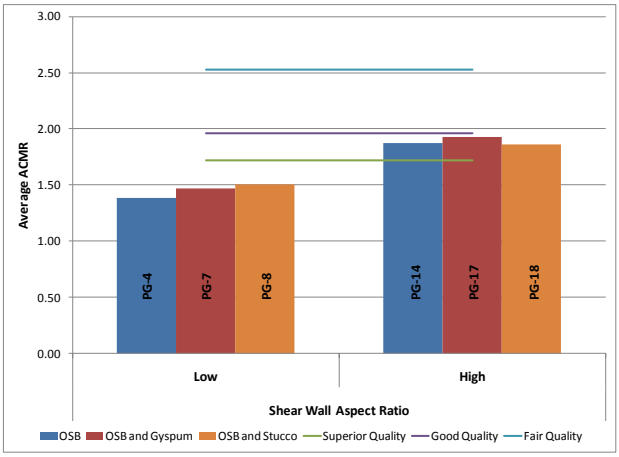

Figure 27 – Comparison plot of average $ACMR$ for performance groups with and without finishes included in building model (SDC = D_{max})

Results indicate a relatively minor influence of finishes (gypsum or stucco) on the $ACMR$. This indicates that the FEMA P695 methodology emphasizes post-capping displacement capacity and that the increase in initial stiffness and the increase in the peak force provided by the finishes are either offset by the changes in the deformation behavior or do not play a significant role in the procedure for determining $ACMR$.

The conclusions drawn from this analysis are evaluated relative to the results from the CUREE-Caltech two-story house tests with (CUREE Test 10.S.5) and without finishes (CUREE Test 9.S.5) for the Rinaldi ground motion with PGA scaled at 0.89g (Table 20). Comparison of peak displacements between the two tests suggest a significant influence of finishes on the performance of the test house at the MCE levels of ground motions with reduction in drift ranging from a factor of 1.8 to 3.4. Similarly, a significant influence of finishes was observed in the CUREE three-story house test with a tuck-under garage and the NEESWood Benchmark Test of a two-story townhouse.

Table 20 – CUREE-Caltech two-story full scale house test results

Direction of Ground Motion	Relative Displacement, inch			
	Without Finishes – CUREE Test 9.S.5 (With Finishes – CUREE Test 10.S.5)			
	East Wall		West Wall	
	1st Floor	2nd Floor	1st Floor	2nd Floor
Positive	1.54 (0.87)	2.59 (1.14)	1.34 (0.59)	2.40 (0.88)
Negative	-2.60 (-1.05)	-4.27 (-1.36)	-2.18 (-0.77)	-3.81 (-1.11)

There are several potential considerations with regard to the apparent negligible influence of finishes on the FEMA P695 collapse performance. On the resistance side of the problem, full-building load distribution and load-sharing effects not captured by the shear wall models as well as the dynamic response effects (e.g., increased damping due to finishes) may not be accurately represented in the dynamic analysis. On the loading side, the FEMA P695 collapse performance is anchored to ground motions scaled to levels significantly higher than the MCE ground motion. At those levels of ground motion, the displacement capacity at large deformations dominates the results of the analysis, and therefore controls the collapse performance. Therefore, FEMA P695 may not be the appropriate tool for analyzing the influence of finishes on building performance for ground motions at the MCE level and below.

System Performance Characteristics – Influence of Archetype Configurations

This study evaluates the influence of the different archetype configurations on the $ACMR$ over a range of seismic design categories. High and low aspect ratio walls are evaluated separately in this study (Figure 28 and Figure 29). A shear wall amount optimization was implemented as discussed in the SDC study to remove the bias associated with "overbuilding" the walls in lower SDCs where the required wall amounts are often less than the amounts specified in the actual archetype wall configurations. The results of the analysis indicate that the $ACMR$ improves with the increase in the number of stories, i.e., results for a single story structure provide the most conservative results with regard to evaluation of the system's *R*-factor. This trend is consistent for all seismic design categories. Similar to the rationale provided in the study of the seismic design categories, an increase in the building period associated with taller structures results in an improved $ACMR$. In actual residential buildings, this trend will not be as definitive because significant "overbuild" is typically present in one and two-story homes relative to minimum shear wall requirements, particularly in seismic design categories lower than D_{max}, due to wind requirements or architectural/building configurations.

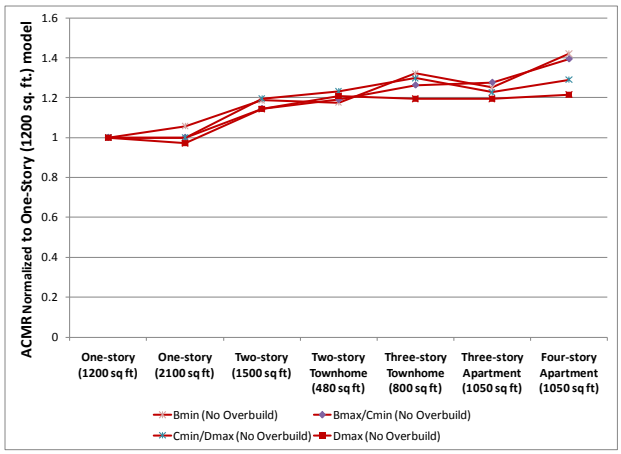

Figure 28 – *ACMR* for low aspect ratio performance groups by archetype configuration (normalized to one-story 1,200 sq ft building)

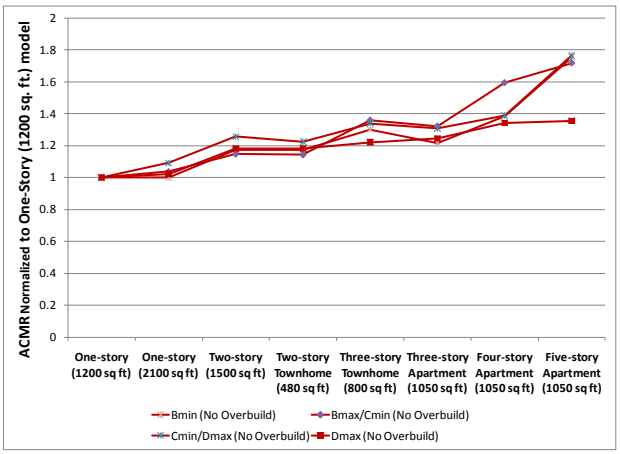

Figure 29 – *ACMR* for high aspect ratio performance groups by archetype configuration (normalized to one-story 1,200 sq ft building)

System Performance Characteristics – Soft-Story Configuration

This study investigates the effect of soft-story configurations on the *ACMR* for low-rise residential construction at SDC D_{max}. The archetypes are designed such that the stiffness of the first story is 70 percent or 60 percent of the stiffness of the story above in accordance with ASCE 7 Table 12.3-2 conditions for soft-story behavior. This condition can occur in some types of residential buildings where the lower stories have more openings than upper stories due to architectural considerations. Buildings with high and low aspect ratio walls are analyzed separately. The results of soft-story analyses are compared to the results of the corresponding baseline configurations (PG-4 and PG-14). Only two- and three-story archetypes were used in the analysis (for four- and five-story archetypes, the length of the upper story shear walls required to achieve a soft-story configuration significantly exceeded the size of the building). Table 21 summarizes shear wall amounts for the baselines and the soft-story configurations. The soft-story configuration was achieved by increasing the shear wall length of the second story from the baseline configuration such that the first story was at 70 or 60 percent of the second story. For three story buildings, the shear wall length of the third story was set to equal the length of the second story.

Table 21 – Shear wall design lengths for soft-story index archetypes

Building Configuration	Floor	Shear Wall Design Length (feet)					
		Low Aspect Ratio			High Aspect Ratio		
		Baseline (PG-4)	1st Floor stiffness 70% of 2nd Floor	1st Floor stiffness 60% of 2nd Floor	Baseline (PG-14)	1st Floor stiffness 70% of 2nd Floor	1st Floor stiffness 60% of 2nd Floor
3	1	14.66	14.66	14.66	9.38	9.38	9.38
	2	9.33	20.94	24.43	6.25	13.40	15.63
4	1	6.50	6.50	6.50	3.13	3.13	3.13
	2	6.50	9.29	10.83	3.13	4.47	5.22
5	1	13.33	13.33	13.33	9.38	9.38	9.38
	2	10.66	19.04	22.22	6.25	13.40	15.63
	3	6.50	19.04	22.22	3.13	13.40	15.63
6	1	22.66	22.66	22.66	12.50	12.50	12.50
	2	17.33	32.37	37.77	9.38	17.86	20.83
	3	8.00	32.37	37.77	6.25	17.86	20.83

Figure 30 summarizes average $ACMR$ results for buildings with low and high aspect ratio walls. Some reduction in $ACMR$ is observed for both aspect ratio configurations relative to the respective baselines. The difference in performance of soft-story configurations is associated with the deformation demand on the first floor. The fundamental response mode shapes (Figure 31 and Figure 32) show an increase in the deformation demand for the bottom story of the soft-story configurations relative to the baseline. Practically undetectable differences are observed between 60 percent and 70 percent conditions. Although these results indicate some influence of soft-story configurations of the ACMR, the difference does not appear sufficient to suggest a reevaluation of the current design provisions for soft-story buildings.

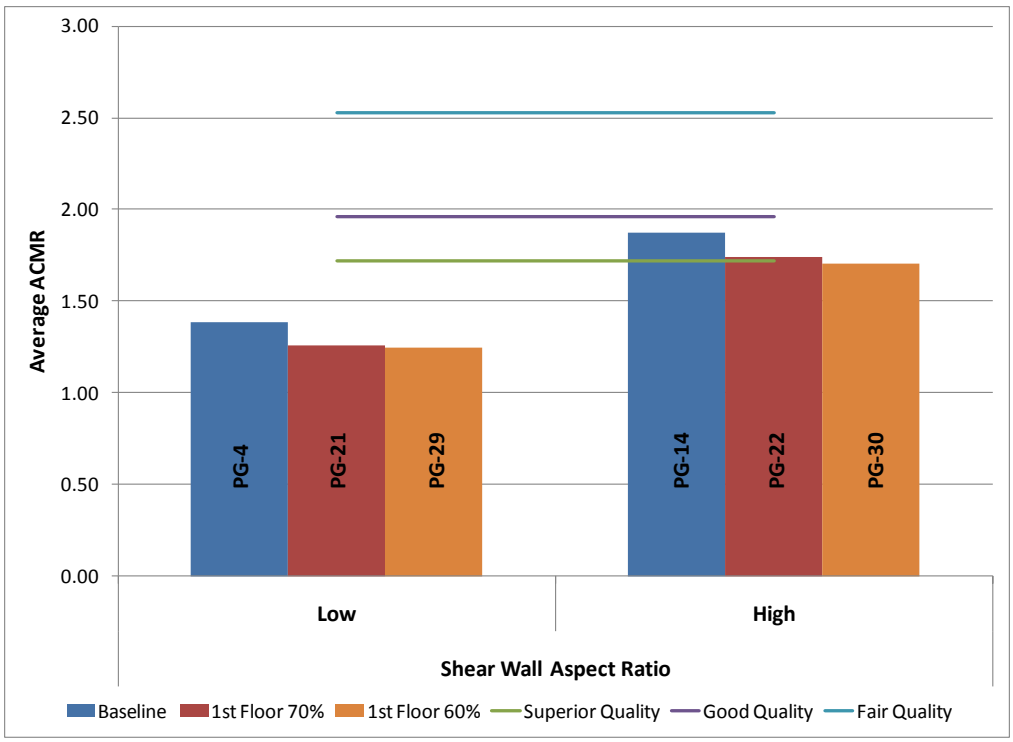

Figure 30 – Comparison plot of average *ACMR* for performance groups with and without 1st floor soft-stories (SDC = D_{max})

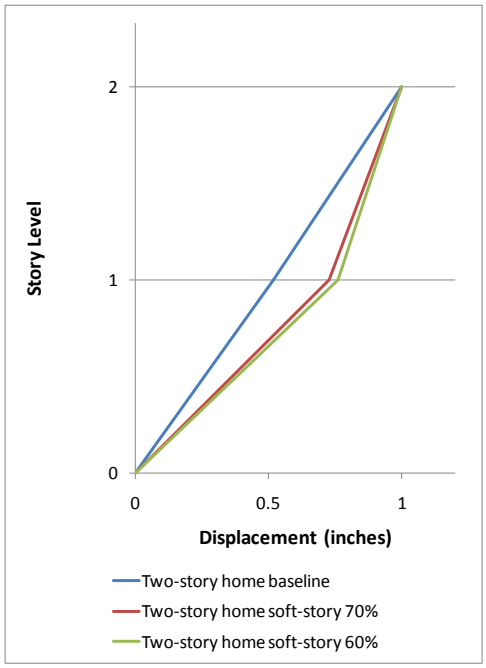

Figure 31 – Mode shape comparison for two-story single family home baseline and soft-story archetype configurations with PG-4 shear wall configuration

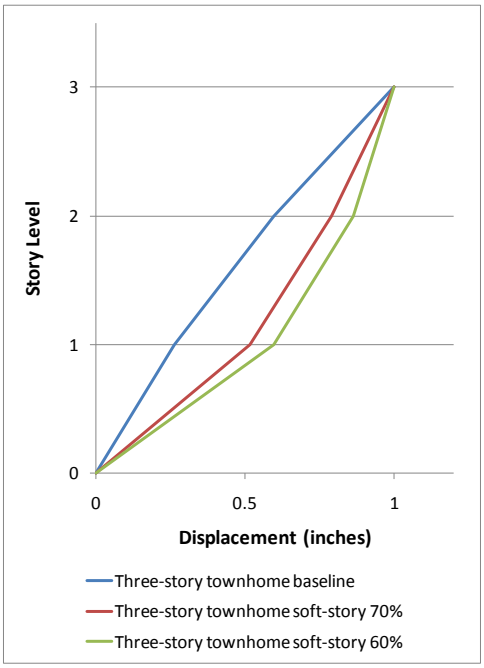

Figure 32 – Mode shape comparison for three-story townhouse baseline and soft-story archetype configurations with PG-4 shear wall configuration

System Analysis Methods – CASHEW vs. Phenomenological Models

This study evaluates the influence of the shear wall modeling methodology on the $ACMR$. The shear wall models are developed using CASHEW analytical software or by fitting a phenomenological CUREE model into experimental data. High and low aspect ratio shear wall models are evaluated separately in this study. The experimental data for shear walls tested using a CUREE cyclic protocol is used. Figure 33 shows cyclic backbone curves for both shear wall response modeling methods. The phenomenological model indicates higher peak loads for both high and low aspect ratio walls, whereas the CASHEW model predicts a higher displacement capacity for low aspect ratio walls and a lower displacement capacity for high aspect ratio walls. The difference in displacement capacity for low aspect ratio walls is likely associated with CASHEW's capability to accurately relate the failure of individual sheathing connections with varying edge distances and associated force vectors to the global failure of the entire shear wall. (However, it also should be noted and is recognized by the authors that response of a shear wall in a complete 3-D building may be different from that measured in a test of an individual shear wall.) For high aspect ratio walls, CASHEW underestimates the displacement capacity because the model does not include the contribution of the uplift component to the global wall displacement (the uplift contribution becomes more significant as the aspect ratio gets higher). The test-based models directly include the contribution of the uplift deformation in the measured global wall response.

Figure 34 shows results of the FEMA P695 analysis in terms of $ACMR$. With the modeling method showing a significant influence on the $ACMR$ value, the effect is also different for the two aspect ratio categories. For low aspect ratio walls, the test-based shear wall model resulted in a lower $ACMR$ than the CASHEW model; for high aspect ratio walls, the test-based shear wall model resulted in a higher $ACMR$ than the CASHEW model. These results reflect the backbone response such that the walls with the greater deformation capacity (i.e., low aspect ratio CASHEW and high aspect ratio test-based models) resulted in increased $ACMR$.

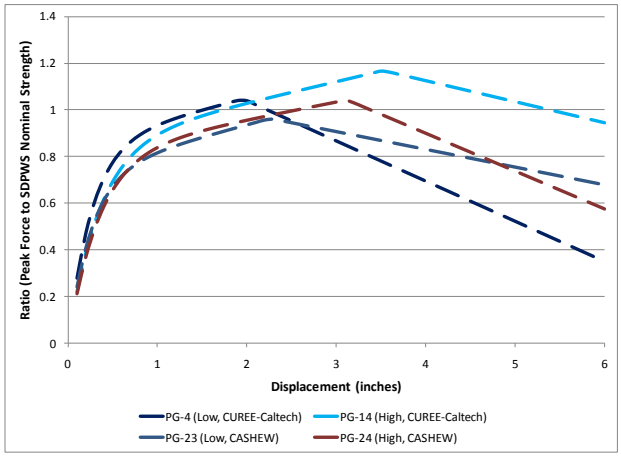

Figure 33 – Low and high aspect ratio shear wall envelope behaviors in parenthesis (aspect ratio, data source)

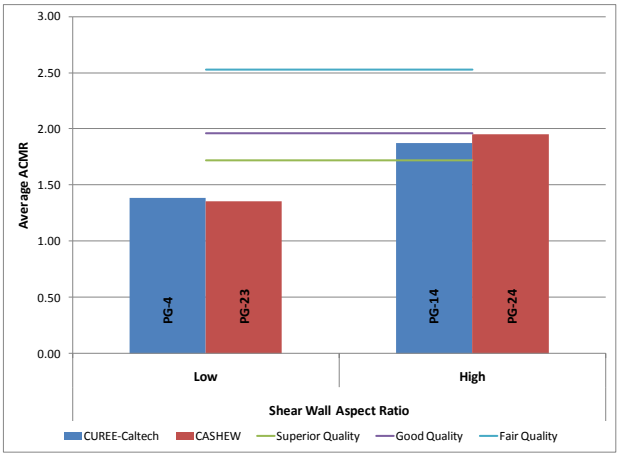

Figure 34 – Comparison plot of average $ACMR$ for performance groups with phenomenological or CAHSEW responses (SDC = D_{max})

In summary, the choice of the methodology selected to model the shear wall response can have a significant influence on the results of the FEMA P695 analysis. Limitations inherent to a specific modeling methodology can have different influences on different configuration of walls. Because the $ACMR$ is sensitive to the deformation capacity, the use of models capable of capturing the wall's response at post-capping deformations should be recommended. The limitations of the CASHEW model are evident for high aspect ratio walls where the uplift component has a significant contribution to the deformation capacity (the CASHEW model significantly underestimates ACMR). A better understanding is also needed with regard to the deformation capacity of individually tested shear walls and the story drift in full-size buildings leading to loss of global stability (i.e., building collapse).

System Analysis Methods – SAWS vs. OpenSEES

This study evaluates the potential sensitivity of the results of the FEMA P695 methodology to different analytical engines. Two software modules with different analytical engines are used to perform identical simulations: SAWS and OpenSEES. A CUREE shear wall model is used with both SAWS and OpenSEES. In addition, a different shear wall model (Pinching4) available in OpenSEES is used to perform simulations. Figure 35 compares backbone curves for CUREE and Pinching4 models for high and low aspect ratio walls. A good correlation between the two models was achieved with a minor degree of divergence in the area of initial yielding for deformations less than 1 inch.

Figure 36 compares the $ACMR$ results for SAWS and OpenSEES. For low aspect ratio walls, the OpenSEES CUREE model results in a slightly higher $ACMR$ compared to SAWS with all other variables equal. The OpenSEES Pinching 4 model matches the SAWS CUREE model, but falls below the OpenSEES CUREE model. For high aspect ratio walls, all three options result in nearly identical ACMRs suggesting that models with larger deformation capacities are less sensitive to (1) the choice of the modeling software and (2) variability of response (actual or modeled) in the initial range of displacements.

A comparison of overstrength values (Figure 37) indicates near identical results for the respective high and low aspect ratio segments. The good repeatability is expected in this case as the overstrength values are determined based on pushover analysis – a more stable analysis procedure when compared to nonlinear dynamic simulations. The period-based ductility calculated using OpenSEES (Figure 38) is noticeably lower than that calculated using SAWS for both categories of aspect ratios. However, the observed difference would not affect the outcome of the analysis because FEMA P695 assigns the same spectral shape factor for all period-based ductility's exceeding 8.

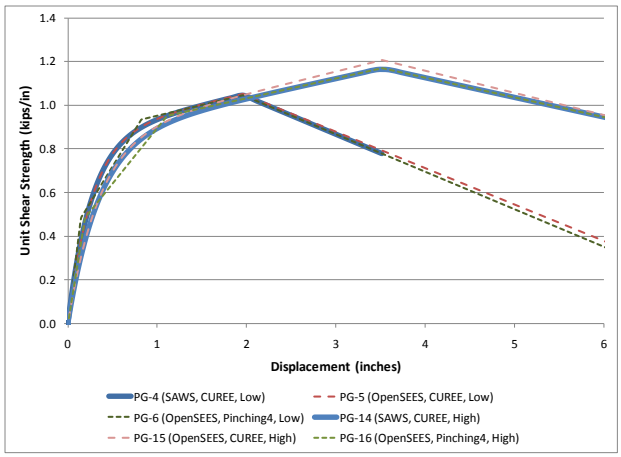

Figure 35 - Unit shear capacity for CUREE and Pinching4 hysteretic models from SAWS and OpenSEES in parenthesis (software platform, hysteretic model, aspect ratio)

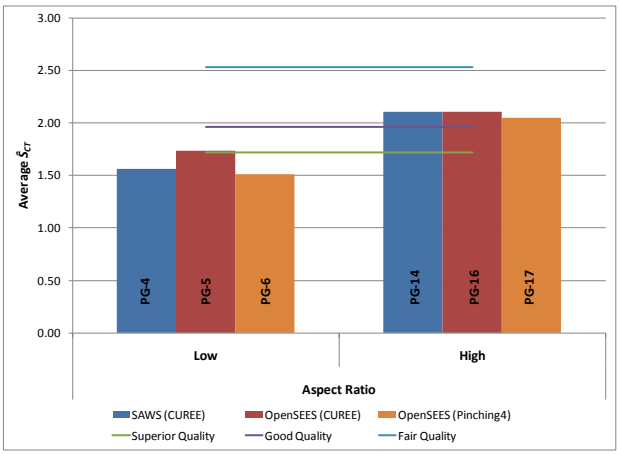

Figure 36 – Comparison plot of *ACMR* for low and high aspect ratio shear wall archetypes in different software platforms (SDC D_{max}) in parenthesis (hysteretic model)

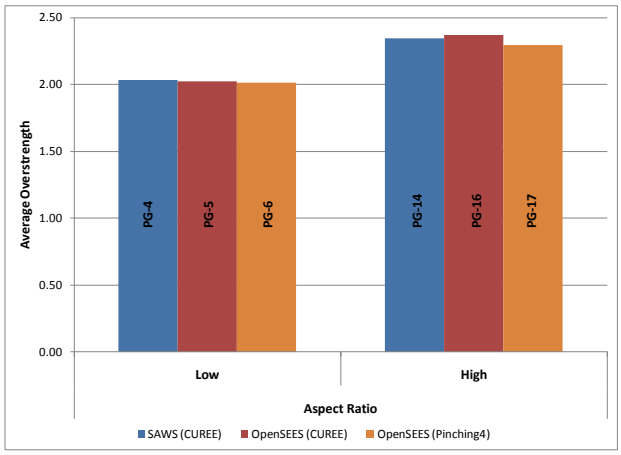

Figure 37 – Comparison plot of overstrength for low and high aspect ratio shear wall archetypes in different software platforms (SDC *D_{max}*) in parenthesis (hysteretic model)

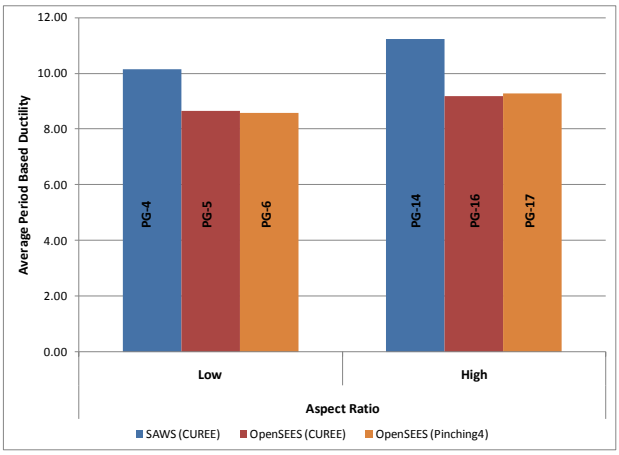

Figure 38 – Comparison plot of period based ductility for low and high aspect ratio shear wall archetypes in different software platforms (SDC *D_{max}*) in parenthesis (hysteretic model)

System Analysis Methods – Damping Ratio

Damping has a significant influence on the dynamic response of structures. In structures subject to inelastic deformations, energy is dissipated through viscous damping and nonlinear hysteresis. The energy dissipated through nonlinear hysteresis is modeled directly using the shear wall load-deformation relationship. The value of viscous damping is assigned based on measurements in full-size buildings and engineering judgment. The FEMA P695 example application for wood-frame buildings used a lower bound of viscous damping of 1%. This study evaluates the influence of the possible range of viscous damping on the results of a FEMA P695 analysis.

The measured values of viscous damping (in terms of damping ratio), available in the literature, range widely from as low as 2.8 percent to as high as 16 percent [22]. The sources of the measured viscous damping values for homes include (1) recorded building response during seismic events by instruments pre-installed in the structure, (2) forced vibration response of existing buildings, and (3) measured response of test structures in a laboratory environment (subjected to free vibration or a ground motion). The average damping ratio of building response during actual seismic events for 5 different buildings (1 to 3 stories) in 8 different earthquakes ranges from 7 to 16 percent. The damping ratio from forced excitation ranges from 2.8 to 6.6 percent for three buildings studied (2 to 3 stories). Measurements from a two-story structure tested in a laboratory (CUREE research program) provided an average damping ratio of 7.6 percent [18].

Nonlinear dynamic analysis of light-frame wood buildings, and particularly its linkage to building code design procedures, is currently at a developmental stage. The use of a lower bound of viscous damping range (e.g., 1%) affects the accuracy of modeling of the initial response prior to onset of yielding, potentially leading to an early onset of inelastic deformations. It also affects the total energy dissipation throughout the entire response history.

Figure 38 shows the influence of higher viscous damping (3% and 5%) on the $ACMR$ values for high and low aspect ratio shear walls. Results show a consistent increase in $ACMR$ with an increase in damping for both aspect ratio categories. This difference is sufficient to make an influence on the decision making process in evaluating performance of a system. Figure 40 compares the energy dissipated through damping with the energy dissipated through yielding for a single ground motion record for systems with 1%, 3%, or 5% viscous damping. (Note that kinetic damping is not a significant source of energy dissipation for these types of systems and is not included in the charts for improved clarity.) The observed trend indicates that a 2% increase in viscous damping results in about a 10% change in the balance of energy dissipation (i.e., 1% viscous damping accounts for less than 10% of total energy dissipation, whereas 3% viscous damping accounts for about 20% of total energy dissipation).

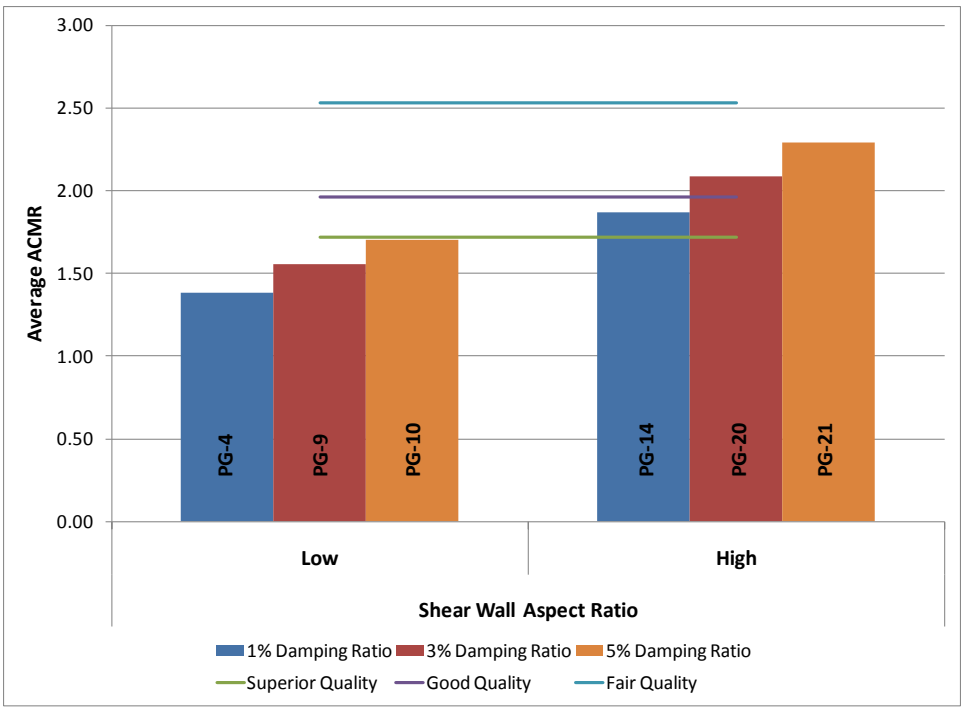

Figure 39 – Comparison plot of $ACMR$ for low and high aspect ratio shear wall archetypes with 1%, 3% and 5% damping ratios (SDC D_{max})

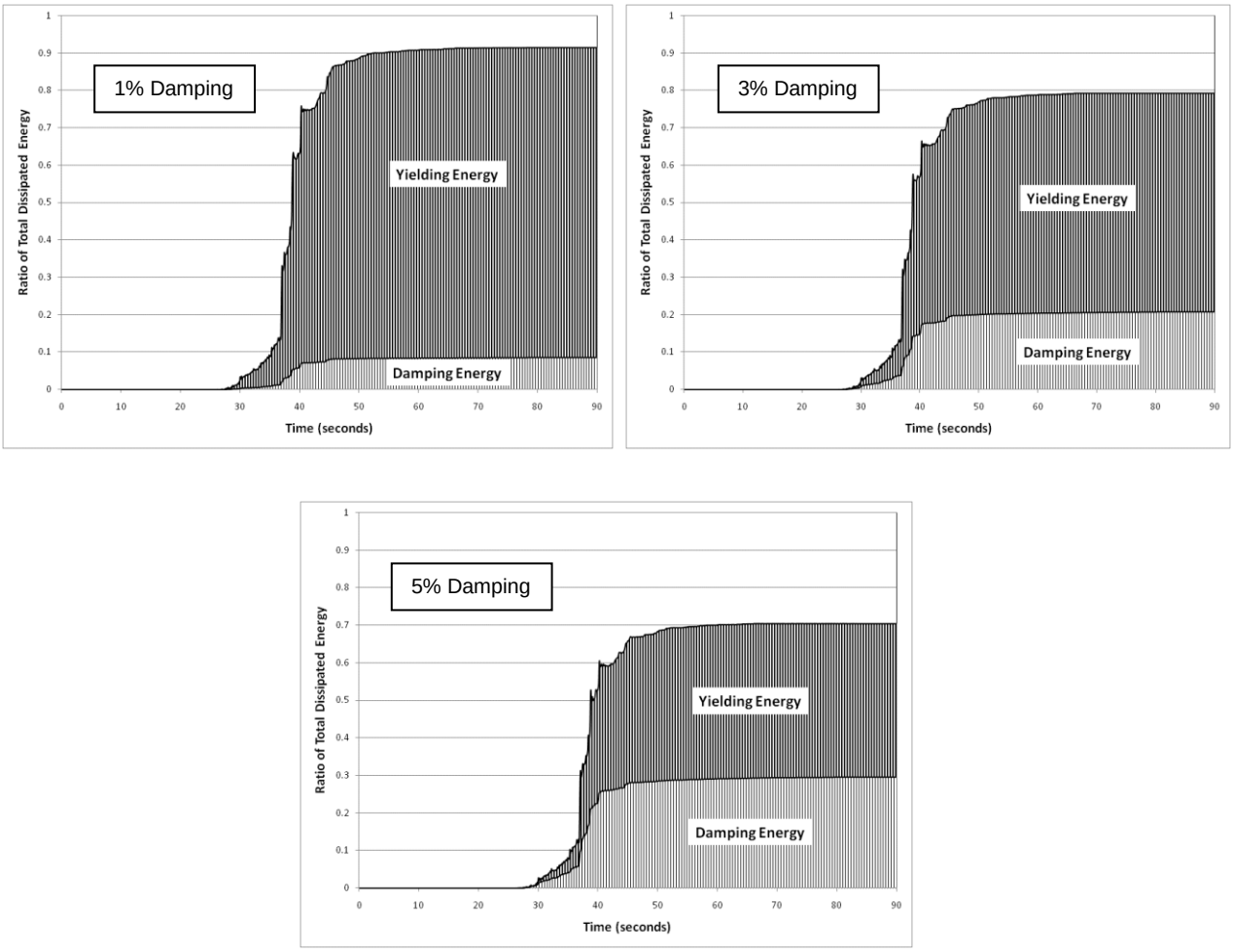

Figure 40 – Dissipated energy for low aspect ratio shear wall archetypes (far-field record #38)

In accordance with Equation (6) through Equation (9) outlining the relationship between $ACMR$ and the R-factor, a change in $\hat{S}_{CT}{}^{*}SSF$ for models with the same $ACMR_{10\%}$ is equivalent to the change in R. Table 22 summarizes the potential influence of using different viscous damping on the R-value of a system. For low and high aspect ratio walls, increasing viscous damping from 1 to 5 percent increases the R factor by 22 and 23 percent, respectively.

$$ACMR_{10\%} = \frac{\hat{S}_{CT}}{S_{MT}} SSF \qquad \textbf{Equation (6)}$$

$$V = \frac{S_{DS}}{R} W$$ **Equation (7)**

$$S_{MT} = 1.5 S_{DS}$$ **Equation (8)**

$$R = \frac{\hat{S}_{CT} * SSF * W}{1.5 ACMR_{10\%} * V}$$ **Equation (9)**

Table 22 – Effect of viscous damping on the R-factor

Performance Group	Aspect Ratio	Damping Ratio	$\hat{S}_{CT}$*SSF	Factor Increase of R
4	Low	1%	2.08	1.00
9		3%	2.33	1.12
10		5%	2.55	1.23
14	High	1%	2.81	1.00
20		3%	3.13	1.11
21		5%	3.44	1.22

System Analysis Methods – Uncertainty

This study evaluates the range of influence of the assigned quality ratings (i.e., uncertainty levels) on the R-factor for one of the baseline performance groups. For this comparison, the shear wall amounts were optimized where needed (one- and two-story structures only) such that the exact shear wall length required by design was used. This optimization was performed to remove any bias associated with "overbuilding" the walls such that the largest change in R can be achieved for a given level of assigned uncertainty. The analysis was performed iteratively finding an R-factor that results in meeting the corresponding $ACMR_{10\%}$ requirement.

The results (Figure 41 and Table 23) indicate that the R-factor can change by as much as a factor of 2.4 (from R=7.5 to R=3.1) when the uncertainty rating is changed from Superior to Fair for all inputs that require an assigned quality rating per FEMA P695. In addition, the change in R is not linear relative to the assigned uncertainty level, such that a downgrade from Good to Fair has twice the influence of a downgrade from Superior to Good. These results underscore the

significance of quality ratings on the outcome of the analyses. As an example of complexities involved with assigning quality ratings, the FEMA P695 example downgraded the quality rating for CASHEW for high aspect ratio shear walls due to the limitations of the model in capturing all components of the wall's response including uplift deformations. However, the study of the influence of shear wall models on $ACMR$ summarized earlier in this report indicates that the limitations of the CASHEW models result in a penalty for high aspect ratio walls. The total influence was a double penalty on the results of the FEMA P695 example analysis – first due to the limitations of the model and second due to the assigned quality rating.

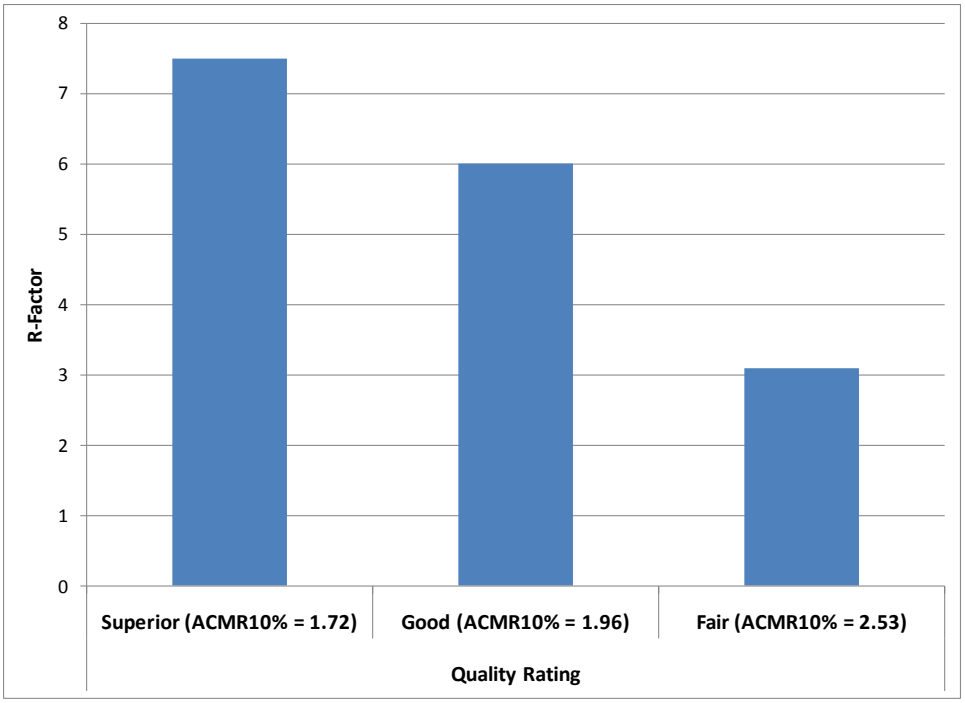

Figure 41 – Maximum R-factors for the high aspect ratio baseline performance group 14 based on assigned uncertainty

Table 23 – Effect of assigned uncertainty on the R-factor for baseline performance group 14

Baseline Performance Group	Maximum R-factor based on assigned uncertainty		
	Superior ($ACMR_{10\%}$ = 1.72)	Good ($ACMR_{10\%}$ = 1.96)	Fair ($ACMR_{10\%}$ = 2.53)
14	7.5	6.0	3.1

Summary

This study was designed to (1) highlight implementation considerations for the FEMA P695 methodology when applied wood light-frame shear wall systems and (2) improve the knowledge of the seismic performance of wood light-frame shear wall systems. The FEMA P695 methodology provides a useful metric for evaluation of seismic resisting systems with the simulated frequency of building collapse under ground motions exceeding the MCE as the primary criteria of performance. However, the results of the analyses are highly dependent on the inputs used: including shear wall models, shear wall configurations, archetypes, level of confidence in those inputs, etc. Specific findings based on the results of this study include:

- Results of FEMA P695 analyses indicate that wood light-frame buildings have improved collapse performance characteristics in lower seismic design categories (e.g., SDC B and SDC C).
- For short-period structures, such as wood light-frame buildings, the influence of the actual building period on FEMA P695 results should be evaluated (as opposed to using the simplified ASCE-7 building period) to improve the accuracy of the analyses.
- Where hysteretic models are strictly based on results from different cyclic load protocols, results of the analysis show a significant influence of the test protocol on the $ACMR$ with the difference between the CUREE and the SPD protocol being as high as 0.5 $ACMR$ value.
- Aspect ratio has a significant influence on the $ACMR$, with the higher aspect ratio walls exhibiting higher deformation capacity, leading to a higher $ACMR$. The improvement in $ACMR$ is achieved without applying strength reductions for high aspect ratio shear walls required by the design standards. Therefore, the FEMA P695 methodology can provide the basis for re-evaluation of the applicability of the triggers for the high aspect ratio strength reductions. The influence of gravity loads on the performance of WSP walls with high aspect ratio walls should be also investigated.
- Results indicate a relatively minor influence of finishes (gypsum or stucco) on the $ACMR$. This indicates that the FEMA P695 methodology emphasizes post-capping displacement capacity, and that the increase in initial stiffness and the increase in the peak force provided by the finishes are either offset by the changes in the deformation behavior or do not play a significant role in the procedure for determining $ACMR$. This conclusion is inconsistent with the results of full-scale shake-table tests of homes. Thus, FEMA P695 may not be the appropriate tool for analyzing the influence of finishes on the buildings' performance for ground motions at the MCE level and below. The influence of gravity loads on the performance of WSP walls with finishes should be also investigated.
- ACMR improves with the increase in the number of stories, i.e., results for a single story structure provide the most conservative results with regard to evaluation of the system's collapse performance. However, in actual residential buildings, this trend will not be as definitive because significant "overbuild" is typically present in one and two-story homes relative to minimum shear wall requirements, particularly in seismic design categories lower than *D*, due to wind requirements or architectural/building configurations.

- The soft-story configuration resulted in an incremental increase in deformation demand on the first story of the building, leading to a small reduction in $ACMR$ for both high and low aspect ratio walls.
- The choice of the methodology selected to model the shear wall response (phenomenological or component) can have a significant influence on the results of the FEMA P695 analysis. Limitations inherent to a specific modeling methodology can have different influences on different configuration of walls. Because the $ACMR$ is sensitive to the deformation capacity, the models capable of capturing the wall's response at post-capping deformations should be recommended. The limitations of the CASHEW model are evident for high aspect ratio walls where the uplift component has a significant contribution to the deformation capacity.
- Good overall repeatability of results was obtained by using two independent analytical engines (SAWS vs. OpenSEES) and different hysteretic models (CUREE vs. Pinching4).
- Selection of viscous damping ratio can have a significant influence on the results of the analysis. A better correlation between the damping ratios obtained from forced vibration measurements and the damping ratios used in the analysis should be defined.
- The assigned quality ratings have a significant influence on a system's R-factor. A downgrade in quality ratings from Superior to Fair for an example analysis influenced the R-factor by a factor of 2.4.

Works Cited

1. **American Society of Civil Engineers.** *ASCE/SEI 7-10: Minimum Design Loads for Buildings and Other Structures.* Reston, VA : American Society of Civil Engineers, 2010.

2. **FEMA P695.** *Quantification of Building Seismic Performance Factors.* Washington, D.C. : FEMA P695 Federal Emergency Management Agency, 2009.

3. **International Code Council.** *International Building Code.* Country Club Hills, IL : International Code Council, Inc., 2009.

4. **American Forest & Paper Association, Inc. (AF&PA).** *SDPWS, Special Design Provisions for Wind and Seismic.* Washington D.C. : American Forest & Paper Association, 2005.

5. —. *NDS, National Design Specification for Wood Construction.* Washington, DC : AF&PA American Wood Council, 2005. 2005.

6. **Christovasilis, Ioannis P., Filiatrault, Andre and Wanitkorkul, Assawin.** *Seismic Testing of a Full-Scale Two-Story Light-Frame Wood Building : NEESWood Benchmark Test.* Buffalo, NY : University at Buffalo, 2007.

7. **Pardoen, G. C., et al.** *Testing and Analysis of One-Story and Two-Story Shear Walls Under Cyclic Loading, CUREE Publication No. W-25.* Richmond, Ca : Consortium of Universities for Research in Earthquake Engineering, 2003.

8. **Martin, Z.** *Effects of Green Lumber on Wood Structural Panel Shear Wall Performance. APA Report T2002-53.* Tacoma, Wa : APA-The Engineered Wood Association, 2002.

9. **Martin, Z. and Skaggs, T.** *Shear Wall Lumber Framing: Double 2x's vs. Single 3x,s at Adjoining Panel Edges. APA Report T2003-22.* Tacoma, Wa : APA-The engineered Wood Association, 2003.

10. **Martin, Z.** *Wood Structural Panel and Shear Wall Connections with Common, Galvanized Box, and Box Nails. APA Report T2004-14.* Tacoma, Wa : APA-The Engineered Wood Association, 2004.

11. **Skaggs, Thomas D. and Martin, Zeno A.** *Performance of OSB and Plywood Sheathed Shear Walls Tested Monotonically and Cyclically. APA Report T2001-37.* Tacoma, WA : APA-The Engineered Wood Association, 2001.

12. **Fischer, David, et al.** *Shake Table Tests of a Two-Story Woodframe House, CUREE Publication No. W-06.* Richmond, CA : Consortium of Universities for Research in Earthquake Engineering, 2001. W-06.

13. **Folz, Bryan and Filiatrault, Andre.** *A Computer Program for Cyclic Analysis of Wood Shear Walls, CUREE Publication No. W-08.* Richmond, Ca : Consortium of Universities for Research in Earthquake Engineering, 2000.

14. —. *A Computer Program for Seismic Analysis of Woodframe Structures, CUREE Publication No. W-21.* Richmond, Ca : Consortium of Universities for Research in Earthquake Engineering, 2001.

15. **Mazzoni, S., et al.** *The OpenSees Command Language Manual.* Berkeley, CA : Pacific Earthquake Engineering Center U.C. Berkeley, 2007.

16. **ASTM International.** *E2126-09 Standard Test Methods for Cyclic (Reversed) Load Test for Shear Resistance of Vertical Elements of the Lateral Force Resisting Systems for Buildings.* West Conshohocken, PA : ASTM International, 2009.

17. **Skaggs, Thomas D. and Martin, Zeno A.** *Performance of OSB Sheathed Shear Walls Tested Cyclically. APA Report T2001L-47.* Tacoma, WA : APA-The Engineered Wood Association, 2001.

18. *Seismic Analysis of Woodframe Structures. II: Model Implementation and Verification.* **Folz, Bryan and Filiatrault, Andre.** 9, s.l. : Journal of Structural Engineering, 2004, Vol. 130.

19. **Isoda, Hiroshi, Folz, Bryan and Filiatrault, Andre.** *Seismic Modeling of Index Woodframe Buildings.* Richmond, Ca : Consortium of Universities for Research in Earthquake Engineering, 2002.

20. **Pei, Shiling and van de Lindt, John W.** *SAPWood for Windows, Seismic Analysis Package for Woodframe Structures.* Fort Collins, CO : Colorado State University, 2007.

21. **Rammer, Douglas.** Personal Communication.

22. **Camelo, Vanessa, Beck, James and Hall, John.** *Dynamic Characteristics of Woodframe Structures, CUREE Publication No. W-11.* Richmond, CA : Consortium of Universities for Research in Earthquake Engineering, 2002.

APPENDIX A (FEMA P695 Analysis Procedure Flow Chart)

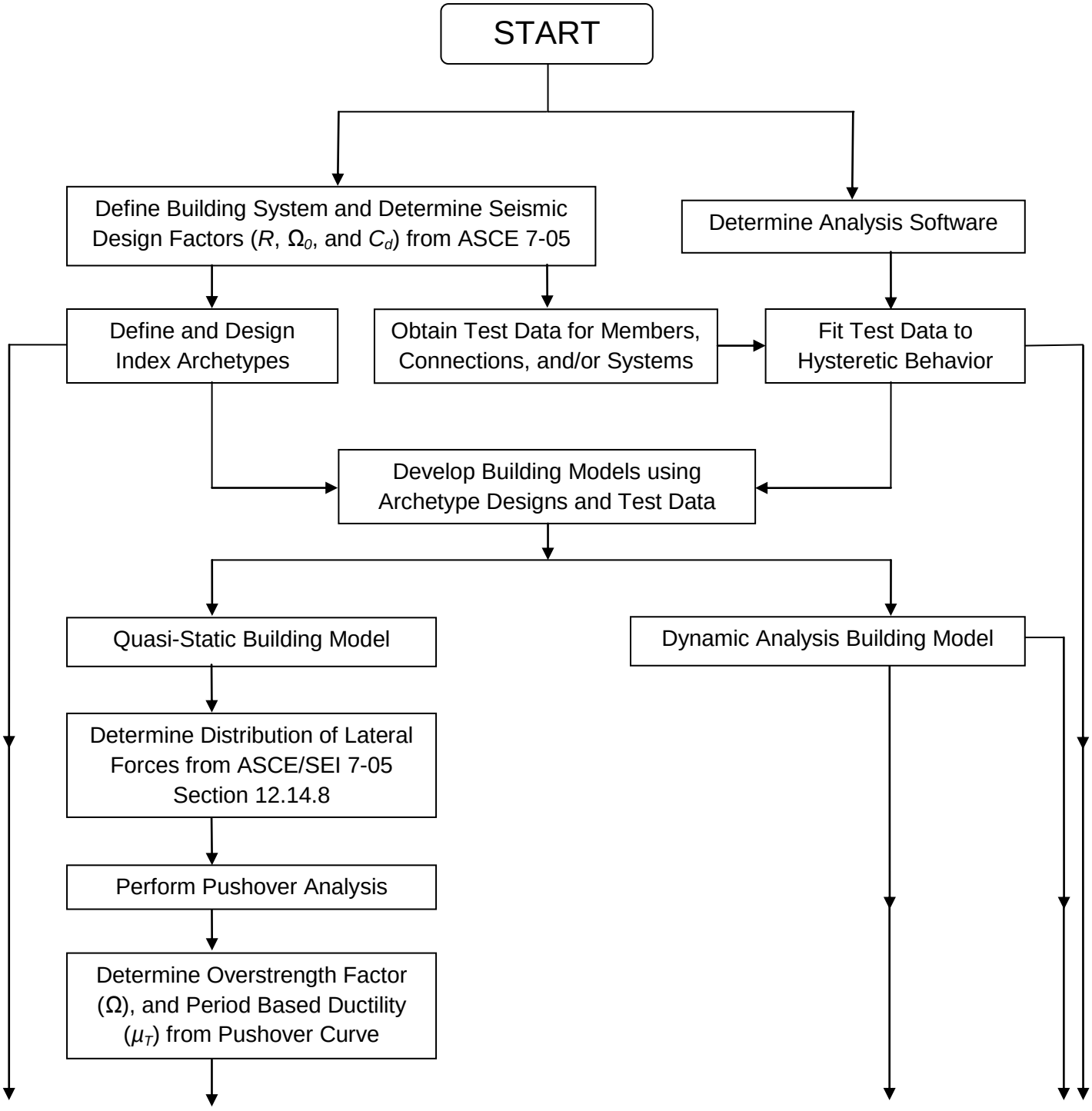

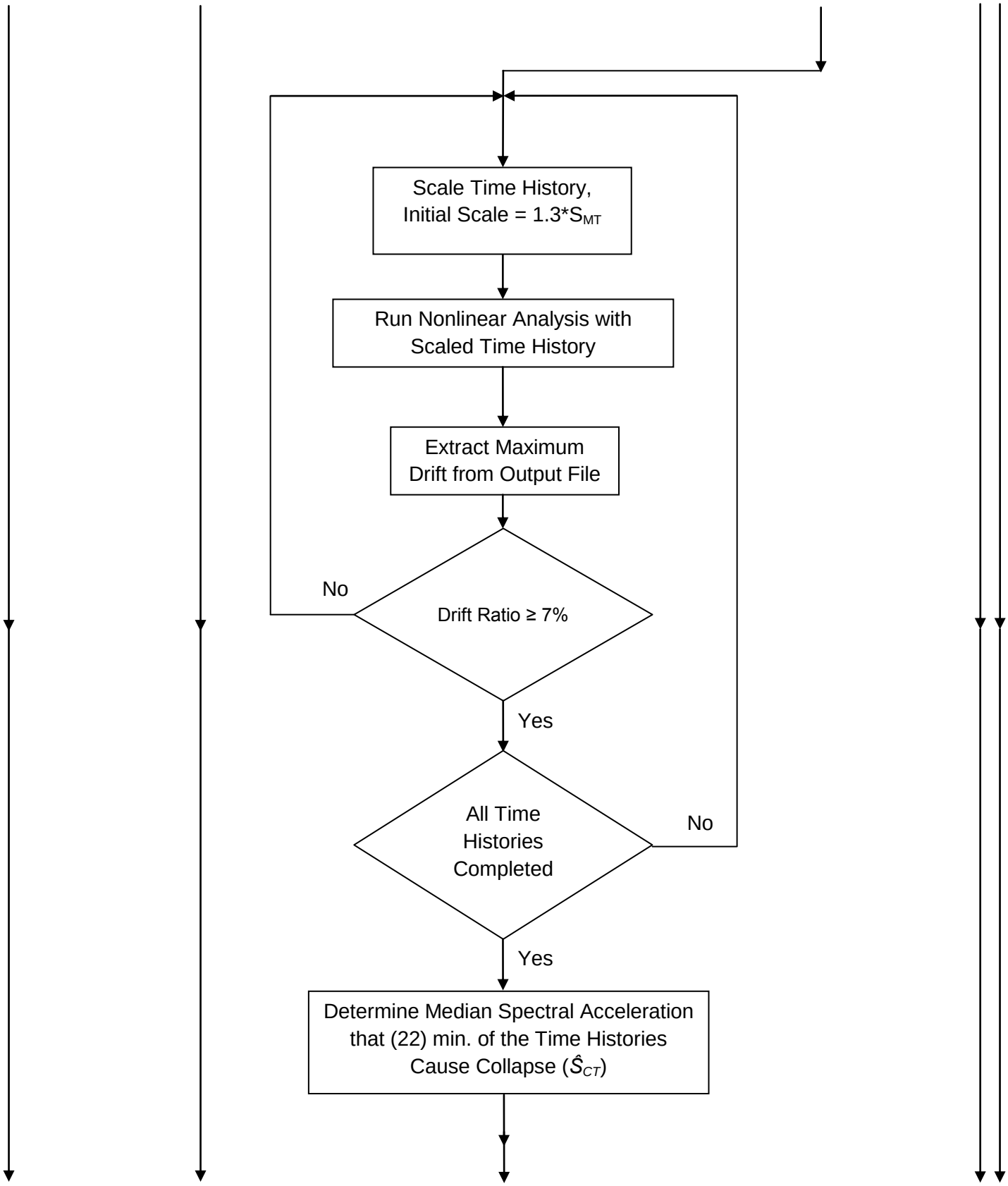
Scale Time History,
Initial Scale = 1.3*S_{MT}
Run Nonlinear Analysis with
Scaled Time History
Extract Maximum
Drift from Output File
Drift Ratio ≥ 7%
No
Yes
All Time
Histories
Completed
No
Yes
Determine Median Spectral Acceleration
that (22) min. of the Time Histories
Cause Collapse ($\hat{S}_{CT}$)

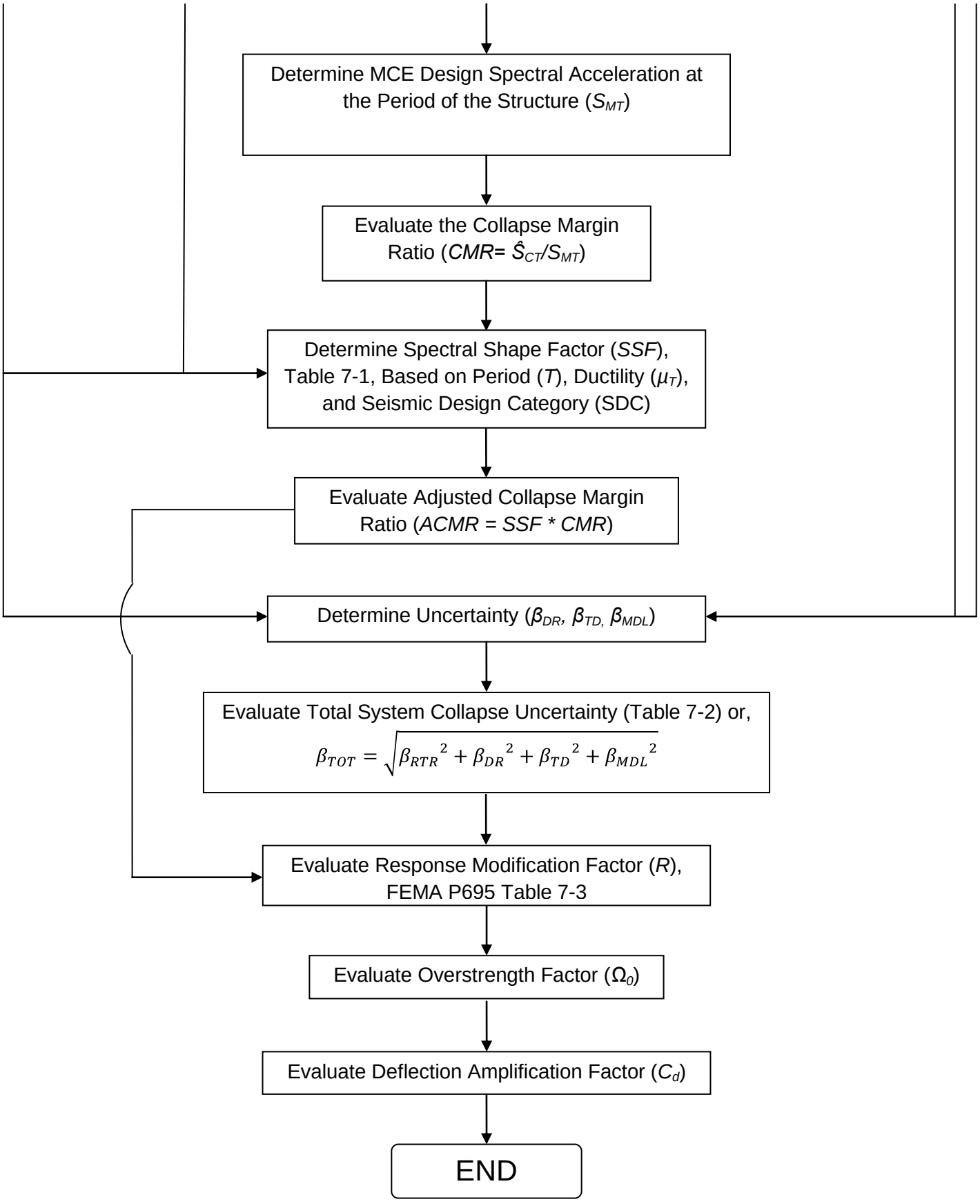
Determine MCE Design Spectral Acceleration at the Period of the Structure (S_{MT})
Evaluate the Collapse Margin Ratio ($CMR = \hat{S}_{CT}/S_{MT}$)
Determine Spectral Shape Factor (SSF), Table 7-1, Based on Period (T), Ductility (μ_T), and Seismic Design Category (SDC)
Evaluate Adjusted Collapse Margin Ratio ($ACMR = SSF * CMR$)
Determine Uncertainty (β_{DR}, β_{TD}, β_{MDL})
Evaluate Total System Collapse Uncertainty (Table 7-2) or,
$\beta_{TOT} = \sqrt{\beta_{RTR}^2 + \beta_{DR}^2 + \beta_{TD}^2 + \beta_{MDL}^2}$
Evaluate Response Modification Factor (R), FEMA P695 Table 7-3
Evaluate Overstrength Factor (Ω_0)
Evaluate Deflection Amplification Factor (C_d)
END

APPENDIX B (Building Configurations Floor Plans)

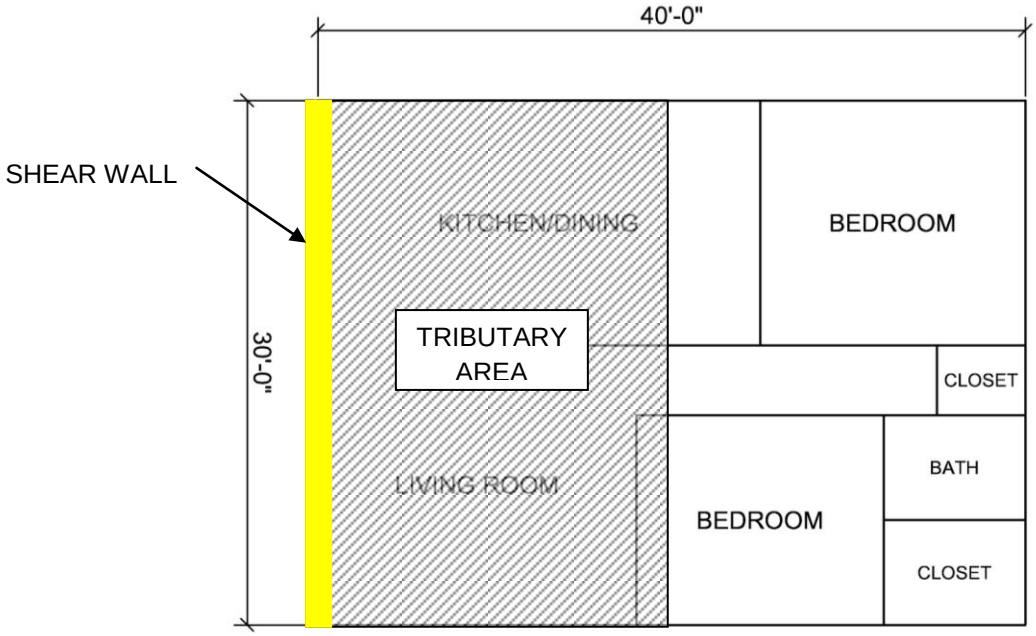

Figure 42 – One-family 1200 ft^2 home (Archetype Configuration #1)

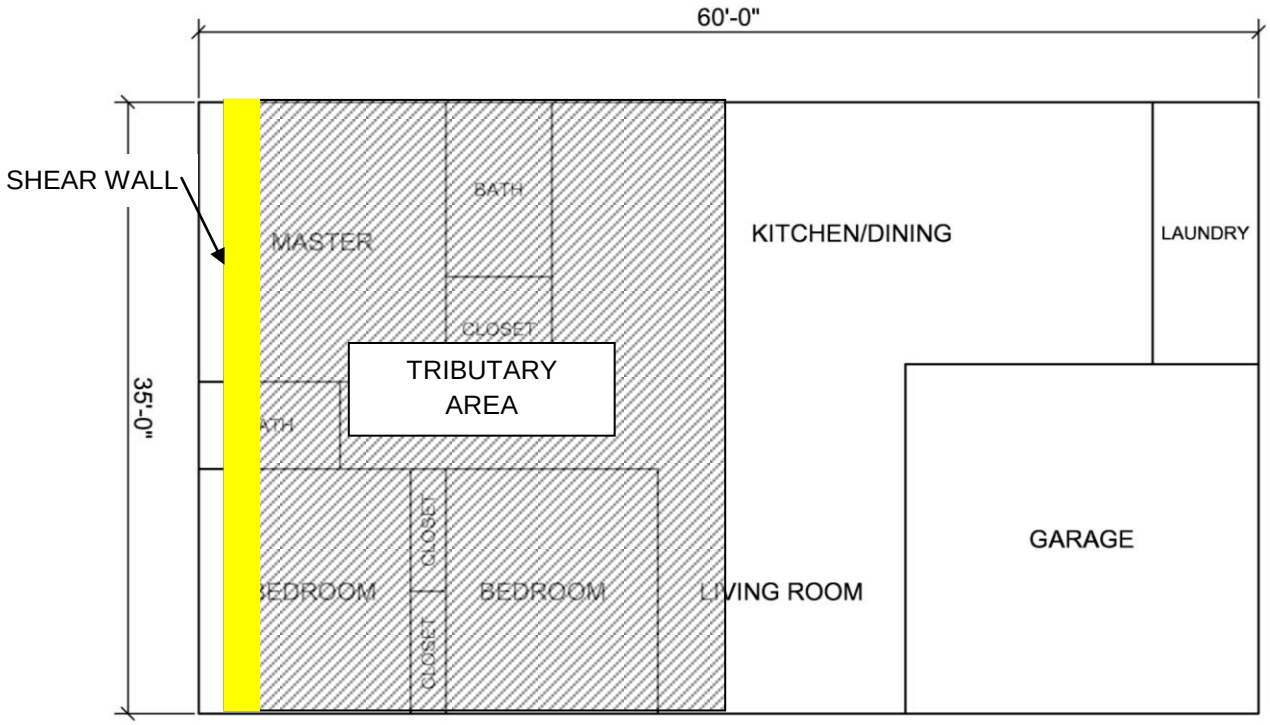

Figure 43 – One-family 2100 ft^2 home (Archetype Configuration #2)

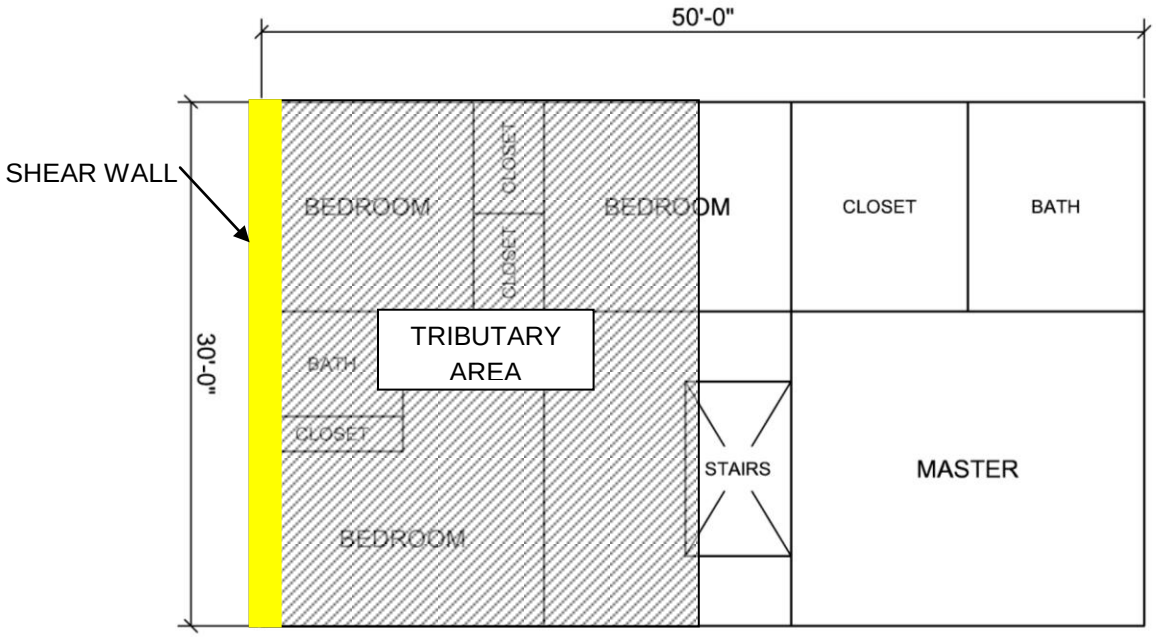

2nd Floor Plan

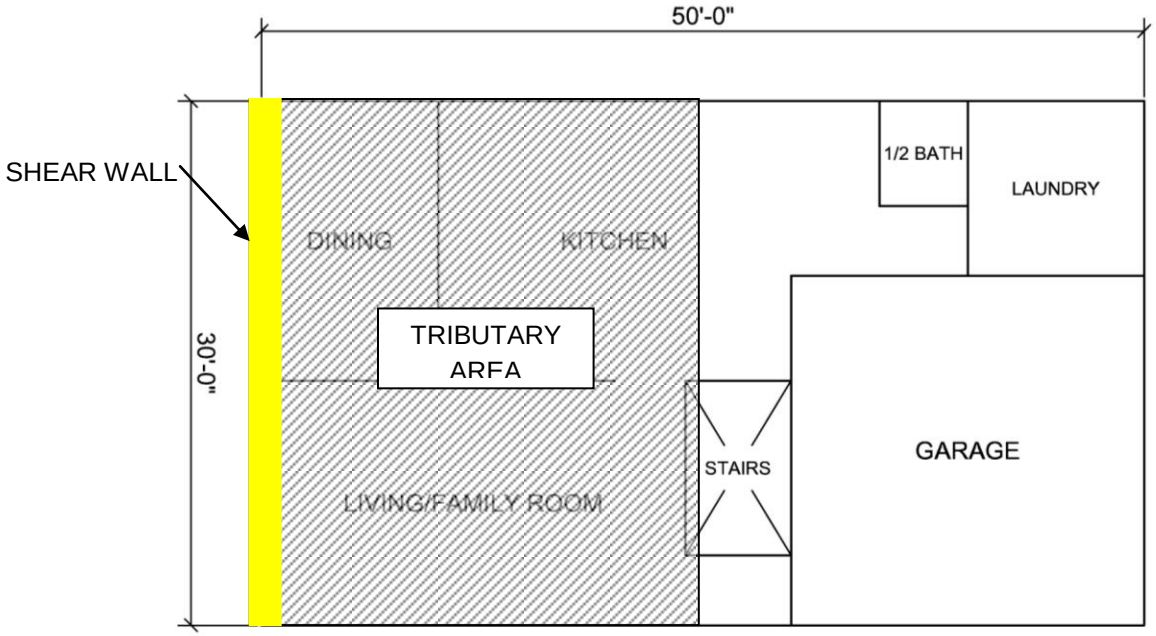

1st Floor Plan

Figure 44 – One-family 3000 ft^2 home (Archetype Configuration #3)

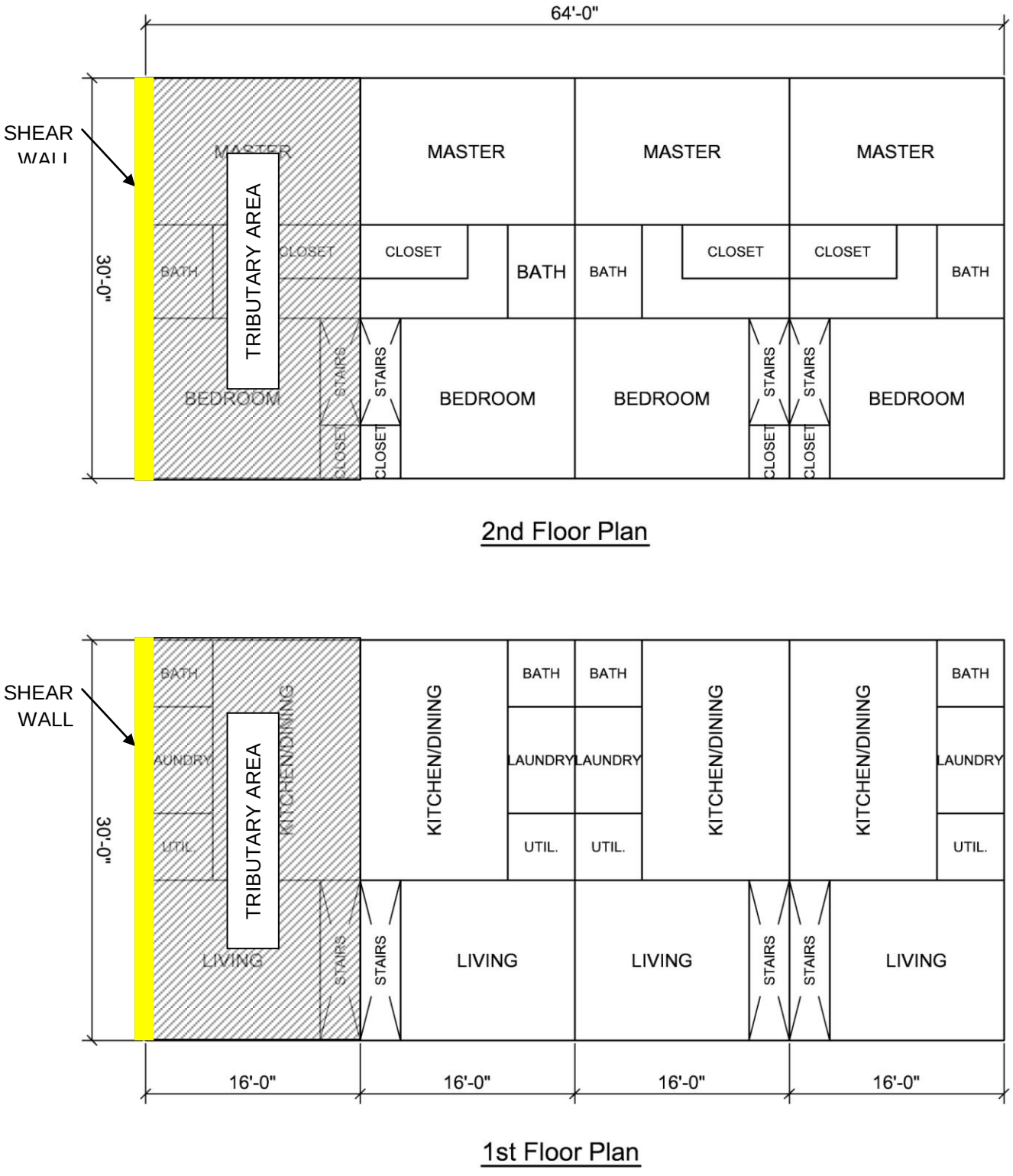

Figure 45 – Townhouse 960 ft^2 (Archetype Configuration #4)

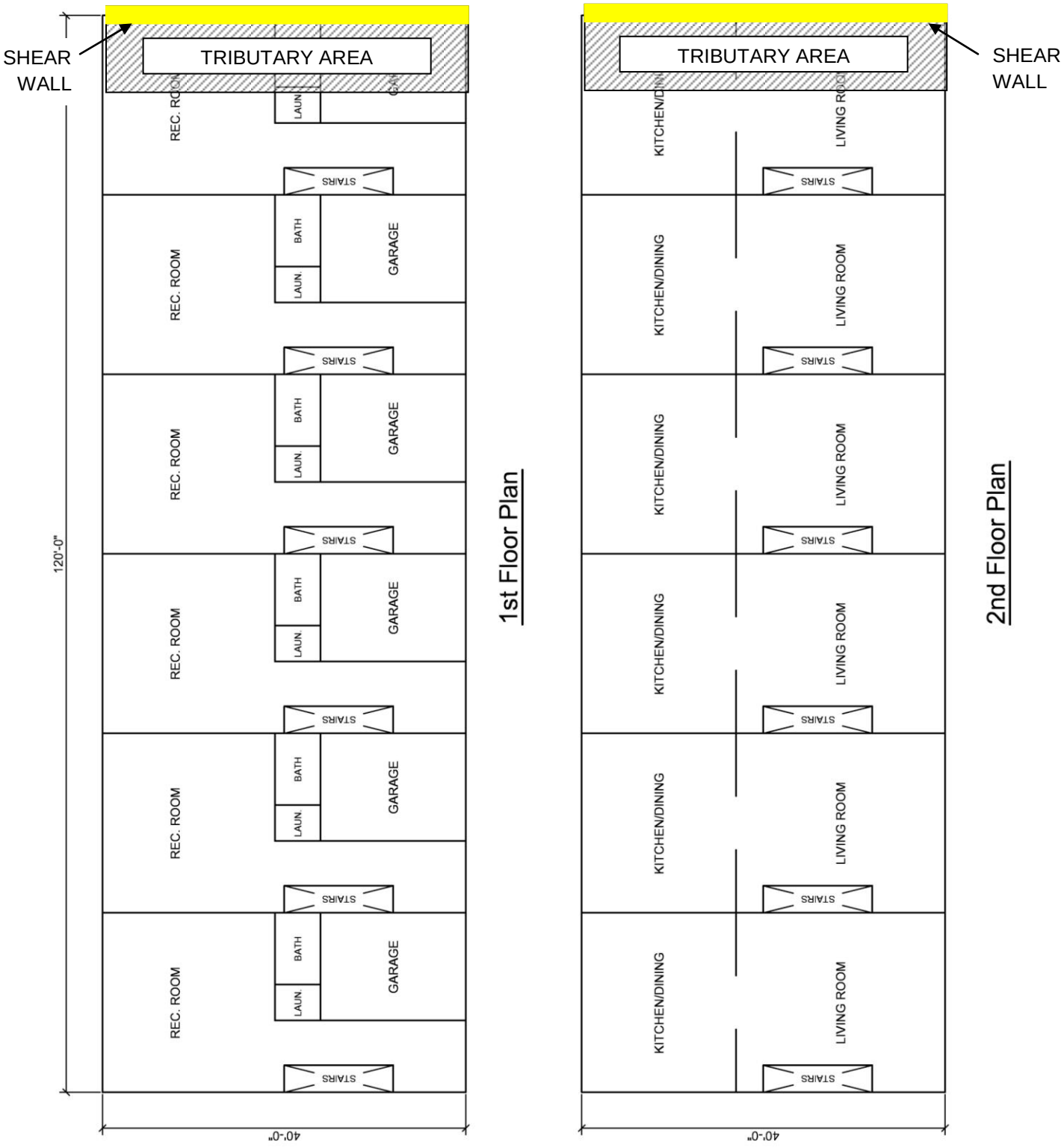

Figure 46 – Townhouse 2400 ft^2 (Archetype Configuration #5)

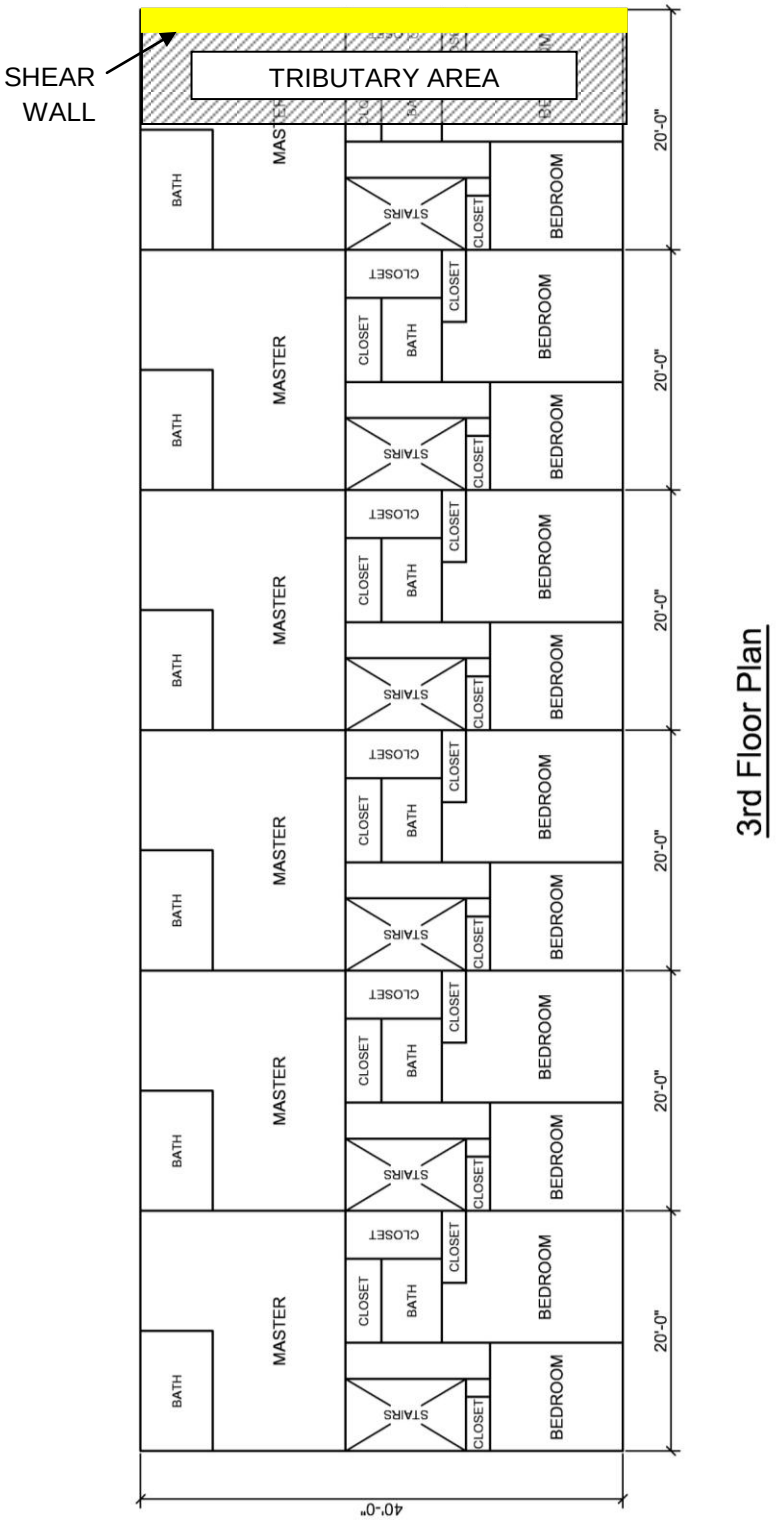

Figure 47 – Townhouse 2400 ft^2 (Archetype Configuration #5)

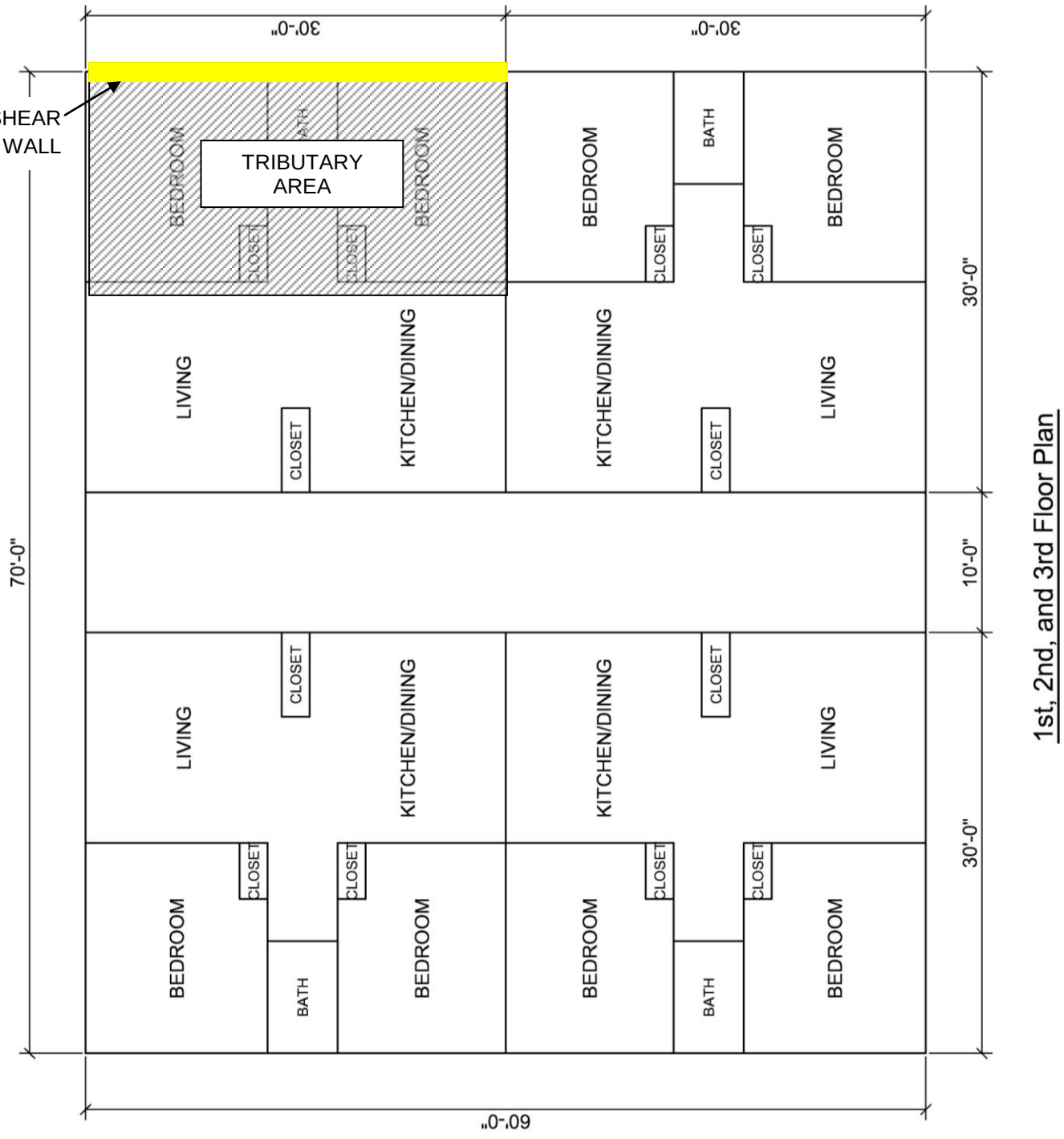

Figure 48 – Multi-family 900 ft^2 apartment (Archetype Configuration #6)

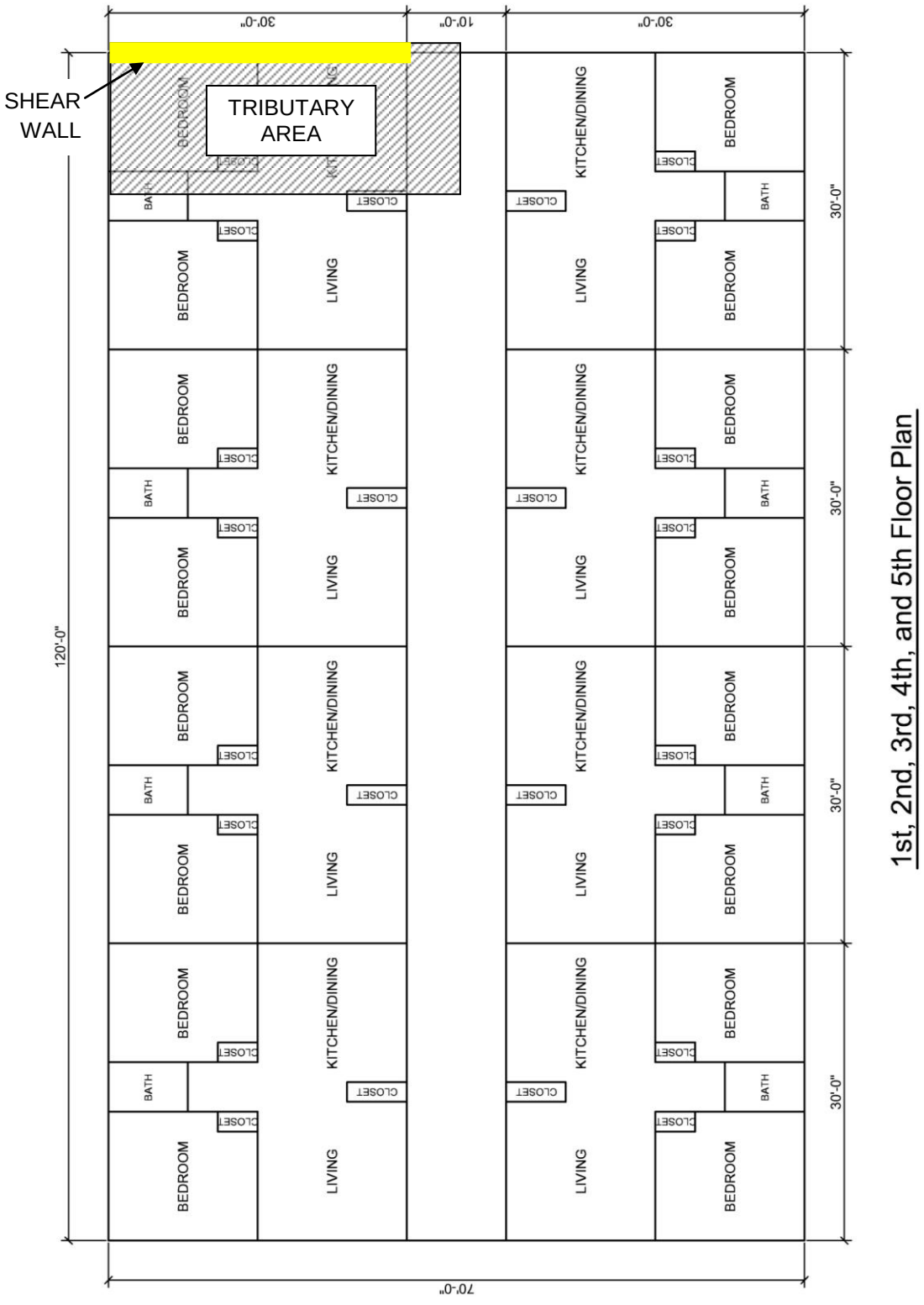

Figure 49 – Multi-family 900 ft^2 apartment (Archetype Configurations #7 and #8)

APPENDIX C (Building Configurations Floor Weight and Loading Calculations)

Table 24 – One-family and townhouse unit area loads

System	Component	Unit Weight[1] (psf)
Roof/ Ceiling	Gypsum	2.2
	2x Wood Truss	8
	7/16" OSB	1.4
	Insulation	1.2
	Single Ply Felt	0.7
	Asphalt Shingles	2
	Total	16
Floor/ Ceiling	Gypsum	2
	2x10 @ 16 Joist	6
	Subfloor	3
	Carpet & Pad	2
	Misc (Electrical, Plumbing, HVAC)	1
	Total	14
Exterior Wall	2x4 Framing	4
	Gypsum	2
	7/16" OSB	1.4
	Vinyl Siding	1
	Insulation	1
	Misc (Electrical, Plumbing)	0
	Total	9
Interior Wall	2x4 Framing	4
	Gypsum	4
	Misc (Electrical, Plumbing)	0
	Total	8

1. Source: ASCE 7 Table C3-1.

Table 25 – Apartment unit area loads

System	Component	Unit Weight[1] (psf)
Roof/ Ceiling	Gypsum	2.2
	2x Wood Truss	8
	7/16" OSB	1.4
	Insulation	1.2
	Single Ply Felt	0.7
	Asphalt Shingles	2
	Total	16
Floor/ Ceiling	Gypsum	2.75
	2x12 @ 16 Joist	7
	Insulation	2
	3/4" T&G Plywood	3
	Gypcrete	10
	Carpet & Pad	2
	Misc (Electrical, Plumbing, HVAC)	2
	Total	29
Exterior Wall	2x4 Framing	4
	Gypsum	2.75
	7/16" OSB	1.4
	Vinyl Siding	1
	Insulation	1
	Misc (Electrical, Plumbing)	1
	Total	11
Interior Wall	2x4 Framing	4
	Gypsum	4
	Misc (Electrical, Plumbing)	1
	Total	9

Table 26 – Building archetype loading

Building Archetype	Level	Area (ft^2)				Total Weight (kips)	# of Living Units	Shear Wall Weight (kips)	C_{vx}	V_x (kips)[1]			
				Wall						SDC			
		Roof	Floor	Exterior	Interior					B_{min} (Cs=0.026)	B_{max}/C_{min} (Cs=0.051)	C_{max}/D_{min} (Cs=0.077)	D_{max} (Cs=0.15)
1	1	1200		560	400	27.44	1	13.72	1.00	0.35	0.70	1.06	2.11
2	1	2100		760	824	47.03	1	23.52	1.00	0.60	1.19	1.81	3.62
3	1		1500	1280	1264	42.63	1	21.32	0.37	1.01	2.00	3.03	6.06
	2	1500		640	800	36.16		18.01	0.63	0.64	1.26	1.91	3.82
4	1		1920	1504	2752	62.43	4	7.80	0.39	0.36	0.71	1.08	2.15
	2	1920		752	1496	49.46		6.18	0.61	0.22	0.43	0.66	1.31
5	1		4800	2560	5312	132.74	6	11.06	0.17	0.84	1.66	2.51	5.03
	2		4800	2560	5896	137.41		11.45	0.36	0.70	1.38	2.09	4.17
	3	4800		1280	4184	121.79		10.15	0.47	0.39	0.78	1.18	2.36
6	1		4200	2080	4448	188.91	12	23.61	0.22	1.53	3.02	4.58	9.17
	2		4200	2080	4448	188.91		23.61	0.44	1.18	2.33	3.53	7.06
	3	4200		1040	2224	98.66		12.33	0.33	0.50	1.00	1.51	3.03
7	1		8400	3040	11232	386.53	32	24.16	0.13	1.92[2]	3.81[2]	6.49[2]	13.10
	2		8400	3040	11232	386.53		24.16	0.25	1.69[2]	3.35[2]	5.71[2]	11.53
	3		8400	3040	11232	386.53		24.16	0.38	1.21[2]	2.40[2]	4.09[2]	8.25
	4	8400		1520	5616	201.66		12.60	0.25	0.48[2]	0.95[2]	1.62[2]	3.28
8	1		8400	3040	11232	386.53	40	24.16	0.08	2.08[2]	4.13[2]	7.04[2]	16.82
	2		8400	3040	11232	386.53		24.16	0.16	1.92[2]	3.80[2]	6.48[2]	15.48
	3		8400	3040	11232	386.53		24.16	0.24	1.58[2]	3.14[2]	5.35[2]	12.78
	4		8400	3040	11232	386.53		24.16	0.32	1.08[2]	2.15[2]	3.66[2]	8.75
	5	8400		1520	5616	201.66		12.60	0.20	0.42[2]	0.83[2]	1.41[2]	3.36

1. The seismic coefficient (C_s) used in shear calculation is determined by S_{DS}/R.
2. The seismic coefficient (C_s) used in shear calculation is determined by $S_{D1}/T/R$.

APPENDIX D (Cyclic Test Data and Curve Fitting Results Comparisons)

NAHB Research Center Curve Fitting Procedure Results

CUREE (CUREE, Low) Shear Wall with 0.5:1 Aspect Ratio

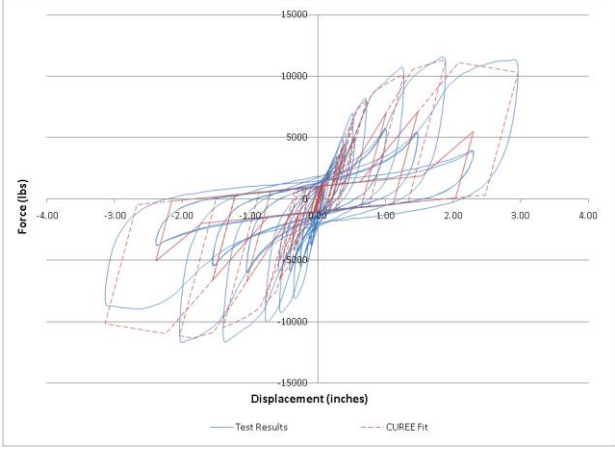

Figure 50 – CUREE-Caltech specimen 4a-p hysteresis

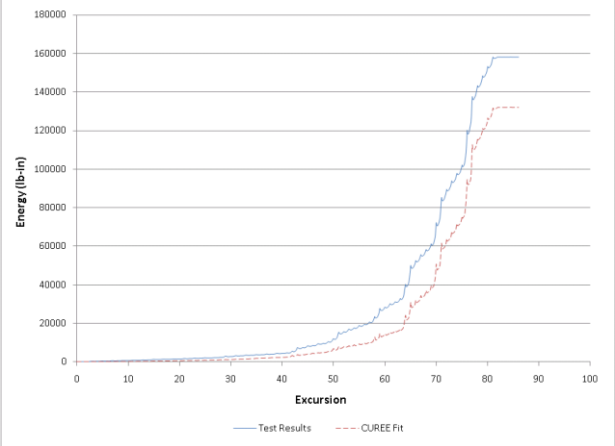

Figure 51 – CUREE-Caltech specimen 4a-p dissipated energy

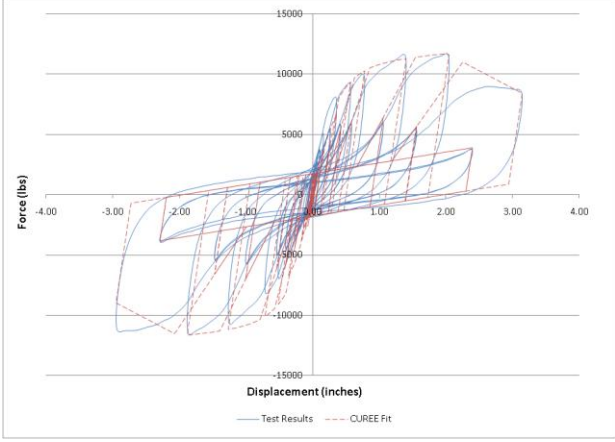

Figure 52 – CUREE-Caltech specimen 4a-n hysteresis

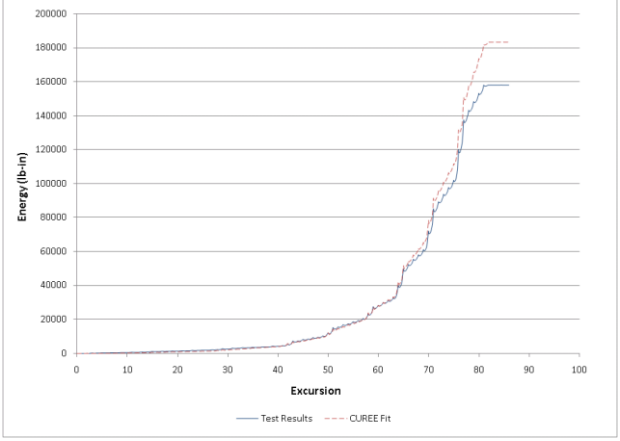

Figure 53 – CUREE-Caltech specimen 4a-n dissipated energy

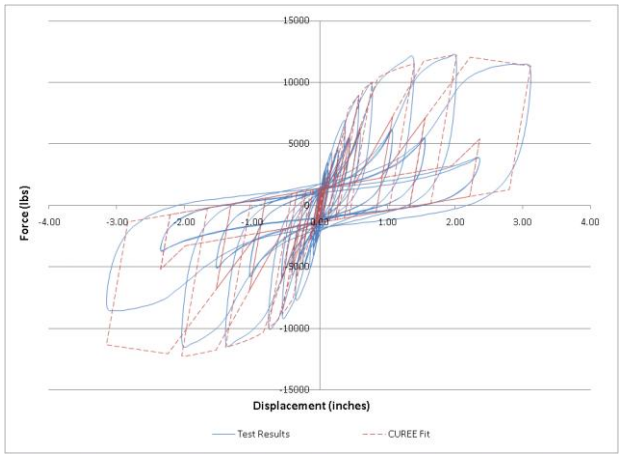

Figure 54 – CUREE-Caltech specimen 4b-p hysteresis

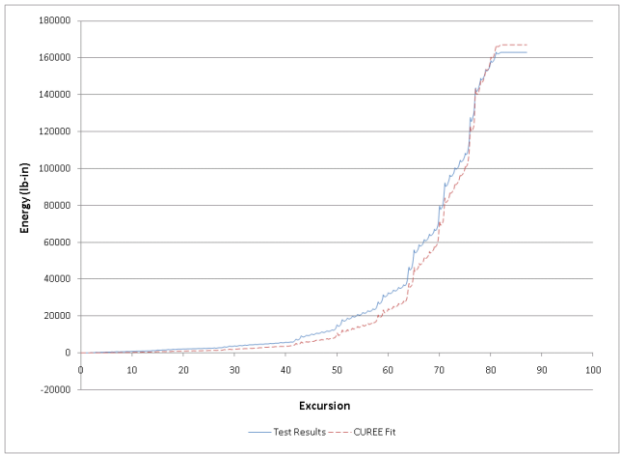

Figure 55 – CUREE-Caltech specimen 4b-p dissipated energy

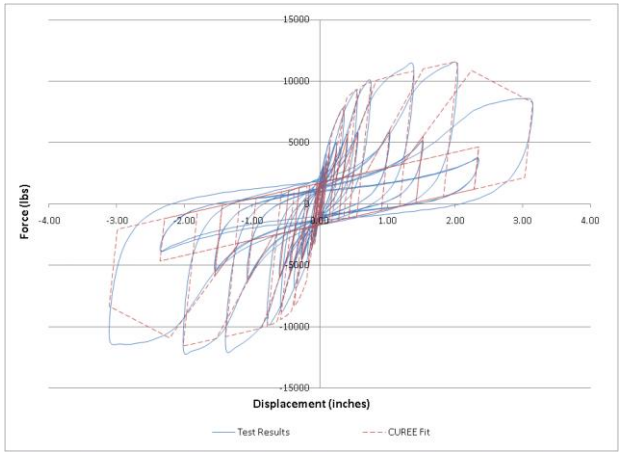

Figure 56 – CUREE-Caltech specimen 4b-n hysteresis

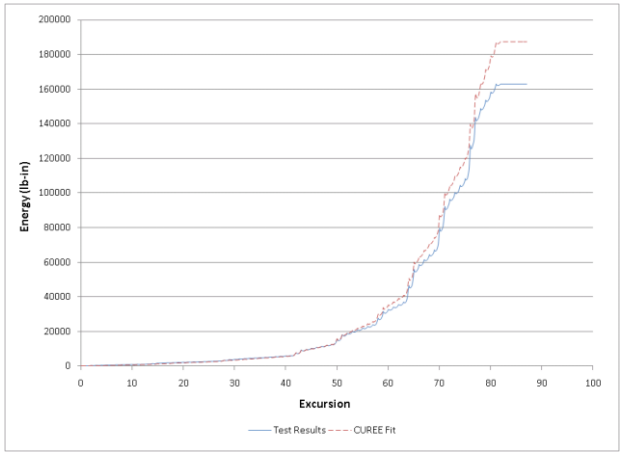

Figure 57 – CUREE-Caltech specimen 4b-n dissipated energy

CUREE (CUREE, Low) Shear Wall with 1.23:1 Aspect Ratio

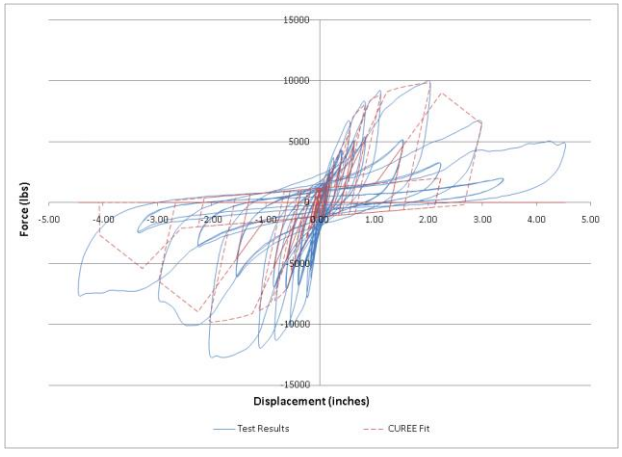

Figure 58 – CUREE-Caltech specimen 6a-p hysteresis

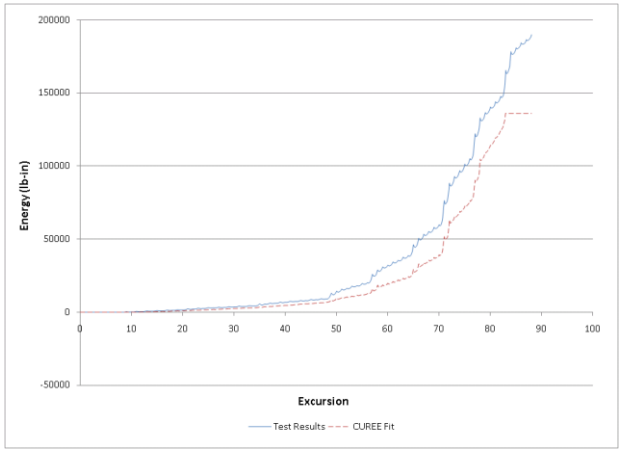

Figure 59 – CUREE-Caltech specimen 6a-p dissipated energy

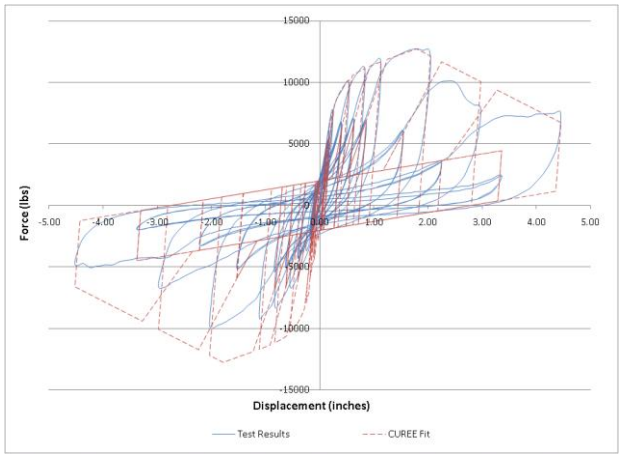

Figure 60 – CUREE-Caltech specimen 6a-n hysteresis

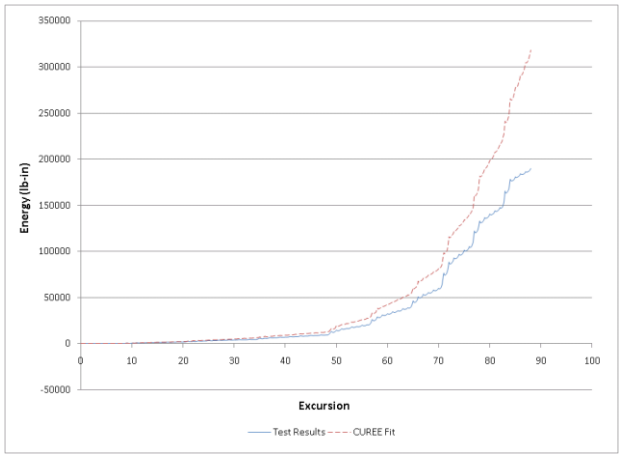

Figure 61 – CUREE-Caltech specimen 6a-n dissipated energy

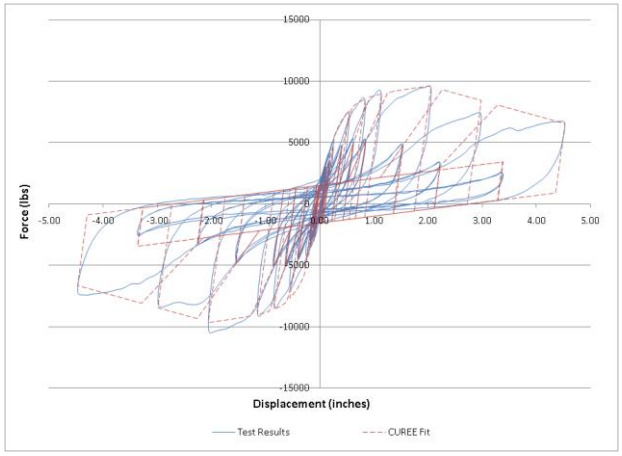

Figure 62 – CUREE-Caltech specimen 6b-p hysteresis

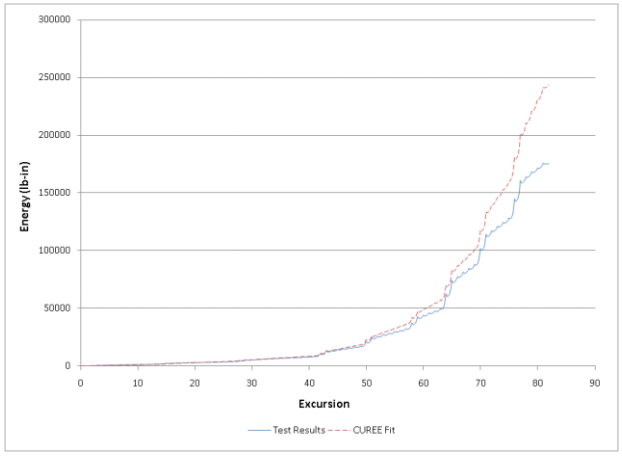

Figure 63 – CUREE-Caltech specimen 6b-p dissipated energy

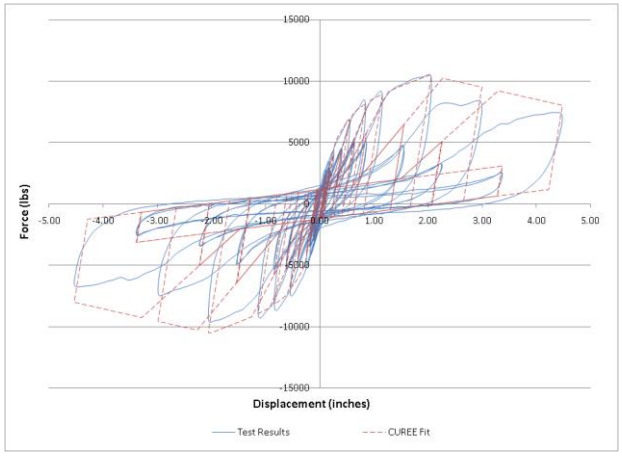

Figure 64 – CUREE-Caltech specimen 6b-n hysteresis

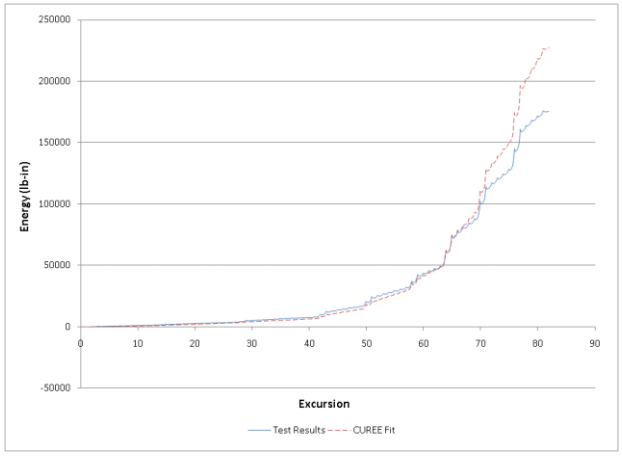

Figure 65 – CUREE-Caltech specimen 6b-n dissipated energy

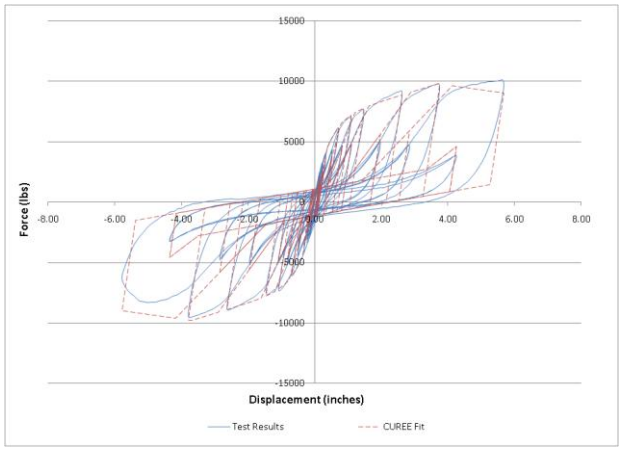

Figure 66 – CUREE-Caltech specimen 8a-p hysteresis

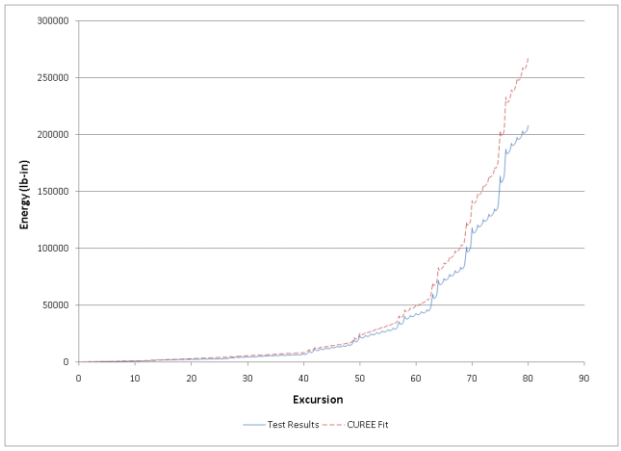

Figure 67 – CUREE-Caltech specimen 8a-p dissipated energy

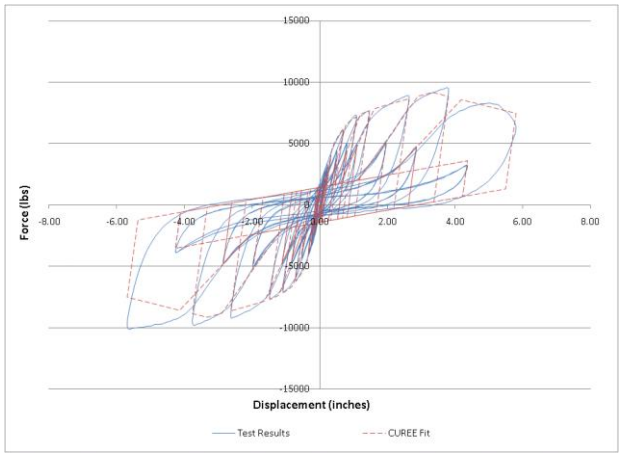

Figure 68 – CUREE-Caltech specimen 8a-n hysteresis

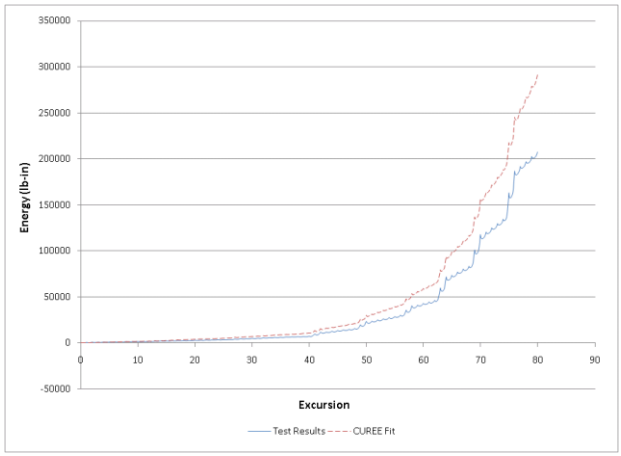

Figure 69 – CUREE-Caltech specimen 8a-n dissipated energy

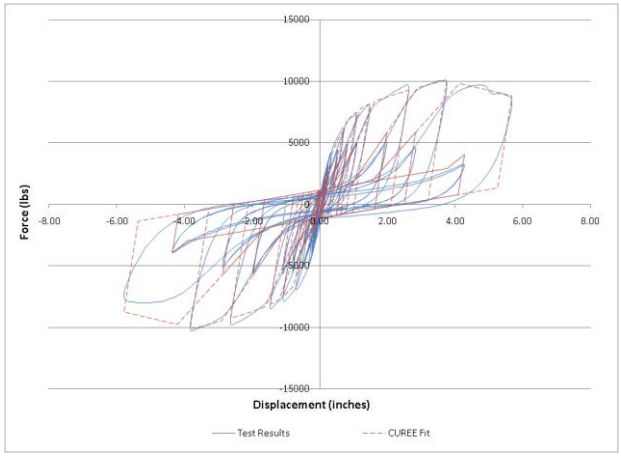

Figure 70 – CUREE-Caltech specimen 8b-p hysteresis

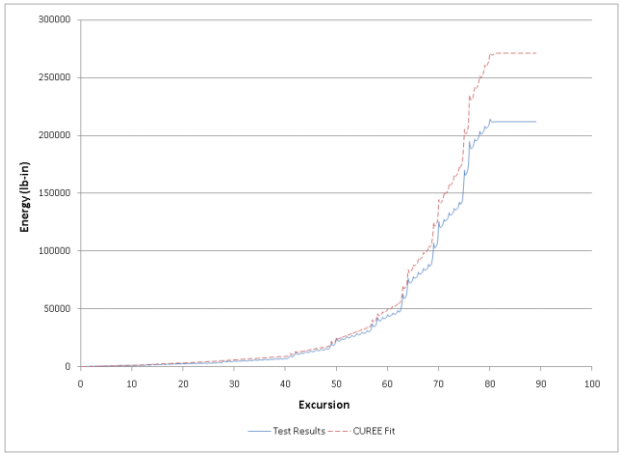

Figure 71 – CUREE-Caltech specimen 8b-p dissipated energy

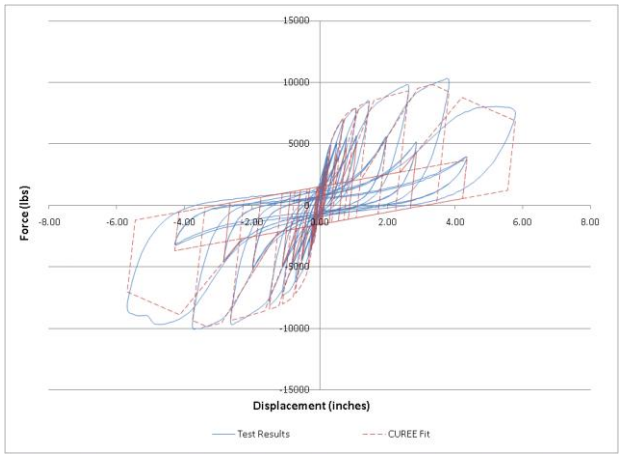

Figure 72 – CUREE-Caltech specimen 8b-n hysteresis

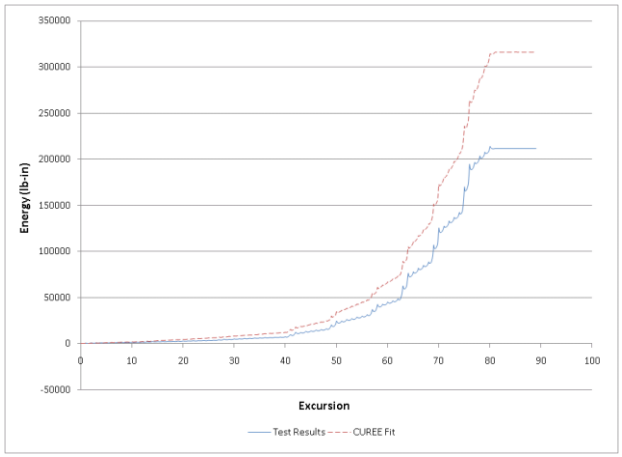

Figure 73 – CUREE-Caltech specimen 8b-n dissipated energy

CUREE (CUREE, High) Shear Wall with 2.56:1 Aspect Ratio

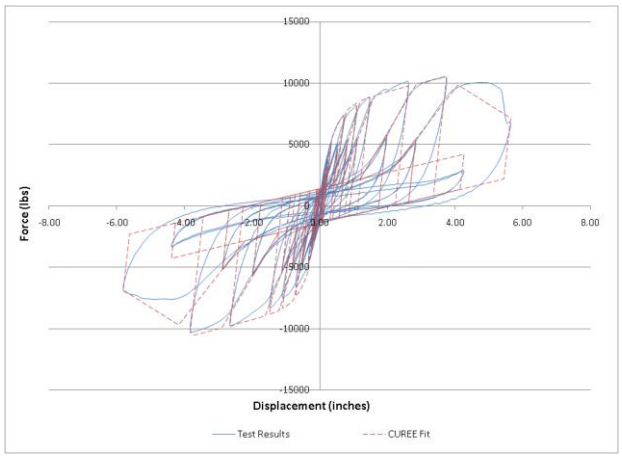

Figure 74 – CUREE-Caltech specimen 10a-p hysteresis

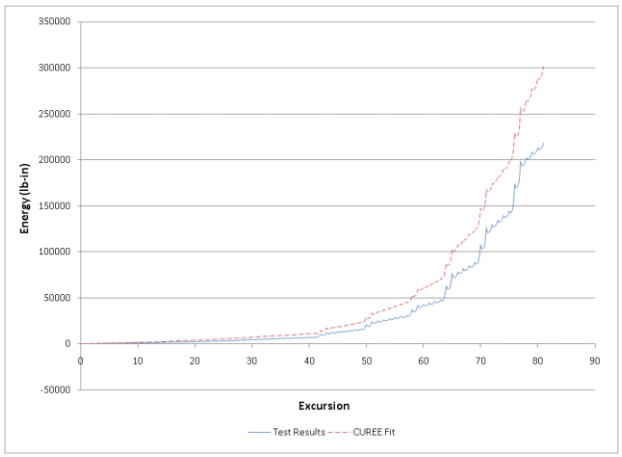

Figure 75 – CUREE-Caltech specimen 10a-p dissipated energy

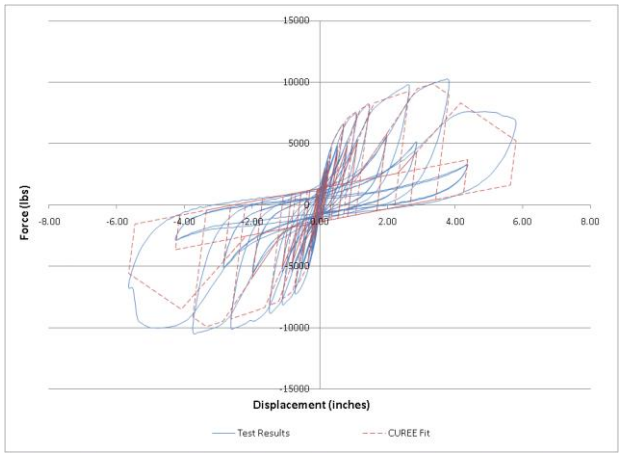

Figure 76 – CUREE-Caltech specimen 10a-n hysteresis

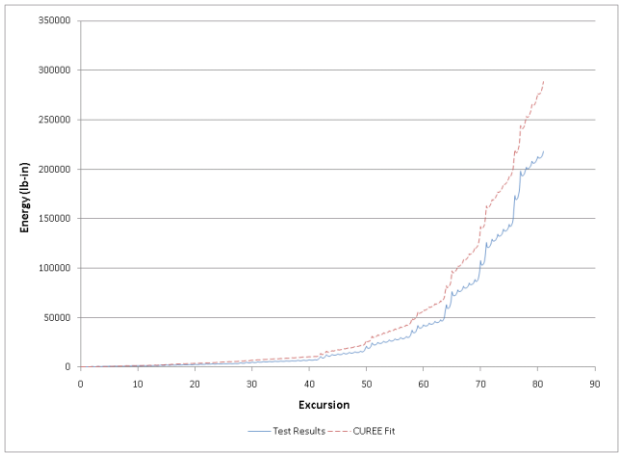

Figure 77 – CUREE-Caltech specimen 10a-n dissipated energy

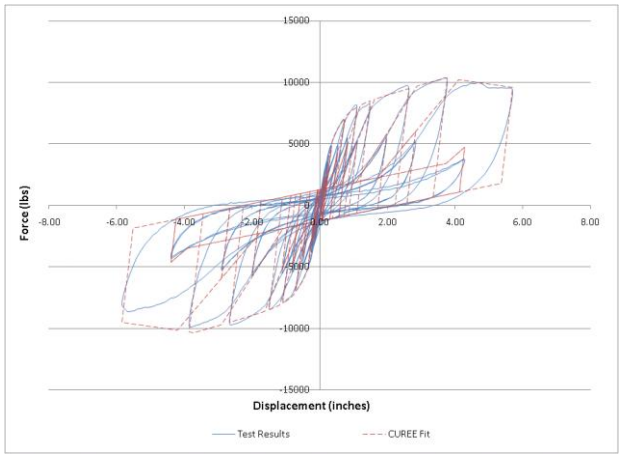

Figure 78 – CUREE-Caltech specimen 10b-p hysteresis

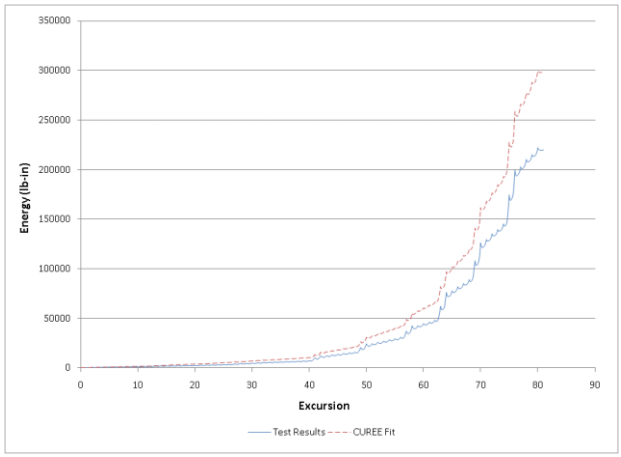

Figure 79 – CUREE-Caltech specimen 10b-p dissipated energy

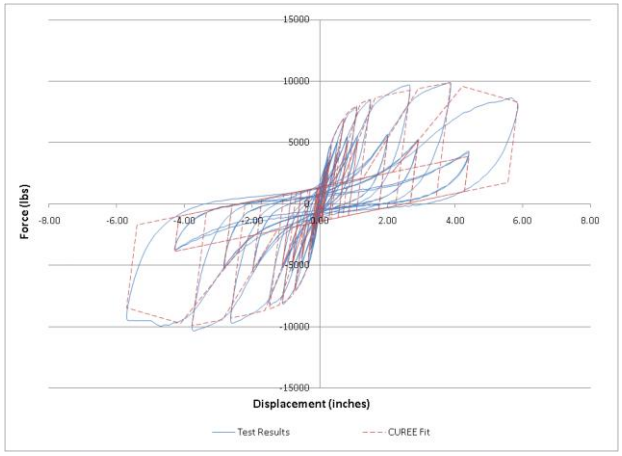

Figure 80 – CUREE-Caltech specimen 10b-n hysteresis

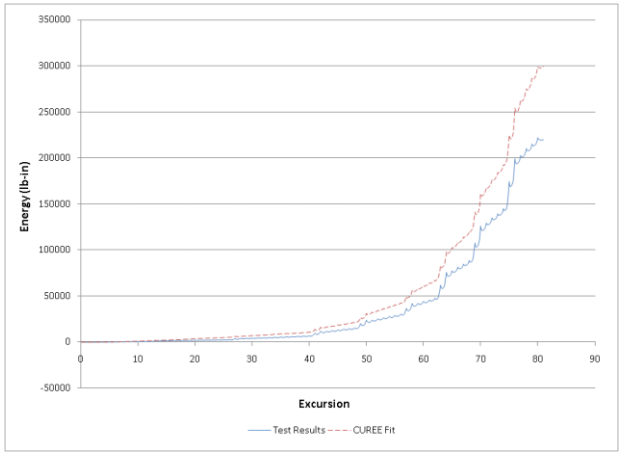

Figure 81 – CUREE-Caltech specimen 10b-n dissipated energy

FPL Curve Fitting Procedure Results

APA (SPD, Low) Shear Wall with 1:1 Aspect Ratio

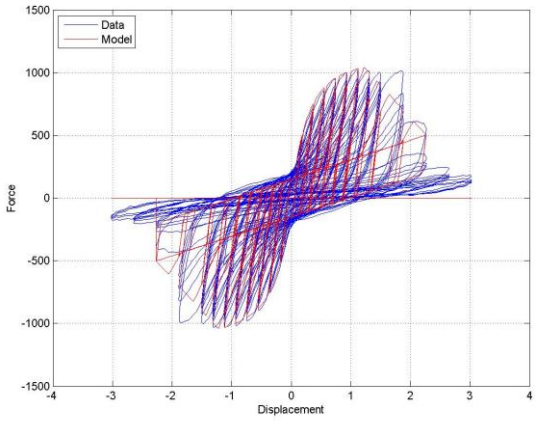

Figure 82 – APA specimen a4a hysteresis

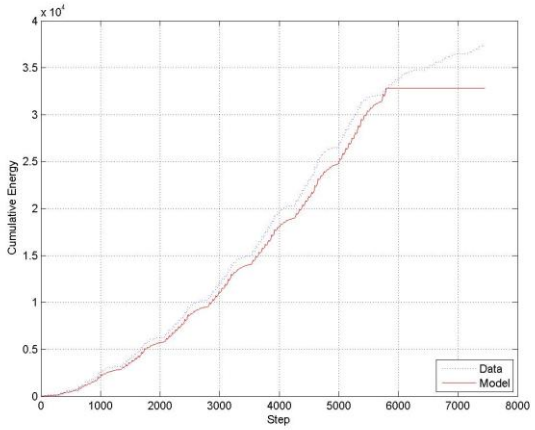

Figure 83 – APA specimen a4a dissipated energy

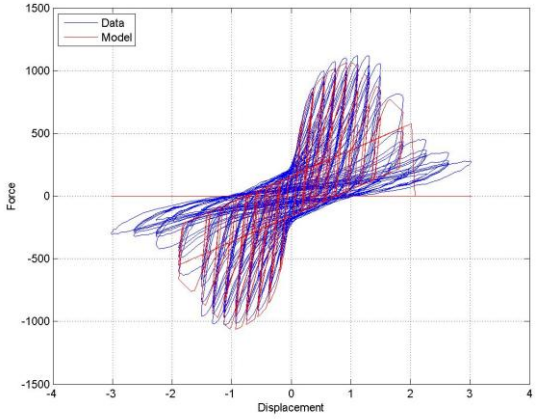

Figure 84 – APA specimen a4b hysteresis

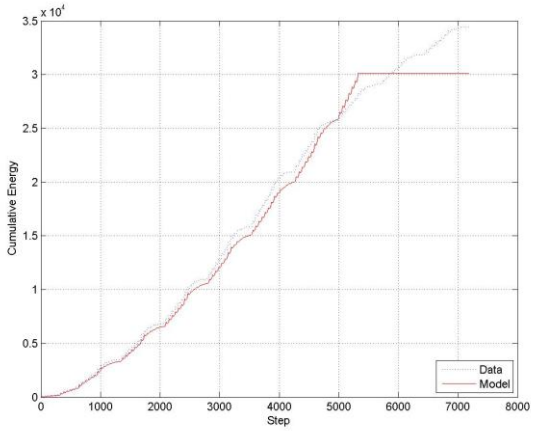

Figure 85 – APA specimen a4b dissipated energy

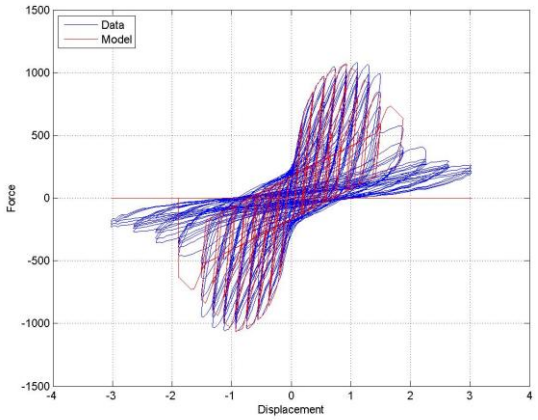

Figure 86 – APA specimen a4c hysteresis

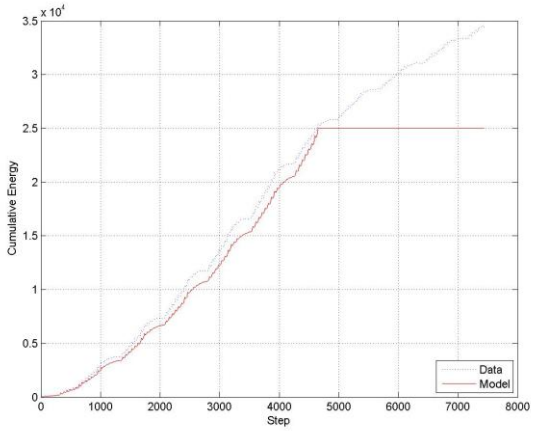

Figure 87 – APA specimen a4c dissipated energy

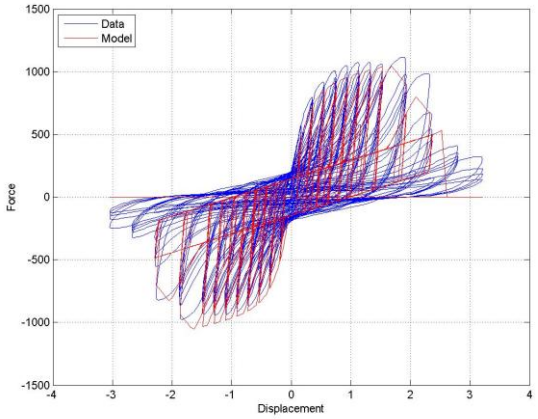

Figure 88 – APA specimen b1a hysteresis

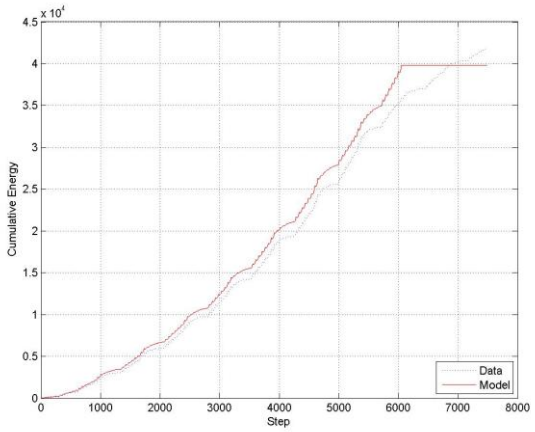

Figure 89 – APA specimen b1a dissipated energy

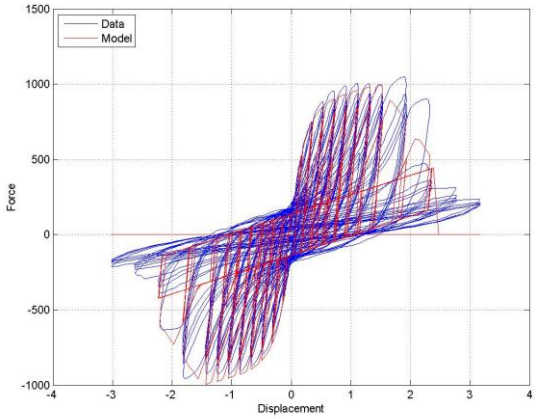

Figure 90 – APA specimen b1b hysteresis

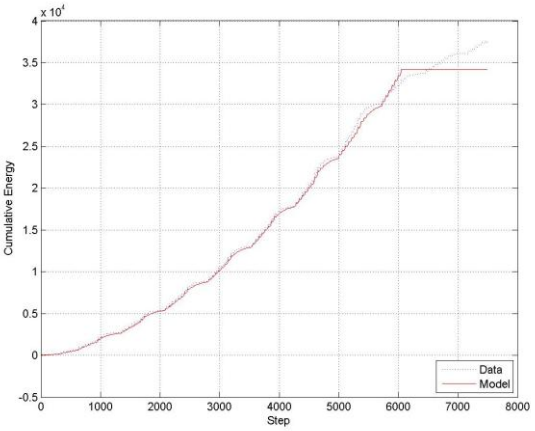

Figure 91 – APA specimen b1b dissipated energy

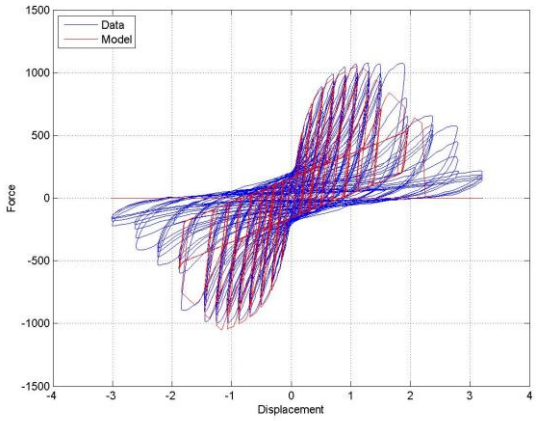

Figure 92 – APA specimen b2a hysteresis

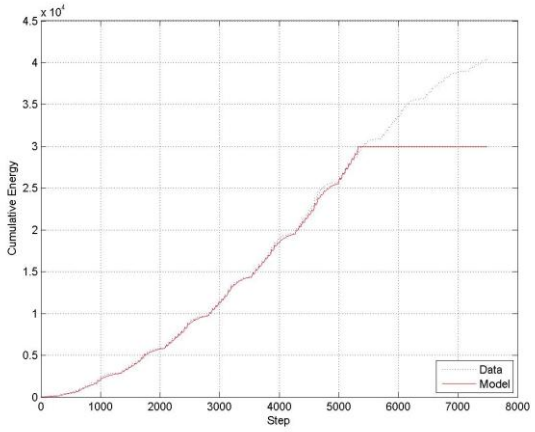

Figure 93 – APA specimen b2a dissipated energy

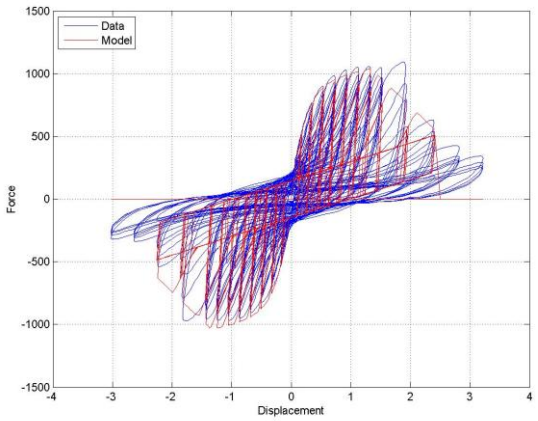

Figure 94 – APA specimen b2b hysteresis

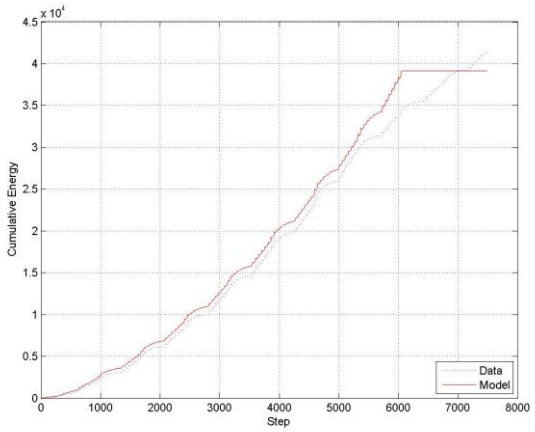

Figure 95 – APA specimen b2b dissipated energy

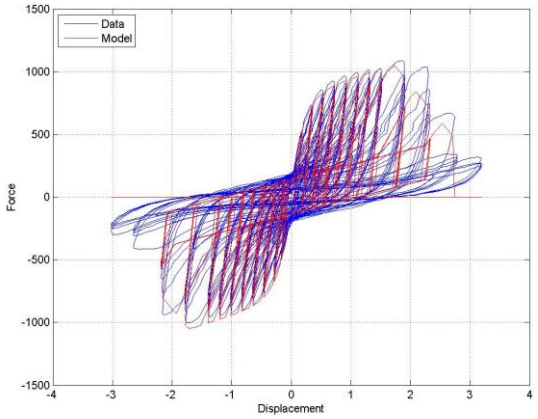

Figure 96 – APA specimen b3a hysteresis

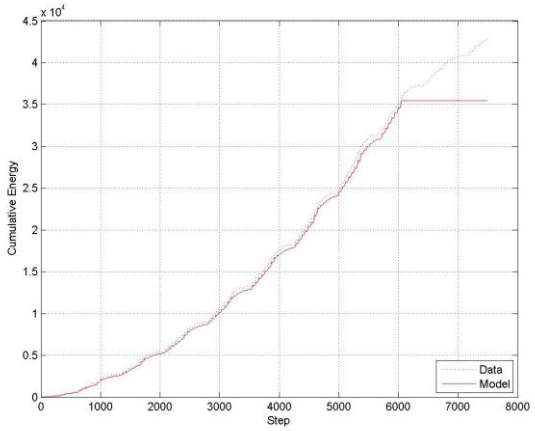

Figure 97 – APA specimen b3a dissipated energy

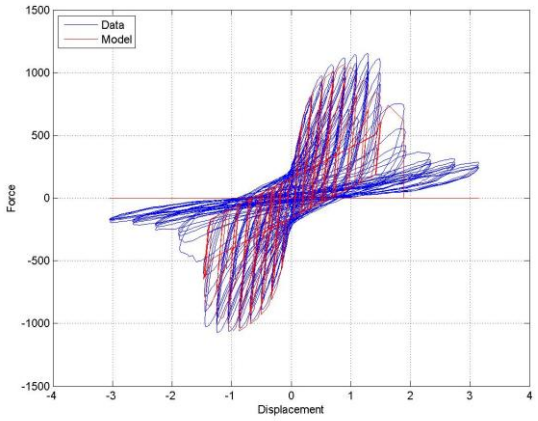

Figure 98 – APA specimen b4a hysteresis

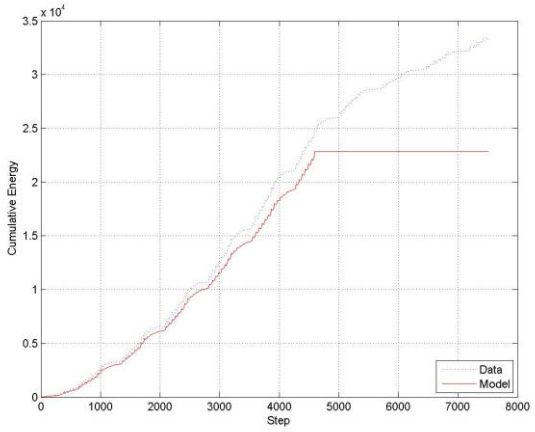

Figure 99 – APA specimen b4a dissipated energy

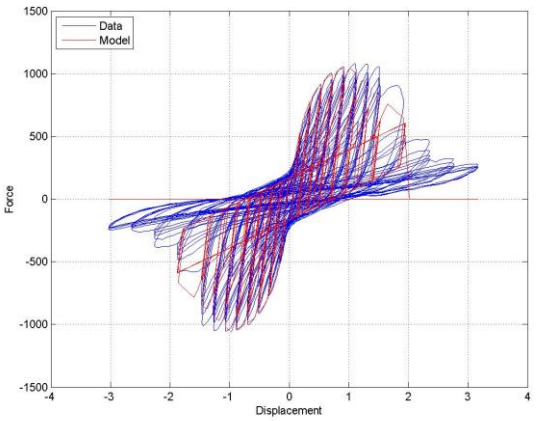

Figure 100 – APA specimen b4a hysteresis

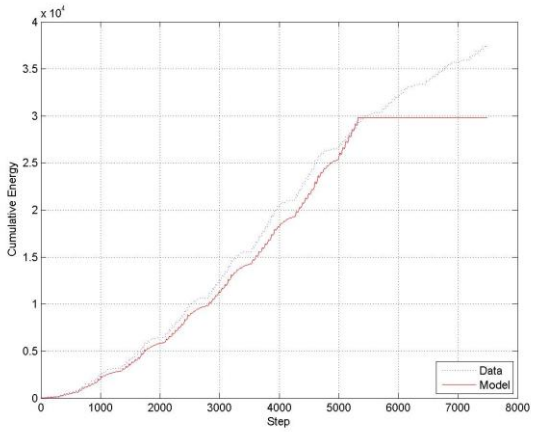

Figure 101 – APA specimen b4a dissipated energy

APA (SPD, Mid) Shear Wall with 2:1 Aspect Ratio

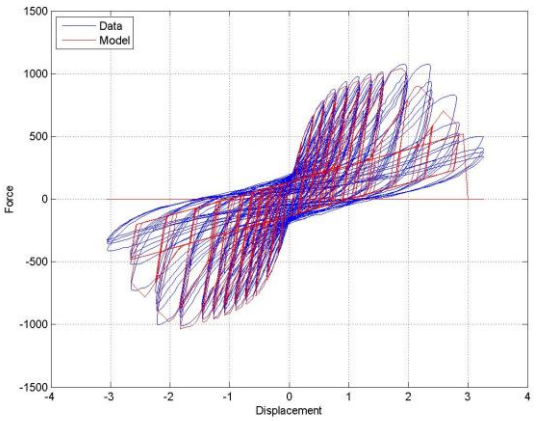

Figure 102 – APA specimen c2a hysteresis

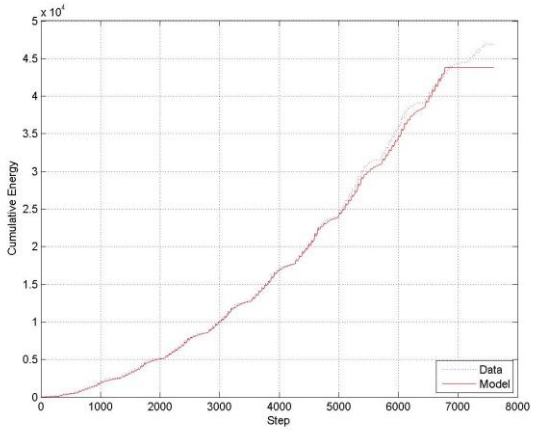

Figure 103 – APA specimen c2a dissipated energy

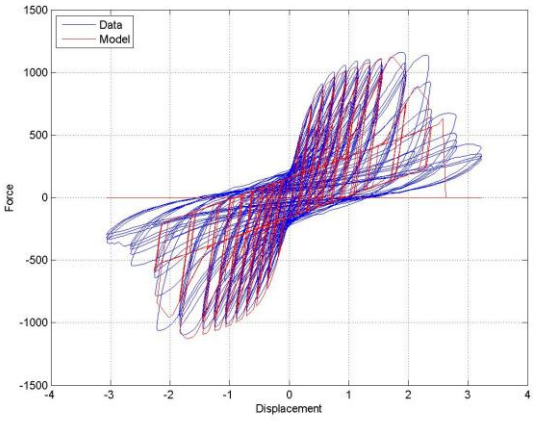

Figure 104 – APA specimen c2b hysteresis

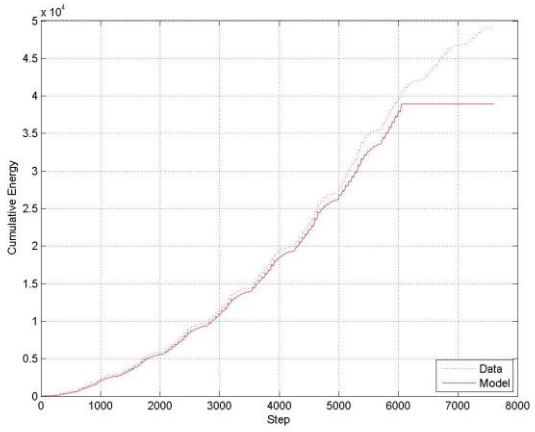

Figure 105 – APA specimen c2b dissipated energy

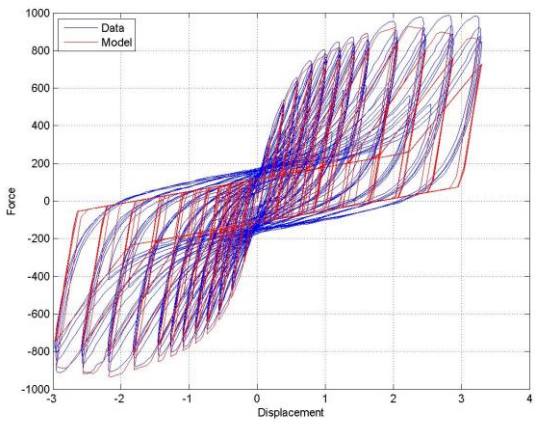

Figure 106 – APA specimen c3a hysteresis

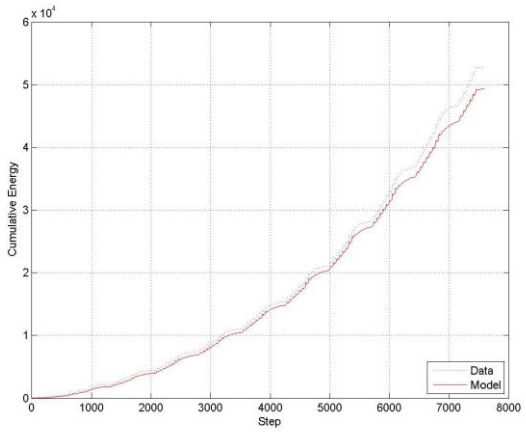

Figure 107 – APA specimen c3a dissipated energy

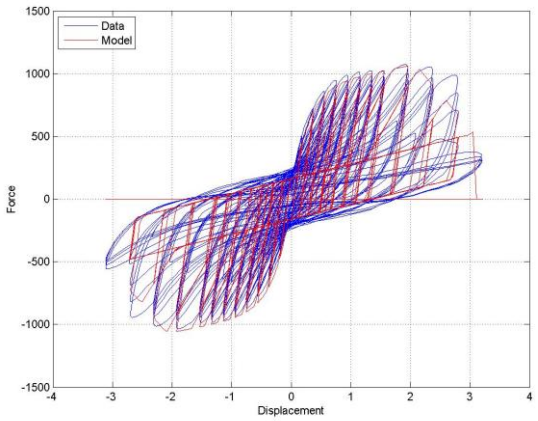

Figure 108 – APA specimen c3b hysteresis

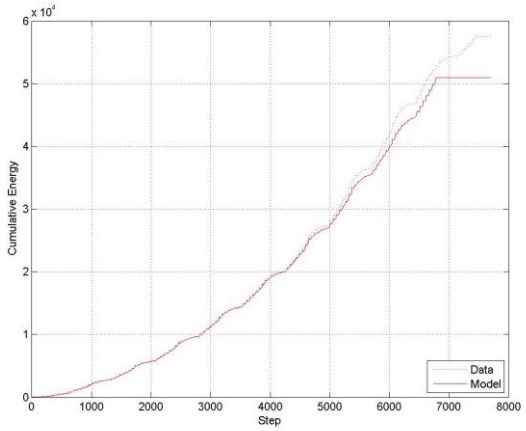

Figure 109 – APA specimen c3b dissipated energy

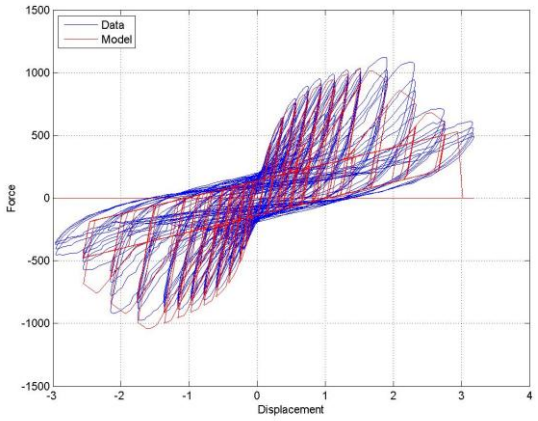

Figure 110 – APA specimen c4a hysteresis

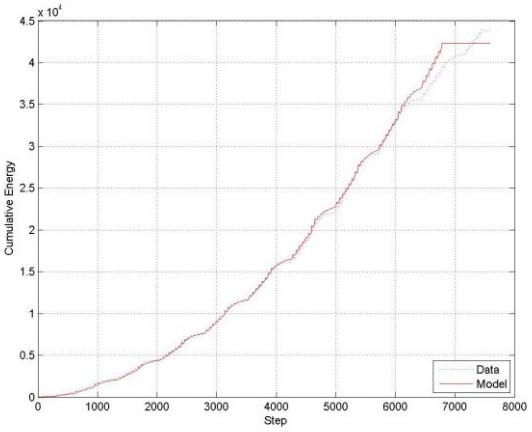

Figure 111 – APA specimen c4a dissipated energy

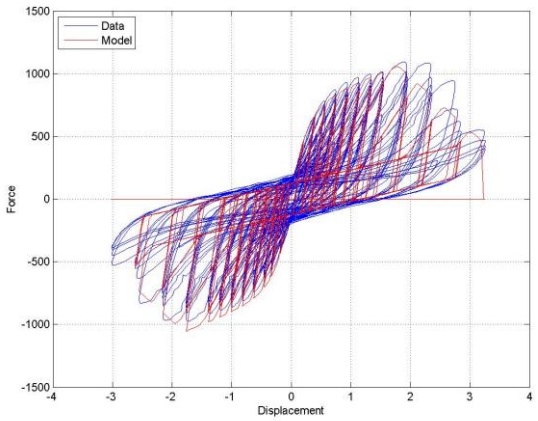

Figure 112 – APA specimen c4b hysteresis

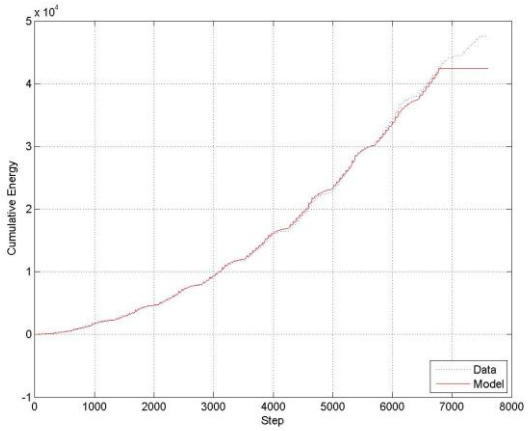

Figure 113 – APA specimen c4b dissipated energy

APA (SPD, High) Shear Wall with 4:1 Aspect Ratio

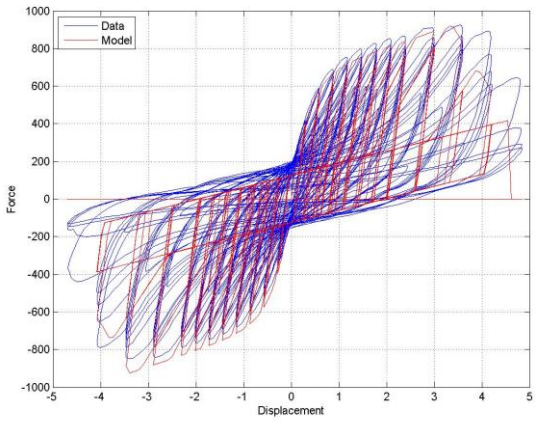

Figure 114 – APA specimen c1a hysteresis

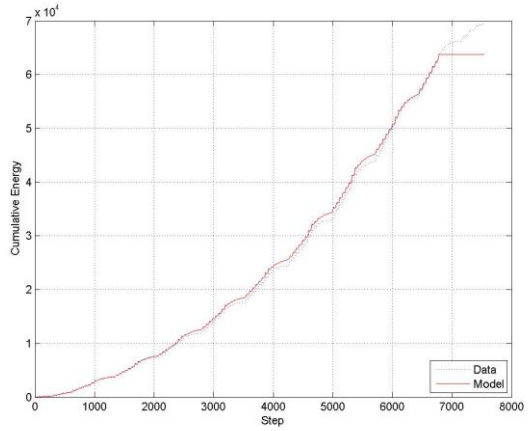

Figure 115 – APA specimen c1a dissipated energy

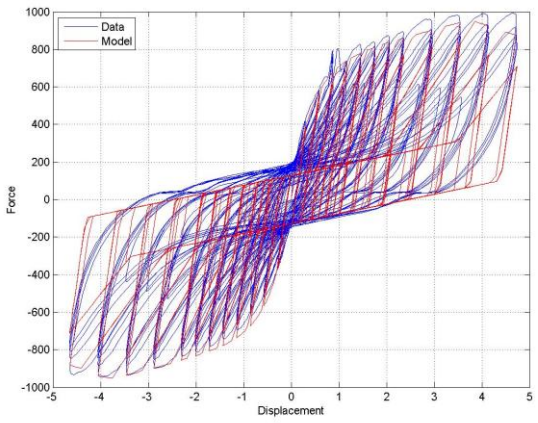

Figure 116 – APA specimen c1b hysteresis

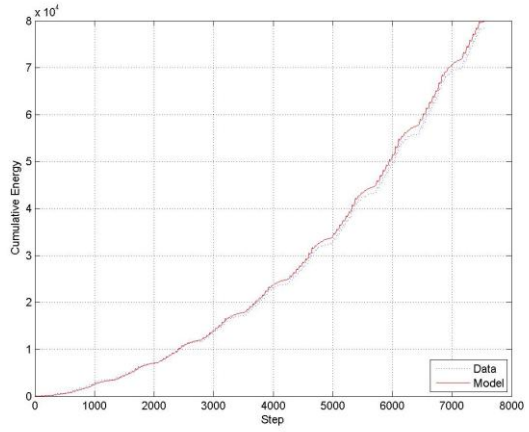

Figure 117 – APA specimen c1b dissipated energy

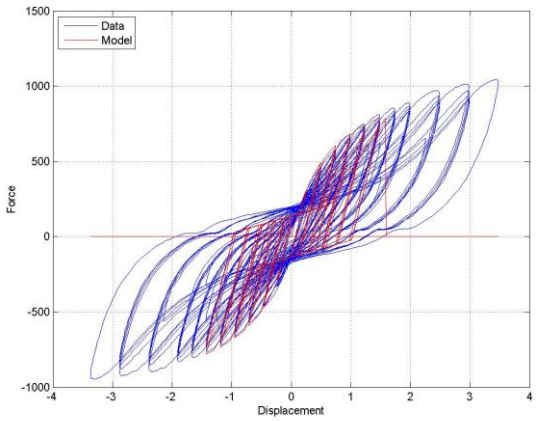

Figure 118 – APA specimen c1c hysteresis

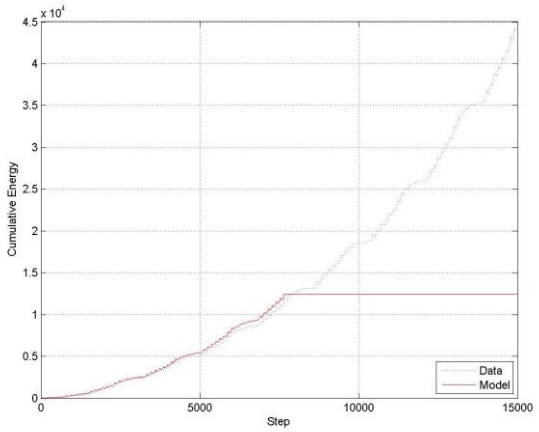

Figure 119 – APA specimen c1c dissipated energy

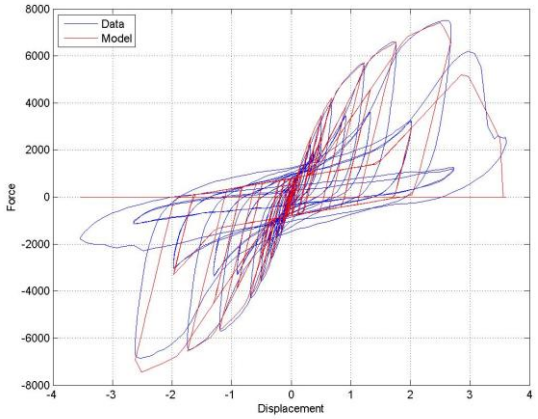

Figure 120 – APA specimen c1d hysteresis

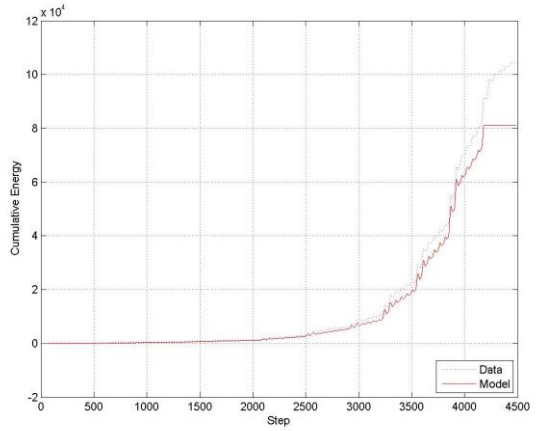

Figure 121 – APA specimen c1d dissipated energy

APA (CUREE, Low) Shear Wall with 1:1 Aspect Ratio

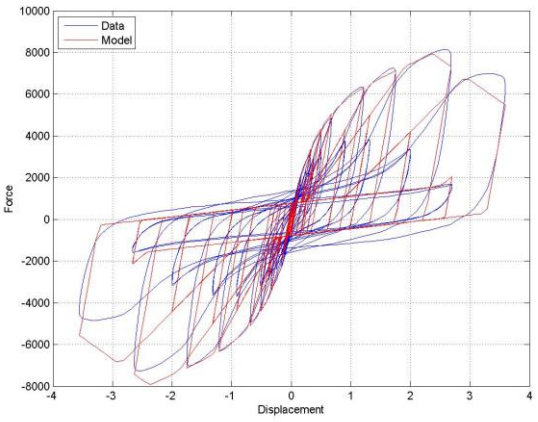

Figure 122 – APA specimen GD2 hysteresis

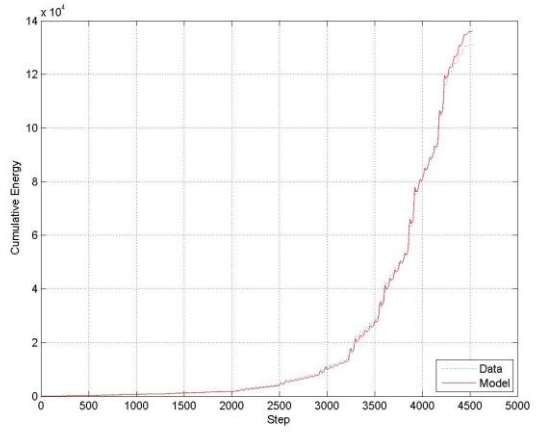

Figure 123 – APA specimen GD2 dissipated energy

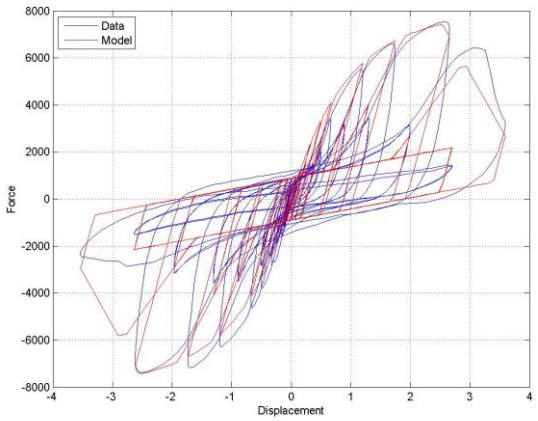

Figure 124 – APA specimen GD3 hysteresis

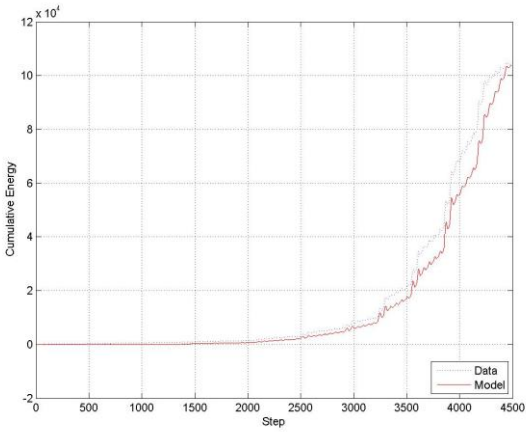

Figure 125 – APA specimen GD3 dissipated energy

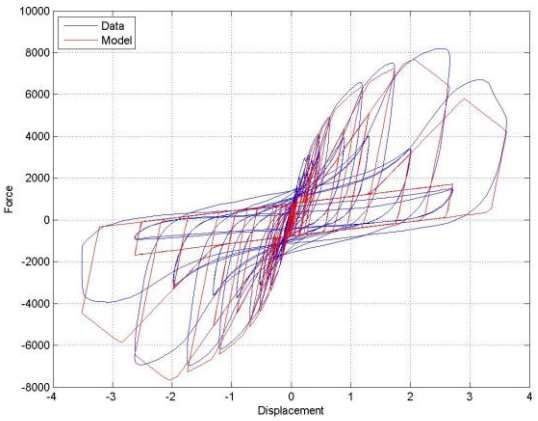

Figure 126 – APA specimen GD4 hysteresis

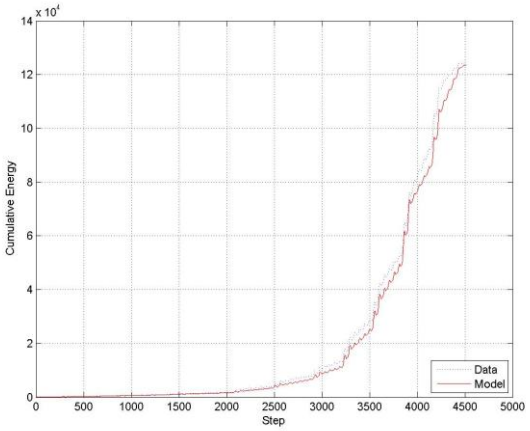

Figure 127 – APA specimen GD4 dissipated energy

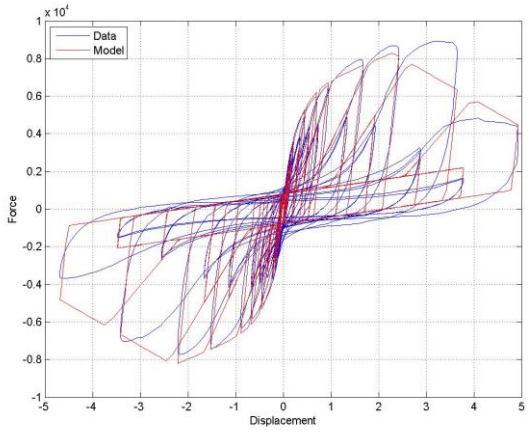

Figure 128 – APA specimen 2-8dgb hysteresis

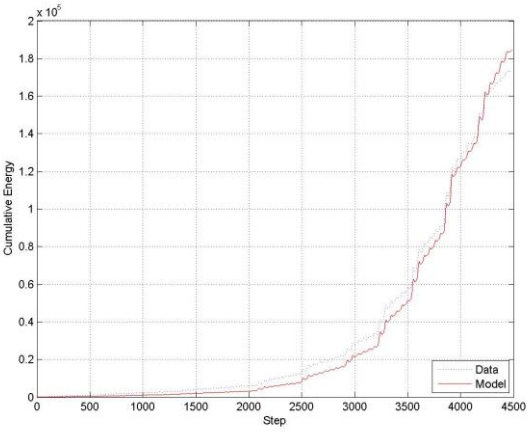

Figure 129 – APA specimen 2-8dgb dissipated energy

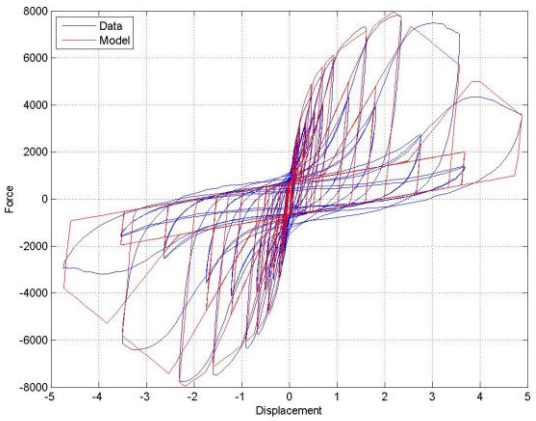

Figure 130 – APA specimen 3-8db hysteresis

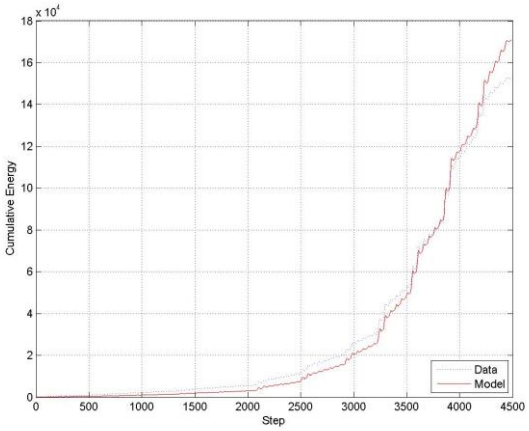

Figure 131 – APA specimen 3-8db dissipated energy

APPENDIX E (CUREE Parameters from NAHB Research Center Curve Fitting Procedure)

Table 27 – CUREE parameters for CUREE-Caltech test data

Test Program	Test Config.	F_0 (plf)	F_I (plf)	K_0 (plf/in)	r_1	r_2	r_3	r_4	δ_u (in)	α	β
CUREE-Caltech	4a	0.87	0.12	2.45	0.032	-0.062	1.000	0.026	1.925	0.76	1.09
	4b	0.84	0.13	3.54	0.027	-0.041	1.000	0.028	1.993	0.76	1.09
	6a	1.02	0.17	4.09	0.021	-0.105	1.000	0.015	1.893	0.76	1.09
	6b	0.82	0.14	3.14	0.040	-0.037	1.000	0.019	2.019	0.76	1.09
	8a	0.78	0.15	2.22	0.042	-0.028	1.000	0.026	3.516	0.76	1.09
	8b	0.86	0.16	2.45	0.036	-0.043	1.000	0.024	3.520	0.76	1.09
	10a	0.84	0.15	2.68	0.035	-0.080	1.000	0.025	3.525	0.76	1.09
	10b	0.89	0.16	2.61	0.030	-0.027	1.000	0.026	3.770	0.76	1.09

APPENDIX F (CUREE Parameters from FPL Curve Fitting Procedure)

Table 28 – CUREE parameters for APA test data

Test Program	Test Config.	F_0 (plf)	F_I (plf)	K_0 (plf/in)	r_1	r_2	r_3	r_4	δ_u (in)	α	β
APA Report T2001L-47	a4a	0.72	0.12	3.06	0.031	-0.134	1.000	0.040	1.218	0.76	1.09
	a4b	0.73	0.13	3.99	0.032	-0.092	1.000	0.041	1.002	0.76	1.09
	a4c	0.76	0.13	3.92	0.024	-0.095	1.000	0.049	0.953	0.76	1.09
	b1a	0.68	0.12	3.11	0.031	-0.149	1.000	0.038	1.662	0.76	1.09
	b1b	0.67	0.11	3.63	0.023	-0.124	1.000	0.028	1.490	0.76	1.09
	b2a	0.67	0.13	3.39	0.044	-0.105	1.000	0.045	1.152	0.76	1.09
	b2a	0.72	0.12	3.48	0.023	-0.103	1.000	0.034	1.339	0.76	1.09
	b3a	0.63	0.11	3.56	0.034	-0.128	1.000	0.027	1.722	0.76	1.09
	b4a	0.67	0.13	4.18	0.048	-0.090	1.000	0.046	0.928	0.76	1.09
	b4b	0.75	0.13	3.32	0.031	-0.106	1.000	0.054	0.983	0.76	1.09
	c2a	0.63	0.11	2.46	0.042	-0.157	1.000	0.042	1.888	0.76	1.09
	c2b	0.73	0.12	2.81	0.035	-0.168	1.000	0.048	1.730	0.76	1.09
	c3a	0.56	0.09	1.73	0.048	-0.030	1.000	0.030	2.145	0.76	1.09
	c3b	0.70	0.13	2.70	0.026	-0.163	1.000	0.035	2.084	0.76	1.09
	c4a	0.59	0.11	2.47	0.062	-0.125	1.000	0.043	1.612	0.76	1.09
	c4b	0.56	0.10	2.66	0.059	-0.127	1.000	0.032	1.796	0.76	1.09
	c1a	0.54	0.10	1.67	0.045	-0.086	1.000	0.023	3.331	0.76	1.09
	c1b	0.50	0.10	1.61	0.042	-0.213	1.000	0.032	3.384	0.76	1.09
	c1c	0.56	0.10	1.41	0.039	-0.048	1.000	0.031	3.755	0.76	1.09
	c1d	0.48	0.11	1.26	0.085	-0.346	1.000	0.071	3.568	0.76	1.09
APA Report T2003-22 and T2004-14	1	0.67	0.10	3.92	0.038	-0.063	1.000	0.011	2.032	0.76	1.09
	2	0.65	0.10	3.60	0.047	-0.058	1.000	0.016	1.370	0.76	1.09
	3	0.72	0.10	2.81	0.025	-0.094	1.000	0.014	2.637	0.76	1.09
	4	0.62	0.09	3.48	0.034	-0.073	1.000	0.008	2.298	0.76	1.09
	2-8dgb	0.75	0.10	2.99	0.045	-0.062	1.000	0.016	2.298	0.76	1.09
	3-8db	0.62	0.09	2.88	0.062	-0.073	1.000	0.016	2.193	0.76	1.09

APPENDIX G (Shear Wall Calculations)

Table 29 – Shear wall design lengths for archetypes with CUREE shear wall configurations in SDCs B_{min}, B_{max}/C_{min}, and C_{max}/D_{min}

Building Configuration	Floor	Shear Wall Configuration							
		CUREE (CUREE, Low)				CUREE (CUREE, High)			
		Seismic Design Category							
		B_{min}	B_{max}/C_{min}	C_{max}/D_{min}	D_{max}	B_{min}	B_{max}/C_{min}	C_{max}/D_{min}	D_{max}
1	1	0.90	1.70	2.60	5.10	0.50	0.90	1.40	2.70
2	1	1.50	2.90	4.40	8.70	0.80	1.60	2.40	4.70
3	1	2.50	4.80	7.30	14.60	1.30	2.60	3.90	7.80
	2	1.60	3.10	4.60	9.20	0.90	1.70	2.50	4.90
4	1	0.90	1.80	2.60	5.20	0.50	1.00	1.40	2.80
	2	0.60	1.10	1.60	3.20	0.30	0.60	0.90	1.70
5	1	2.10	4.00	6.10	12.10	1.10	2.20	3.30	6.50
	2	1.70	3.30	5.00	10.00	0.90	1.80	2.70	5.40
	3	1.00	1.90	2.90	5.70	0.60	1.10	1.60	3.10
6	1	3.70	7.20	10.90	22.00	2.00	3.90	5.90	11.80
	2	2.90	5.60	8.50	17.20	1.60	3.00	4.60	9.20
	3	1.30	2.40	3.70	7.60	0.70	1.30	2.00	4.10
7	1	4.60	9.40	15.50	31.40	2.50	5.00	8.30	16.80
	2	4.00	8.20	13.60	27.50	2.20	4.40	7.30	14.70
	3	2.90	5.90	9.70	19.80	1.60	3.20	5.20	10.60
	4	1.20	2.40	3.90	8.10	0.70	1.30	2.10	4.40
8	1	5.00	10.20	16.90	-	2.70	5.50	9.00	21.50
	2	4.60	9.40	15.50	-	2.50	5.00	8.30	19.80
	3	3.80	7.80	12.80	-	2.10	4.20	6.90	16.40
	4	2.60	5.30	8.80	-	1.40	2.90	4.70	11.30
	5	1.00	2.10	3.40	-	0.60	1.10	1.80	4.50

1. Shear wall design lengths in the 1st floor for archetype configuration 8 with the CUREE (CUREE, Low) shear wall response in SDC D_{max} exceed building wall dimensions and therefore are not included in this analysis.

APPENDIX H (Performance Group Index Archetype FEMA P695 Nonlinear Analysis Results)

Table 30 – Collapse performance results for the performance groups using SWM-1 (CUREE-Caltech, CUREE protocol, low aspect ratio)

Performance Group		FEMA P695 Analysis Parameters				
Archetype		Ω	μ_T	$\hat{S}_{CT}$	SSF	$ACMR$
Performance Group	Building Configuration					
1	1	1.95	10.18	0.70	1.14	3.19
	2	1.89	10.35	0.74	1.14	3.37
	3	1.88	9.50	0.82	1.16	3.79
	4	1.91	8.41	0.82	1.14	3.75
	5	1.91	9.83	0.91	1.16	4.22
	6	1.86	8.70	0.87	1.15	3.99
	7	1.62	8.57	0.86	1.15	4.53
2	1	1.86	10.58	0.86	1.14	1.96
	2	1.85	10.52	0.86	1.14	1.96
	3	0.60	9.37	0.97	1.15	2.24
	4	0.64	13.95	0.97	1.20	2.33
	5	1.84	10.82	1.06	1.17	2.48
	6	1.83	12.07	1.06	1.18	2.50
	7	1.67	8.97	1.09	1.14	2.73
3	1	1.88	10.43	0.97	1.14	1.47
	2	1.85	10.19	0.97	1.14	1.47
	3	1.83	11.08	1.13	1.17	1.76
	4	1.84	10.56	1.17	1.17	1.82
	5	1.85	10.61	1.23	1.17	1.91
	6	1.83	9.62	1.19	1.14	1.81
	7	1.82	9.97	1.23	1.16	1.90
4	1	2.35	11.24	1.48	1.33	1.31
	2	1.96	11.18	1.36	1.33	1.21
	3	1.85	9.51	1.56	1.33	1.38
	4	2.30	7.78	1.48	1.32	1.31
	5	2.00	9.64	1.74	1.33	1.54
	6	1.90	9.24	1.67	1.33	1.48
	7	1.88	12.50	1.66	1.33	1.47

5	1	2.36	10.22	1.67	1.33	1.49
	2	1.98	10.24	1.56	1.33	1.38
	3	1.86	8.97	1.71	1.33	1.52
	4	2.32	7.54	1.71	1.32	1.51
	5	1.96	7.66	1.90	1.32	1.67
	6	1.88	8.06	1.74	1.33	1.55
	7	1.80	7.92	1.85	1.33	1.64
6	1	2.35	10.11	1.48	1.33	1.31
	2	1.97	10.11	1.32	1.33	1.17
	3	1.85	8.86	1.48	1.33	1.31
	4	2.31	7.57	1.44	1.32	1.27
	5	1.95	7.54	1.63	1.32	1.43
	6	1.85	8.05	1.59	1.33	1.41
	7	1.80	7.83	1.62	1.33	1.43
7	1	2.95	10.62	1.60	1.33	1.42
	2	2.47	13.25	1.44	1.33	1.28
	3	2.32	13.77	1.71	1.33	1.52
	4	2.90	9.73	1.52	1.33	1.35
	5	2.51	11.47	1.82	1.33	1.61
	6	2.39	11.28	1.74	1.33	1.55
	7	2.36	14.37	1.77	1.33	1.57
8	1	4.01	6.08	1.71	1.28	1.47
	2	3.40	6.48	1.56	1.29	1.34
	3	3.17	8.17	1.75	1.33	1.55
	4	3.98	5.19	1.71	1.26	1.43
	5	3.44	7.95	1.82	1.34	1.63
	6	3.27	7.99	1.78	1.34	1.59
	7	3.24	7.14	1.77	1.31	1.55
9	1	2.34	10.95	1.67	1.33	1.49
	2	1.96	10.76	1.56	1.33	1.38
	3	1.84	9.71	1.71	1.33	1.52
	4	2.30	8.39	1.67	1.33	1.49
	5	2.00	9.67	1.98	1.33	1.75
	6	1.90	9.17	1.82	1.33	1.61
	7	1.88	12.71	1.85	1.33	1.64
10	1	2.34	10.79	1.87	1.33	1.66
	2	1.96	10.47	1.75	1.33	1.55
	3	1.84	9.94	1.83	1.33	1.62
	4	2.30	8.16	1.83	1.33	1.62
	5	2.00	9.76	2.09	1.33	1.86
	6	1.90	9.85	1.98	1.33	1.75
	7	1.88	12.28	2.07	1.33	1.84

Table 31 – Collapse performance results for the performance groups using SWM-2 (CUREE-Caltech, CUREE protocol, high aspect ratio)

Performance Group		FEMA P695 Analysis Parameters				
Archetype		Ω	μ_T	$\hat{S}_{CT}$	SSF	$ACMR$
Performance Group	Building Configuration					
11	1	2.27	13.38	0.93	1.14	4.24
	2	2.11	13.57	0.93	1.14	4.24
	3	2.05	10.91	1.09	1.14	4.97
	4	2.23	14.66	1.09	1.14	4.97
	5	2.10	10.97	1.21	1.14	5.52
	6	2.11	10.93	1.13	1.14	5.15
	7	1.84	10.31	1.12	1.14	5.87
	8	1.74	10.55	1.23	1.12	7.44
12	1	2.06	13.65	1.09	1.14	2.49
	2	0.71	13.39	1.13	1.14	2.58
	3	2.08	11.65	1.25	1.14	2.85
	4	2.25	14.71	1.25	1.14	2.84
	5	2.12	11.50	1.48	1.14	3.37
	6	2.08	12.36	1.44	1.14	3.28
	7	1.86	10.78	1.54	1.17	3.96
	8	1.78	9.47	1.42	1.15	4.26
13	1	1.72	14.01	1.21	1.14	1.84
	2	2.12	13.96	1.32	1.14	2.01
	3	2.06	11.99	1.52	1.14	2.31
	4	2.08	11.67	1.48	1.14	2.25
	5	2.10	11.91	1.62	1.14	2.46
	6	2.08	11.60	1.58	1.14	2.40
	7	2.04	11.32	1.68	1.14	2.55
	8	1.94	10.66	1.78	1.14	3.25
14	1	2.36	14.00	1.87	1.33	1.66
	2	2.76	14.13	1.99	1.33	1.76
	3	2.47	11.49	2.14	1.33	1.90
	4	2.32	9.81	1.91	1.33	1.69
	5	2.15	12.45	2.05	1.33	1.82
	6	2.15	11.45	2.09	1.33	1.86
	7	2.21	9.02	2.49	1.33	2.20
	8	2.35	7.47	2.32	1.35	2.08

15	1	2.45	12.39	1.91	1.33	1.69
	2	2.85	12.39	1.87	1.33	1.66
	3	2.52	7.31	2.18	1.31	1.91
	4	2.40	9.08	1.95	1.33	1.73
	5	2.19	8.45	2.02	1.33	1.79
	6	2.17	9.04	2.13	1.33	1.89
	7	2.24	7.20	2.37	1.31	2.07
	8	2.15	7.58	2.40	1.32	2.11
16	1	2.37	13.24	1.71	1.33	1.52
	2	2.76	13.00	1.87	1.33	1.66
	3	2.45	7.53	1.99	1.32	1.75
	4	2.33	9.80	1.75	1.33	1.55
	5	2.09	6.09	2.13	1.28	1.82
	6	2.10	9.59	2.13	1.33	1.89
	7	2.17	7.44	2.37	1.32	2.08
	8	2.08	7.57	2.43	1.32	2.14
17	1	2.70	14.75	1.87	1.33	1.66
	2	3.15	14.77	2.03	1.33	1.80
	3	2.82	12.63	2.26	1.33	2.00
	4	2.65	11.04	2.03	1.33	1.80
	5	2.47	14.51	2.17	1.33	1.92
	6	2.45	11.11	2.17	1.33	1.92
	7	2.53	10.13	2.37	1.33	2.10
	8	2.69	7.97	2.51	1.33	2.22
18	1	2.54	19.94	1.79	1.33	1.59
	2	2.97	19.50	1.87	1.33	1.66
	3	2.66	14.53	2.18	1.33	1.93
	4	2.50	13.98	1.91	1.33	1.69
	5	2.31	17.65	1.98	1.33	1.76
	6	2.31	13.39	2.17	1.33	1.92
	7	2.38	11.39	2.45	1.33	2.17
	8	2.54	8.69	2.40	1.35	2.15
19	1	2.37	14.05	2.06	1.33	1.83
	2	2.75	14.51	2.18	1.33	1.93
	3	2.47	11.44	2.34	1.33	2.07
	4	2.33	9.92	2.06	1.33	1.83
	5	2.15	12.31	2.52	1.33	2.23
	6	2.15	11.14	2.40	1.33	2.13
	7	2.21	9.64	2.71	1.33	2.40
	8	2.35	7.50	2.58	1.32	2.27

20	1	2.36	14.40	2.26	1.33	2.00
	2	2.76	13.64	2.41	1.33	2.14
	3	2.47	11.43	2.53	1.33	2.24
	4	2.32	10.13	2.26	1.33	2.00
	5	2.16	13.66	2.95	1.33	2.62
	6	2.15	11.58	2.60	1.33	2.30
	7	2.21	9.80	2.90	1.33	2.57
	8	2.35	7.52	2.81	1.32	2.47

Table 32 – Collapse performance results for the soft-story performance groups using SWM-1 and SWM-2

Performance Group		FEMA P695 Analysis Parameters				
Archetype		Ω	μ_T	$\hat{S}_{CT}$	SSF	$ACMR$
Performance Group	Building Configuration					
21	3	1.84	8.65	1.40	1.33	1.24
	4	2.30	8.93	1.44	1.33	1.28
	5	2.01	7.24	1.47	1.31	1.29
	6	1.90	7.24	1.40	1.31	1.22
22	3	2.47	10.56	1.95	1.33	1.73
	4	2.32	10.92	1.91	1.33	1.69
	5	2.98	9.04	2.17	1.33	1.92
	6	2.20	9.60	1.82	1.33	1.61
29	3	1.84	8.74	1.32	1.33	1.17
	4	2.30	8.80	1.44	1.33	1.28
	5	2.02	7.05	1.47	1.31	1.28
	6	1.90	7.55	1.43	1.32	1.26
30	3	2.46	11.65	1.95	1.33	1.73
	4	2.33	10.91	1.91	1.33	1.69
	5	2.98	9.36	2.02	1.33	1.79
	6	2.20	9.57	1.82	1.33	1.61

Table 33 – Collapse performance results for the performance group using SWM-7 (CASHEW, CUREE protocol, low aspect ratio)

Performance Group		FEMA P695 Analysis Parameters				
Archetype		Ω	μ_T	$\hat{S}_{CT}$	SSF	ACMR
Performance Group	Building Configuration					
23	1	2.22	14.15	1.71	1.33	1.52
	2	1.85	13.35	1.60	1.33	1.42
	3	1.74	11.97	1.83	1.33	1.62
	4	2.17	9.95	1.75	1.33	1.55
	5	1.89	11.24	1.98	1.33	1.75
	6	1.78	10.66	1.98	1.33	1.75
	7	1.77	14.25	1.92	1.33	1.70
	8	2.22	14.15	1.71	1.33	1.52

Table 34 – Collapse performance results for the performance group using SWM-8 (CASHEW, CUREE protocol, high aspect ratio)

Performance Group		FEMA P695 Analysis Parameters				
Archetype		Ω	μ_T	$\hat{S}_{CT}$	SSF	ACMR
Performance Group	Building Configuration					
24	1	2.08	10.36	1.64	1.33	1.45
	2	2.43	11.03	1.71	1.33	1.52
	3	2.18	9.67	1.83	1.33	1.62
	4	2.05	7.96	1.60	1.33	1.42
	5	1.87	9.20	1.63	1.33	1.45
	6	1.89	9.13	1.82	1.33	1.61
	7	1.95	7.46	1.92	1.32	1.69
	8	2.08	6.08	1.91	1.28	1.63

Table 35 – Collapse performance results for the performance group using SWM-6 (APA, CUREE protocol, low aspect ratio)

Performance Group		FEMA P695 Analysis Parameters				
Archetype		Ω	μ_T	$\hat{S}_{CT}$	SSF	$ACMR$
Performance Group	Building Configuration					
25	1	3.66	10.21	1.64	1.33	1.45
	2	2.13	11.26	1.36	1.33	1.21
	3	2.06	10.92	1.13	1.33	1.00
	4	3.56	8.45	1.71	1.33	1.52
	5	1.88	7.88	1.36	1.33	1.20
	6	2.21	8.95	1.05	1.33	0.93
	7	1.78	7.93	1.21	1.33	1.07
	8	2.03	8.27	1.31	1.33	1.16

Table 36 – Collapse performance results for the performance group using SWM-3 (APA, SPD protocol, low aspect ratio)

Performance Group		FEMA P695 Analysis Parameters				
Archetype		Ω	μ_T	$\hat{S}_{CT}$	SSF	$ACMR$
Performance Group	Building Configuration					
26	1	3.93	4.99	1.36	1.25	1.14
	2	2.29	7.81	0.97	1.33	0.86
	3	1.59	5.53	0.82	1.27	0.69
	4	3.83	4.89	1.40	1.25	1.17
	5	1.65	4.92	0.89	1.25	0.74
	6	1.52	5.60	1.01	1.27	0.85
	7	1.47	5.58	0.98	1.27	0.83
	8	1.68	5.06	1.01	1.26	0.85

Table 37 – Collapse performance results for the performance group using SWM-4 (APA, SPD protocol, mid aspect ratio)

Performance Group		FEMA P695 Analysis Parameters				
Archetype		Ω	μ_T	$\hat{S}_{CT}$	SSF	$ACMR$
Performance Group	Building Configuration					
27	1	1.56	7.77	0.97	1.32	0.86
	2	1.80	7.65	1.05	1.32	0.93
	3	1.62	7.12	1.29	1.31	1.12
	4	1.52	5.94	1.01	1.28	0.86
	5	1.31	6.15	1.09	1.28	0.93
	6	1.41	6.06	1.12	1.28	0.96
	7	1.16	5.83	1.21	1.28	1.02
	8	1.33	4.63	1.20	1.27	1.01

Table 38 – Collapse performance results for the performance group using SWM-5 (APA, SPD protocol, high aspect ratio)

Performance Group		FEMA P695 Analysis Parameters				
Archetype		Ω	μ_T	$\hat{S}_{CT}$	SSF	$ACMR$
Performance Group	Building Configuration					
28	1	1.41	8.67	1.32	1.33	1.17
	2	1.24	8.52	1.29	1.33	1.14
	3	1.19	8.68	1.56	1.33	1.38
	4	1.15	7.63	1.64	1.32	1.44
	5	1.09	7.36	1.63	1.31	1.43
	6	1.06	6.82	1.51	1.30	1.31
	7	1.05	7.21	1.66	1.31	1.45
	8	1.20	6.46	1.76	1.29	1.52